NASA TECHNICAL REPORT

NASA TR R-281
C. 1

NASA TR R-281

DESIGN OF A PRECISION TILT
AND VIBRATION ISOLATION SYSTEM

by Herbert Weinstock

Electronics Research Center

Cambridge, Mass.

NATIONAL AERONAUTICS AND SPACE ADMINISTRATION • WASHINGTON, D. C. • MARCH 1968

DESIGN OF A PRECISION TILT AND VIBRATION

ISOLATION SYSTEM

By Herbert Weinstock

Electronics Research Center
Cambridge, Mass.

NATIONAL AERONAUTICS AND SPACE ADMINISTRATION

FOREWORD

The studies described herein have been conducted
under the supervision of Professor Jacob P. Den Hartog
of the Department of Mechanical Engineering at M.I.T.
who served as chairman of the author's thesis committee
which included Professors R. W. Mann and S. Y. Lee of
the Department of Mechanical Engineering and Professor
W. R. Markey of the Department of Aeronautics and Astro-
nautics. The author would like to thank Professor
Den Hartog and the members of the committee for their
consistent encouragement, constructive criticisms and
continuing interest in the author's efforts.

The author was initially introduced to the special
problems of platform stability in the testing of inertial
navigation sensors by Mr. Peter J. Palmer, Deputy Associate
Director, of the M.I.T. Instrumentation Laboratory. The
author is indebted to Mr. Palmer and his friends and
associates at Instrumentation Laboratory for his education
in the arts of inertial navigation sensors and for their
continuous encouragement in the author's formal studies.
Special thanks are due to Professor K. Tsutsumi (Tufts
University) consultant to Instrumentation Laboratory and
Mr. F. Merenda of the Gyro Research Group for the use of
the M.I.T. micromotion drive in the experimental work.

iii

with NASA/ERC.

TABLE OF CONTENTS

TABLE OF CONTENTS (Cont)

LIST OF ILLUSTRATIONS

LIST OF ILLUSTRATIONS (Cont)

LIST OF ILLUSTRATIONS (Cont)

LIST OF TABLES

SECTION I

INTRODUCTION

Improvements in the design and fabrication of the optical and inertial sensors that are used in navigation and guidance systems have resulted in an increase in the accuracies and sensitivities of these instruments by several orders of magnitude over the past decade. These sensitivities and accuracies have improved to the point where the long term tilts and angular vibrations of the platforms on which the instruments are calibrated introduce significant errors in instrument performance tests. For gyroscope instrument testing a one arc second variation in platform position may result in an unwanted component of the angular rate of the Earth's rotation of 0.075 millidegree per hour. Current gyroscope instruments may be obtained having drift rates of 1 millidegree per hour and it is expected that gyroscope drift rates of the order of 0.1 millidegree per hour will be obtained by 1970. For accelerometer testing a one arc second drift of the test platform will result in a testing error of 5 micro-g which is intolerable compared with the one micro-g performance that is expected in 1970.

These considerations have caused the manufacturers and test laboratories concerned with these instruments to search for extremely stable and seismically inactive test locations. Some of these efforts are discussed in the proceedings of the Test Pad Stability Subcommittee of

the American Institute of Aeronautics and Astronautics of 1965 [1] and 1966. [2] Of particular note, is a description of the efforts of the Martin Company [3] in selecting a site for their navigation instrument test facility in a seismically inactive area near Denver, Colorado. In constructing the facility, however, they found that the cultural activity introduced by personnel and equipment necessary to the facility, combined with structural resonances, resulted in vibration and drift levels which were above their stated tolerances. Although it may be possible to locate a sufficiently quiet test location and to take sufficient precautions in facility design to permit testing of current instruments, the accuracy requirements of future instruments will require better definition and control of the test environment than is available at any known seismically inactive location. Furthermore, there are several situations where it is desirable to test instruments at locations having known high seismic activities. For example, a space vehicle launch site. In addition, selection of a site for a test facility is often influenced by the availability of skilled personnel and proximity to complementary test facilities.

In order to overcome the limitations produced by drifts and vibrations on instrument testing, more recent efforts have been directed towards the design of tilt and vibration isolation systems which are intended to isolate

the platform from local ground motions. The conventional passive vibration isolation approach of mounting the platform on a very massive spring supported pendulum was attempted by the Newark Air Force Station at Newark, Ohio.[4] A 24 foot spring supported pendulum having natural frequencies of about 0.2 cps was constructed. Although this system was successful in isolating high frequency vibrations, it was difficult to prevent undesirable oscillations at the pendulum natural frequency that were caused by small disturbance forces (e.g. air currents and drafts). Furthermore a pendulum is incapable of providing rotational isolation at or near its natural frequency. These limitations are discussed in more detail, with reference to the typical environments and specifications given below, in Section II.

A more practical approach to providing low frequency tilt isolation is the use of a tilt servomechanism controlled by high resolution level sensors. One such system has been built by Tsutsumi and Merenda at M.I.T. Instrumentation Laboratory [5] and another by DeBra at Stanford University.[6] The estimated performance of both of these systems is about 0.5 arc seconds. The bandpass of both of these tilt isolation systems is, however, limited to about 0.05 cps. This limitation is caused by the response of the transducer and as discussed in Section II by the high susceptibility of this type of system to horizontal accelerations. A one micro-g horizontal acceleration would force an angular motion of about 0.2 arc seconds. Horizontal accelerations

3

of a hundred micro-g at higher frequencies are not uncommon in typical test laboratories.

A system combining low frequency tilt isolation and high frequency passive vibration isolation has recently been delivered to the Heath Air Force Station at Newark, Ohio by the Barry Wright Corporation at Watertown, Mass.[7] This system is, in principle, a modification of the Barry Serva Level vibration isolation system described in Reference 8 with a signal from a pendulum used to control the low frequency tilts in place of the height control that is usually provided. As in the servomechanism system the bandpass of the low frequency tilt isolation is limited to about 0.05 cps by the horizontal accelerations and the transducer time constants. At frequencies between the low frequency cutoff and twice the system natural frequency (about .6 cps) the system is relatively sensitive to disturbance torques. At the natural frequency there is an amplification of the existing ground motions. Therefore application of this type of system would be recommended only in environments where only very small disturbance forces and angular vibrations exist between the low frequency cutoff and twice the natural frequency and where considerable vibration levels exist at frequencies above the system natural frequency. The accuracy of this system is quoted at $\pm$ 0.25 arc second in the environment of the Heath facility.

A survey of the limitations on inertial sensor testing that are produced by the tilt and vibration environments that would be expected in a typical urban test laboratory is presented in Reference 9. Estimates of the environments that would be expected are obtained in Reference 9 from published measurements. These vibration spectra are presented for reference purposes in Figure 1-1. The errors in accelerometer and gyroscope testing that would be produced by these environments are calculated in the manner indicated in Reference 9 and are tabulated in Tables 1-1 through 1-3. It is seen that the primary errors in both gyroscope and accelerometer testing are those due to the long term tilts and angular vibrations of the test platform. The translational accelerations produce a secondary error in accelerometer tests and a negligibly small error in gyroscope testing.

If long averaging times (heavy filtering) is permissible in the instrument tests, a servomechanism levelling system of the type used at the M.I.T. Instrumentation Laboratory [5] is capable of reducing the major portion of the testing errors introduced by the environment. The use of long averaging times, however, increases the time required to obtain a statistically significant set of performance data. In addition this type of testing provides no information on the short term performance of the instrument. In gimballess (strapdown) inertial navigation systems short term instrument errors (e.g. a noise

5
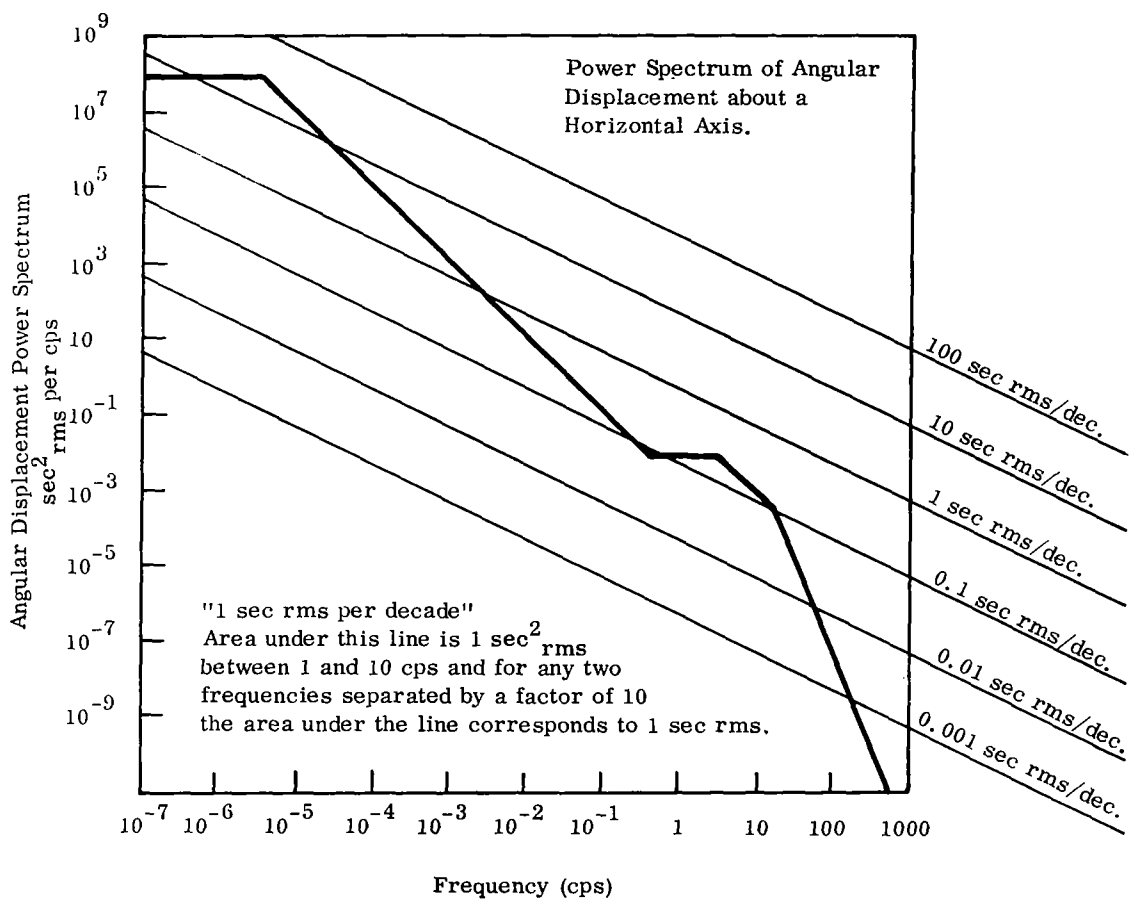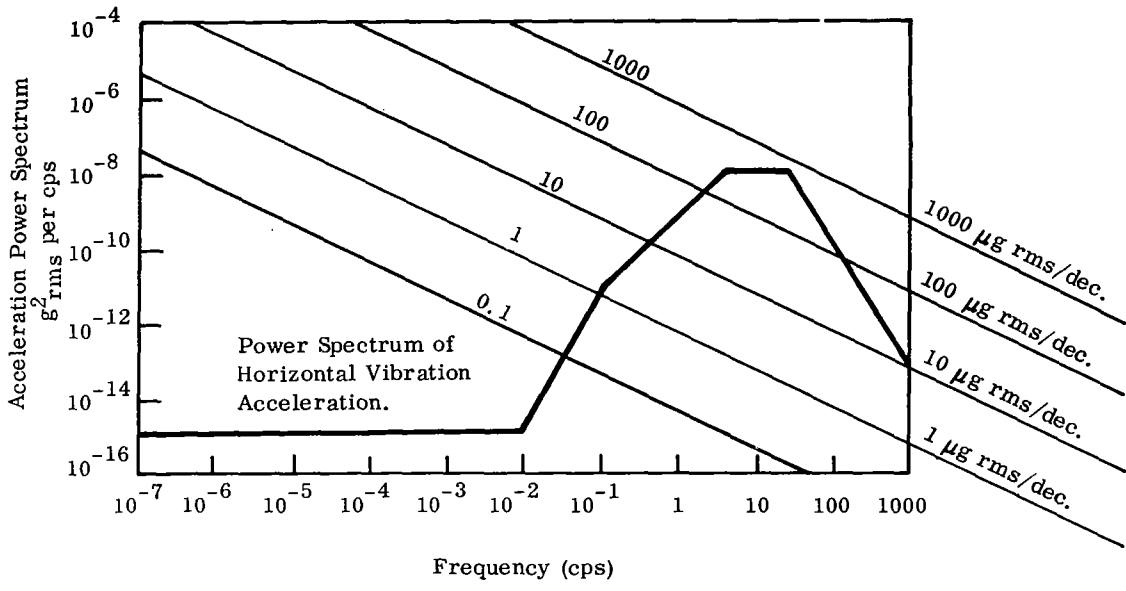
Figure 1-1. Representative Vibration Environment of an Urban Test Laboratory

6

TABLE 1-1

ERROR IN ACCELEROMETER TESTING

PRODUCED BY REFERENCE TRANSLATIONAL VIBRATION SPECTRUM

(micro-g - rms)

FREQUENCY BAND (cps)	AVERAGING TIME			
	SECONDS		MINUTES	
	10	30	10	30
$0 - 10^{-5}$	0.0001*	0.0001*	0.0001*	0.0001*
$10^{-5} - 10^{-4}$	0.0003	0.0003	0.0003	0.0003
$10^{-4} - 10^{-3}$	0.001	0.001	0.0009	0.0005
$10^{-3} - 10^{-2}$	0.003	0.003	0.0005	0.0002
$10^{-2} - 10^{-1}$	0.19	.06	.003	.001
$10^{-1} - 1$	0.95	0.32	0.016	0.005
$1 - 10$	2.1	0.70	0.035	0.012
$10 - 100$	0.84	.28	.014	.005
TOTAL	2.5	0.67	0.041	0.014

*EXCLUSIVE OF EARTH TIDES AND GRAVITATIONAL EFFECTS.

7

TABLE 1-2

ERROR IN ACCELEROMETER TESTING

PRODUCED BY REFERENCE ANGULAR VIBRATION SPECTRUM

(micro-g - rms)

FREQUENCY BAND	AVERAGING TIME			
	SECONDS		MINUTES	
	10	30	10	30
$0 - 10^{-5}$	89.4	89.4	89.4	89.4
$10^{-5} - 10^{-4}$	46	46	46	46
$10^{-4} - 10^{-3}$	14.5	14.5	14.5	12.5
$10^{-3} - 10^{-2}$	4.6	4.6	1.5	0.5
$10^{-2} - 10^{-1}$	1.4	1.1	0.04	0.02
$10^{-1} - 1$	0.09	0.03	0.001	0.0005
$1 - 10$	0.01	0.003	0.0001	0.00005
$10 - 100$	0.001	0.0003	0.00001	0.000005
TOTAL	102	102	102	101

TABLE 1-3

ERROR IN GYROSCOPE TESTING

PRODUCED BY REFERENCE ANGULAR VIBRATION SPECTRUM
FOR SEVERAL FILTERING TIMES

(millideg/hr (rms))

| FREQUENCY BAND (cps) | FILTER TIME CONSTANT (τ) | | | |
| | SECONDS | | MINUTES | |
	10	30	10	30
$0 - 10^{-5}$	2.3	2.3	2.3	2.3
$10^{-5} - 10^{-4}$	4.9	4.9	4.9	4.5
$10^{-4} - 10^{-3}$	11.7	11.7	11.2	3.6
$10^{-3} - 10^{-2}$	20.3	20.0	2.5	0.8
$10^{-2} - 10^{-1}$	35.6	12.2	0.6	0.2
$10^{-1} - 1.0$	11.2	3.7	0.2	0.06
$1 - 10$	20.8	7.0	0.35	0.12
$10 - 100$	8.1	2.7	0.14	0.05
TOTAL	51	28	12.7	6.1

signal at 3 cps) could result in significant system errors.
Heavy filtering would also be unacceptable for navigation
and control of fast highly maneuverable vehicles. In order
to demonstrate gyroscope instrument performance of 0.0001
degrees per hour as will be required in the 1970's and
permit testing with the smaller filtering times required
for strapdown system application, a vibration isolation
system is required that will reduce angular motions of the
test platform about a horizontal axis at all frequencies
below 50 cps. This document presents the results of an
analytical and experimental design study which demonstrates
the feasibility of an angular vibration isolation system
that will meet these requirements.

The design specifications for this system are:

1. The platform is to support a testing device
    having a weight of 5,000 lbs. and contained
    in the volume of a five foot cube.

2. In the presence of the reference vibration
    spectrum shown in Figure 1-1 angular motions
    about a horizontal axis shall be limited to:

    A. 0.1 arc second rms for frequencies
        between 1 cycle per three months to 10^{-5}
        cycles per second (0.86 cycle per day).

    B. 0.03 arc second rms for frequencies
        between 10^{-5} to 10^{-4} cycles per second.

    C. 0.02 arc second rms for frequencies above
        10^{-4} cps.

D. 0.01 arc second rms between any two frequencies above 10^{-4} cps that are separated by a factor of 10.

A graphical representation of these requirements is shown in Figure 1-2.

3. The angular motions are to be limited to those specified above in the presence of disturbance torques of 250 lb-ft. at frequencies less than 0.001 cps, and disturbance pressures of 10^{-5} psi rms per decade that may be due to drafts or sound waves.

4. For a step torque disturbance of 250 lb-ft the maximum platform excursion is to be 3 arc seconds. This excursion is to be reduced to the motions specified above within a five second period.

5. The ratio of the platform angular motions about a horizontal axis to the ground angular motions shall be less than one at all frequencies.

A platform meeting the above specifications will limit the errors in gyroscope testing to 0.2 millidegree per hour for tests using a filter time constant of 100 seconds. For tests employing time constants of 15 minutes the error in gyroscope testing will be reduced to about 0,023 millidegree per hour. For accelerometer tests with averaging times of 30 seconds the platform will reduce the testing error to about 0.75 micro-g and for averaging times of 10 minutes or longer, the error will be reduced to about 0.05 micro-g.
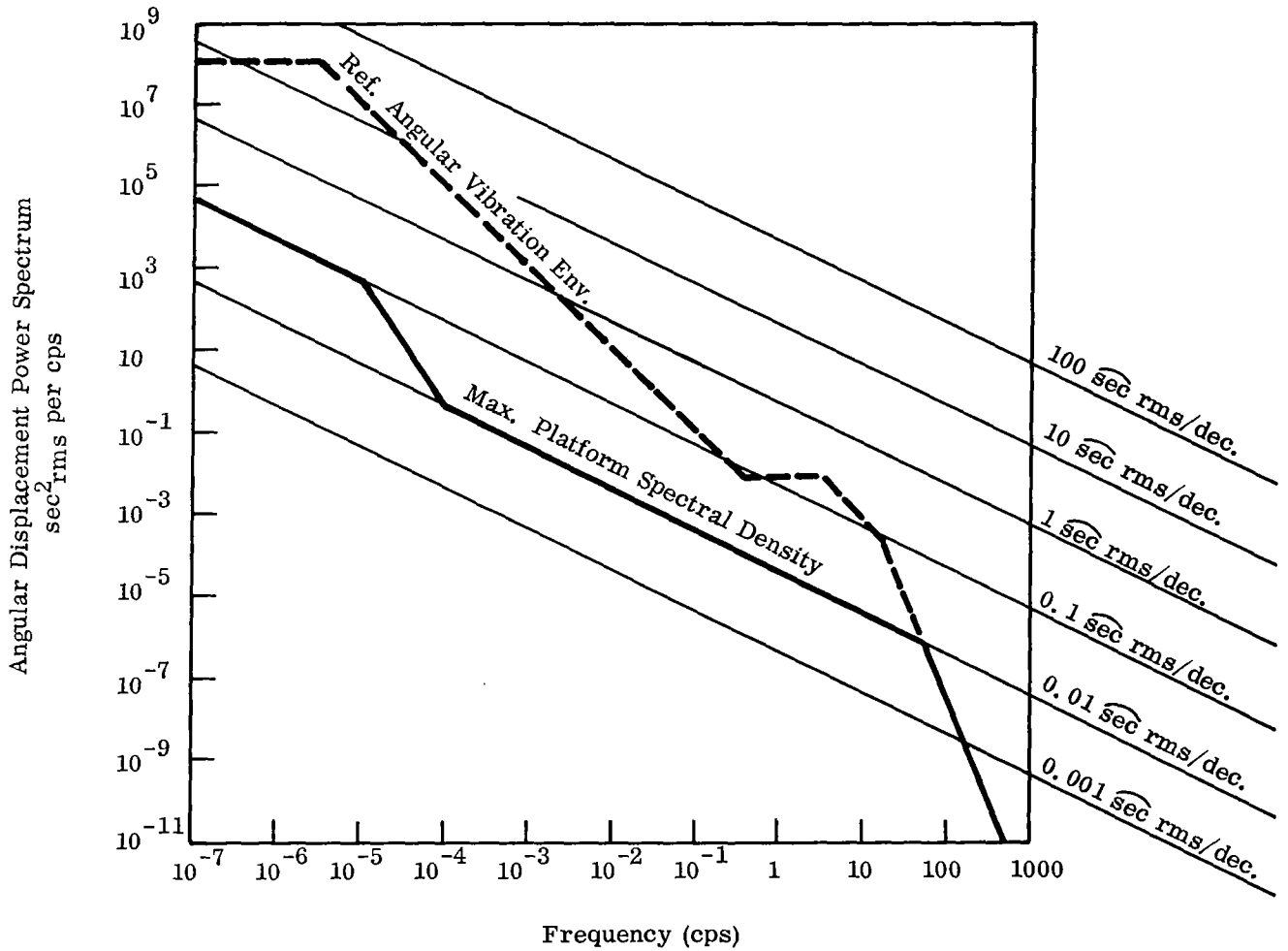
11

Figure 1-2.   Maximum Allowable Angular Motions about Horizontal Axis of Required Isolation System

The platform specification is based on the accuracies of currently available level and rate sensors. An improvement in the accuracies of these instruments would result in corresponding improvements in platform performance.

The design discussed here consists of a two axis servo-mechanism levelling system controlled by gyroscopes and level sensors as indicated in Figure 1-3 which is mounted on a massive conventional pneumatic isolation system of the serva level type built by Barry Wright Corporation as indicated in Figure 1-4.

At frequencies below 0.012 cps the system is controlled by the level sensors. From 0.012 cps to 25 cps the gyroscope instruments maintain control. At frequencies above 25 cps the servomechanism system is locked out and the test device and the massive frame act as a "rigid" body mounted on springs resulting in the isolation that would be provided by a damped 1 cps conventional vibration isolation system.

Section II of this document discusses the design alternatives for this system and the general design parameters required to meet the performance specification.

Section III discusses the specific components required to achieve the design parameters discussed in Section II with particular emphasis on the practical limitations imposed by existing components (e.g., saturation, friction and other non-linear effects)

13
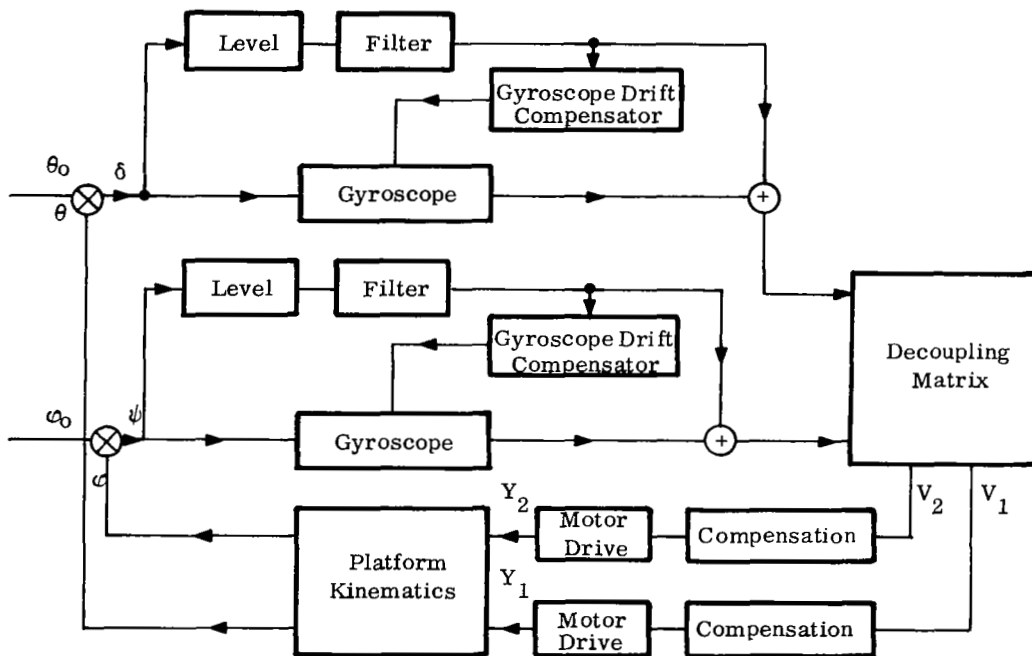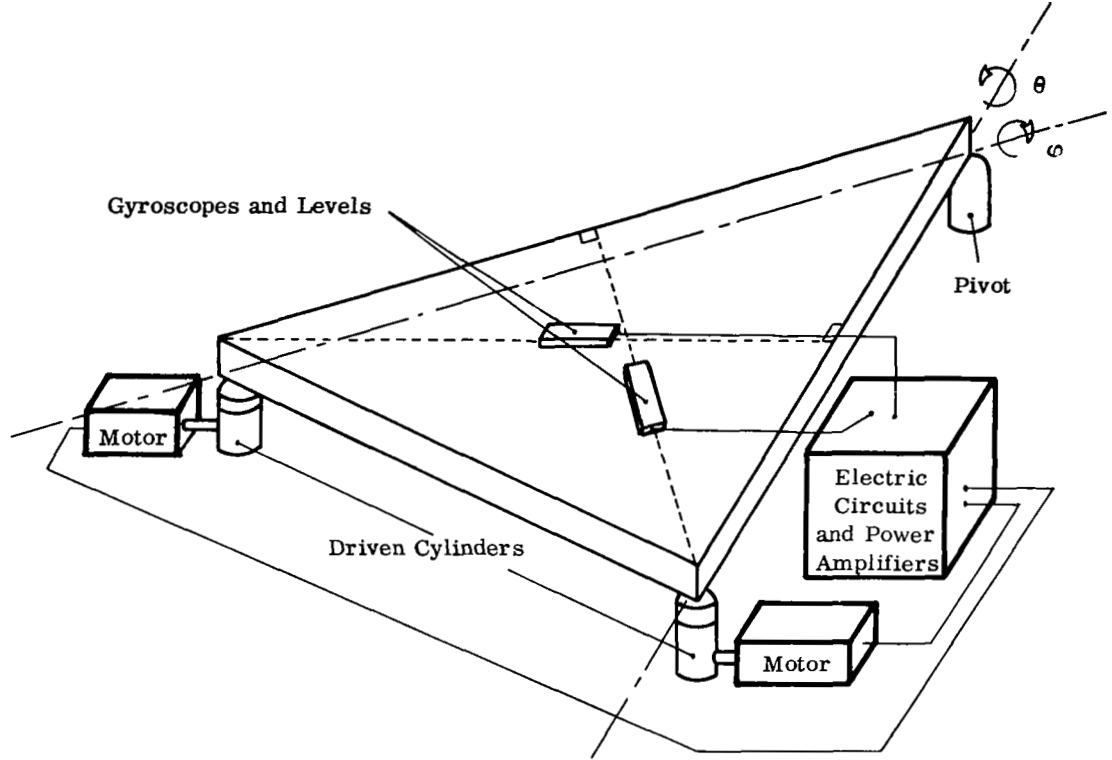
Figure 1-3. Servomechanism System Using Gyroscopes and Levels for Control

14

8 ft

Level control 0 to .012 cps
Gyroscope control .012 cps to 25 cps
Passive isolation from 1 cps up.

Test Table
(5000 lb.)

Laboratory Floor

Laboratory Floor

Steel Frame Passive
System inertia
20,000 lb.-ft.-sec.
35,000 lb.

3 ft

Active System Pivot

Concrete Base

Active System Drive

Air Spring Barry Servo Level
1 cps Natural Frequency
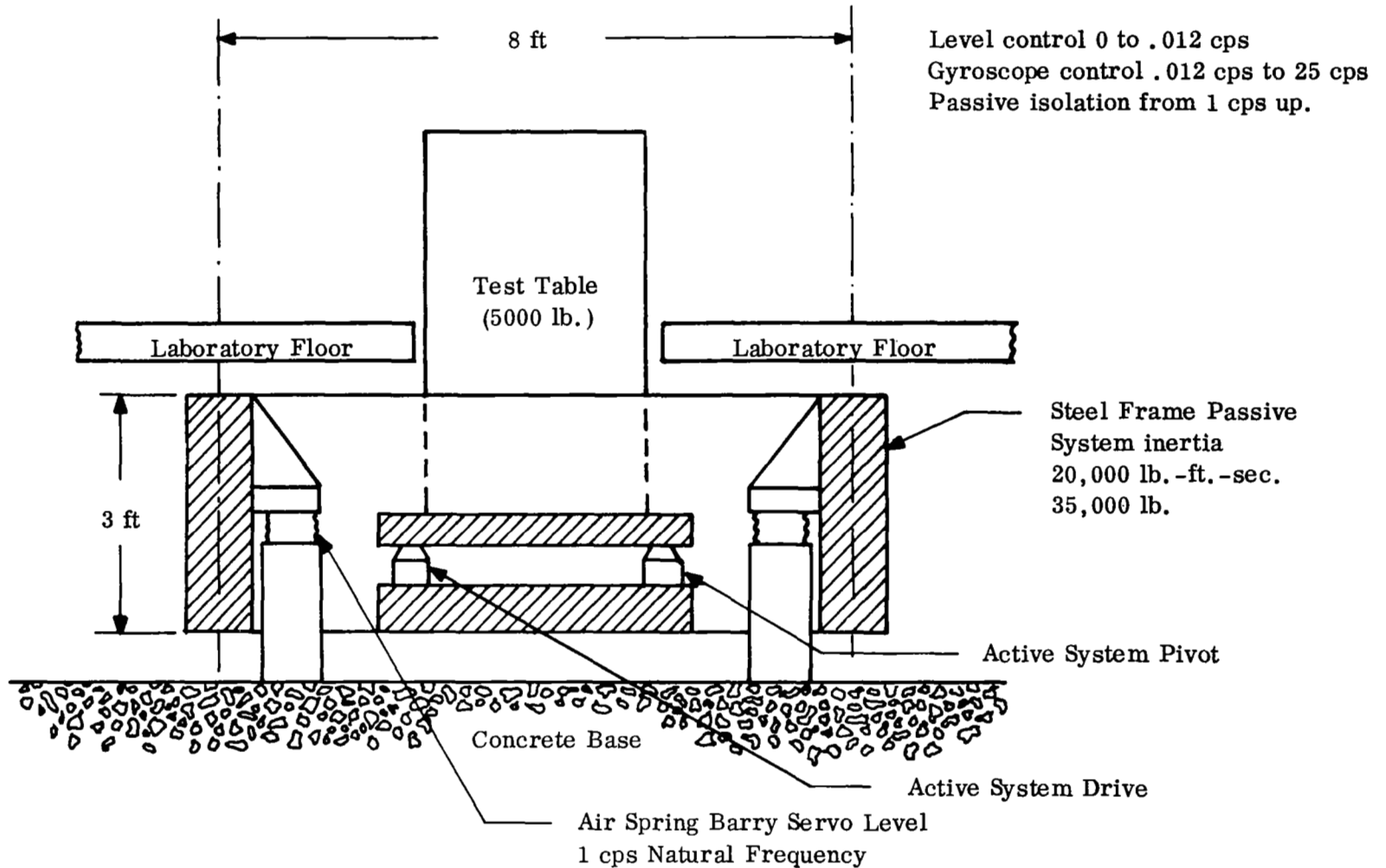
Figure 1-4. Active (servo-controlled) Base Motion Isolation System Mounted on Low Frequency
Air Spring Isolation System

Figure 1-5. Forecast of Gyroscope and Accelerometer Performance
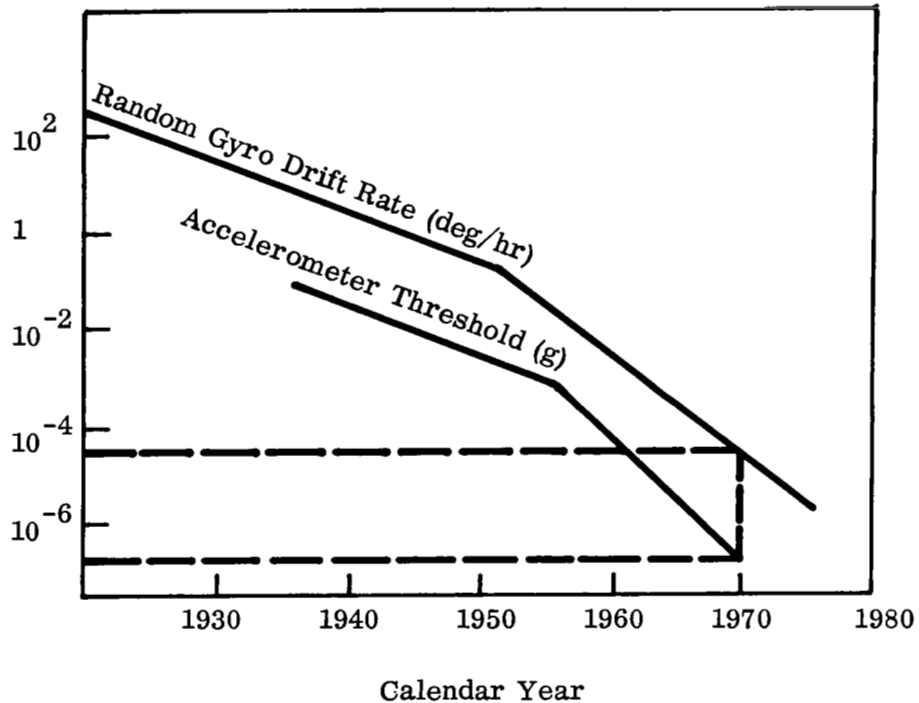
From: Fink, D. J. (Deputy Director Defense Research and Engineering), Communications - Components - Guidance - in "Space Age of FY 2001," 4th Goddard Memorial Symposium of American Astronautical Society, Washington, D. C. , March 1966.

16

and presents the isolation efficiency and other performance functions of a realizable design.

Section IV reviews the design, assembly and test results of an experimental single axis full scale model of the servo-mechanism portion of the system.

SECTION II

GENERAL DESIGN CONSIDERATIONS

2.0 Summary

Alternate methods for achieving the performance requirements outlined in Section I are reviewed. It is concluded that passive vibration isolation systems are incapable of meeting the required performance and that an active isolation system using both gyroscope instruments and level sensors for control is required. The optimum parameters for the general design of an active isolation system that combines servomechanism control at low frequencies with passive (inertia) isolation at high frequencies are obtained. The physical mechanization and practical design of this system is discussed in Section III.

2.1 Passive Isolation Systems

Conceptually, the simplest means of maintaining a surface at level and providing high frequency rotational isolation is the use of a pendulum as shown in Figure 2-1 The differential equation governing the response of the pendulum to ground rotations, translational accelerations and externally applied torques is:

$$(Mgl)\ \delta + C\dot{\delta} + I_0 \ddot{\delta} = C\dot{\theta}_0 + Mla_x + T \qquad (2\text{-}1)$$

where the notation is that indicated in Figure 2-1 and the dot represents differentiation with respect to time

Platform Surface

Hemispheric
Bearing
(Pendulum Pivot)

ℓ

c. g.

a_x

True Level

θ_0

C

δ

ℓ

M = Platform Mass

g = Specific Force of Gravity

ℓ = Distance between platform pivot and platform Gravity center

c = Effective viscous damping

I_0 = Moment of inertia of platform about platform pivot

θ_0 = Ground angular motion

a_x = Ground horizontal acceleration

T = Torque applied to platform

g

$$Mg\,\ell\,\delta + c\,\dot{\delta} + I_0\,\ddot{\delta} = c\,\dot{\theta}_0 + M\,\ell a_x + T$$

Figure 2-1. Pendulum as Passive Isolation System

$(\overset{o}{\delta}$ = angular velocity and $\overset{..}{\delta}$ = angular acceleration).

The response of the platform to a sinusoidal base rotation is:

$$\left|\frac{\delta}{\Theta_o}\right| = \sqrt{\frac{4\beta^2\left(f^2/f_n^2\right)}{\left(1 - f^2/f_n^2\right) + 4\beta^2\, f^2/f_n^2}} \qquad (2-2)$$

The response to horizontal sinusoidal acceleration is:

$$\left|\frac{\delta}{a_x}\right| = \frac{1}{g}\sqrt{\frac{1}{\left(1 - f^2/f_n^2\right) + 4\beta^2\, f^2/f_n^2}} \qquad (2-3)$$

and the response to external torques is:

$$\left|\frac{\delta}{T}\right| = \frac{1}{Mgl}\sqrt{\frac{1}{\left(1 - f^2/f_n^2\right) + 4\beta^2\, f^2/f_n^2}} \qquad (2-4)$$

If the disturbance torques and vibratory motions are random and uncorrelated the power spectral density of the error angle is:

$$\Phi_{\delta\delta}(f) = \frac{4\beta^2\, f^2/f_n^2\, \Phi_{\theta\theta}(f) + \Phi_{aa}(f)/g^2 + \Phi_{TT}(f)/Mgl)^2}{\left(1 - f^2/f_n^2\right)^2 + 4\beta^2\, f^2/f_n^2} \qquad (2-5)$$

and the mean squared error angle is:

$$\overline{\delta^2} = \int_o^\infty \Phi_{\delta\delta}(f)\, df \qquad (2-6)$$

At frequencies well above the pendulum natural frequency

the error angle spectral density due to horizontal acceleration is given by:

$$\Phi_{\delta\delta_a}(f) \simeq \frac{\Phi_{aa}(f)}{g^2 \left(\frac{f}{f_n}\right)^4} \tag{2-7}$$

Between 10^{-4} cps and 50 cps the maximum allowable platform spectral density is given in Figure 1-2 as:

$$\Phi_{\delta\delta_{max}} = \frac{4.35 \times 10^{-5}}{f} \quad \overparen{\sec}^2/cps \tag{2-8}$$

Between 0.01 cps and 0.1 cps the translational acceleration is given in Figure 1-3 as:

$$\Phi_{aa} = 10^{-15} \left(\frac{f}{10^{-2}}\right)^4 \quad g^2/cps \tag{2-9}$$

converting $\Phi_{aa/g}2$ to arc second units:

$$\Phi_{aa/g}2 = 10^{-15} \left(\frac{f}{10^{-2}}\right)^4 (2.06 \times 10^5)^2 \quad \frac{\overparen{\sec}}{cps}^2$$

$$= 4.25 \times 10^3 \, f^4 \quad \overparen{\sec}^2/cps \tag{2-10}$$

To meet the required specification:

$$\frac{4.35 \times 10^{-5}}{f} \lessapprox \frac{4.25 \times 10^3 \, f^4}{f^4/f_n^4} \tag{2-11}$$

21

between 0.01 cps and 0.1 cps. This requires that the natural frequency of the pendulum be less than 0.018 cps.

In order to sustain a torque load of 250 lb-ft at frequencies less than 0.001 cps with an error less than 0.01 arc second, the platform pendulousity must be greater than:

$$Mgl = \frac{250 \text{ lb-ft}}{.01 \text{ sec}} \times 2.06 \times 10^5 \frac{\text{sec}}{\text{rad}}$$

$$= 5.15 \times 10^9 \text{ lb-ft}$$

This would represent a 250 million pound weight at a 20.6 foot arm. Even if the specification could be reduced to disturbance torques of 0.05 lb-ft., a platform pendulousity of a million lb-ft would be required. For this pendulousity and a natural frequency of 0.018 cps, the moment of inertia of the platform would be:

$$I_o = \frac{Mgl}{\left(2\pi f_n\right)^2} = \frac{10^6}{\left(2\pi \times 0.018\right)^2} = \underline{7.84 \times 10^7 \text{ lb-ft-sec}^2}$$

This is the moment of inertia of a 46 foot cube having a weight of about 15 million pounds.

Equations 2-2 and 2-5 show that at the pendulum natural frequency, no angular isolation exists for any finite amount of damping. To minimize the

sensitivity to ground induced motions near the pendulum natural frequency, the damping should be as small as possible. However, this would result in a maximum sensitivity to torques and accelerations at or near the natural frequency and continuous transient oscillations.

If the environment were such that no disturbance torques or ground motions existed at the pendulum natural frequency, it would be conceivably possible to design a pendulum for maintaining level. However, as indicated by the above calculations, construction of such a platform would meet many serious practical limitations. The same considerations introduce practical limitations on the design of any passive isolation system.

2.2 Servo-mechanism Systems Using Level Sensors

Low frequency vibration isolation of rotations about a horizontal axis can be achieved by using a servomechanism controlled by a level sensor as shown in Figure 2-2. Levelling systems of this type are currently in use at the M.I.T. Instrumentation Laboratory (Ref. 5) and Stanford University (Ref. 6). In this type of system, the error angle of the platform is measured by the level transducer and a signal proportional to the error angle is operated on by a filter (G(s)) to produce appropriate frequency charac-

23
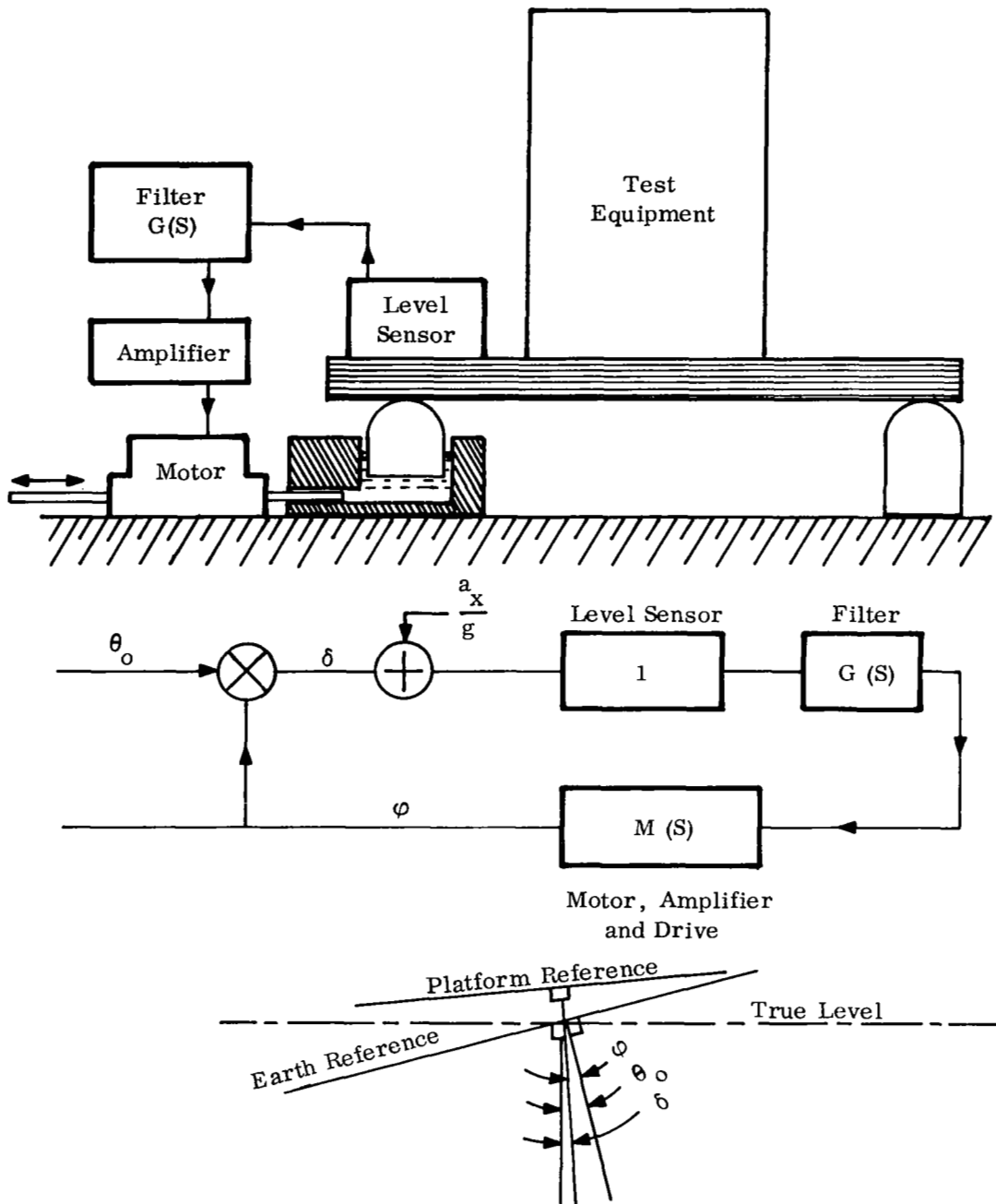
a_x = Horizontal Acceleration

θ_o = Angle between Normal to Earth Surface and "True" Vertical

φ = Angle between Platform Normal and Earth Surface Normal

δ = Angle between Platform Normal and "True" Vertical

Figure 2-2. Servomechanism System Controlled by Level Sensor

24

teristics and is then amplified to drive a motor which attempts to restore the platform to level. The sensitivity of the platform to base rotations is:

$$\frac{\delta(s)}{\Theta_o(s)} = \frac{1}{1 + G(s)M(s)} \qquad (2-12)$$

The sensitivity to horizontal accelerations is:

$$\frac{\delta(s)}{a_x(s)} = \frac{(1/g)G(s)M(s)}{1 + G(s)M(s)} \qquad (2-13)$$

If the operator $L(s)$ is defined as:

$$L(s) = \frac{G(s)M(s)}{1 + G(s)M(s)} \qquad (2-14)$$

the error angle is given by:

$$\delta(s) = (1-L(s)) \, \Theta_o(s) + \frac{L(s)}{g} \, a_x(s) \qquad (2-15)$$

If the accelerations and rotations are random and uncorrelated the spectral density of the error angle is given by:

$$\Phi_{\delta\delta}(\omega) = |(1-L(j\omega))|^2 \, \Phi_{\theta\theta}(\omega) + |L(j\omega)|^2 \, \Phi_{aa}(\omega)$$

25

$$\omega = 2\Pi f \qquad\qquad\qquad\qquad (2\text{-}16)$$

The best conceivable performance of this system occurs if L (jω) is the optimum (Wiener) filter (e.g., see Ref. 10) and is given by:

$$L\ (j\omega)\ =\ \frac{\Phi'_{\theta\theta}\ (\omega)}{\Phi'_{\theta\theta}\ (\omega)\ +\ \Phi'_{aa}\ (\omega)} \qquad\qquad (2\text{-}17)$$

Substitution into Equation (2-16) yields:

$$\Phi_{\delta\delta}\ (\omega)\ =\ \frac{\Phi'_{aa}\ (\omega)\ \Phi'_{\theta\theta}\ (\omega)}{\Phi'_{\theta\theta}\ (\omega)\ +\ \Phi'_{aa}\ (\omega)} \qquad\qquad (2\text{-}18)$$

This spectral density is plotted for the reference spectra in Figure 2-3. It is seen that for this physically unrealizable frequency characteristic the best performance that could be obtained would be an error angle power spectral density corresponding to about 0.2 arc seconds. Although the calculation of Equation (2-18) implies a frequency response characteristic which can not be achieved in a real system, it does provide a simple and rapid bound on the performance that can be achieved. As illustrated in the following paragraphs, this computation indicates an rms error angle for the systems discussed here that is within about a factor of 2 of the performance that would be achieved by the best
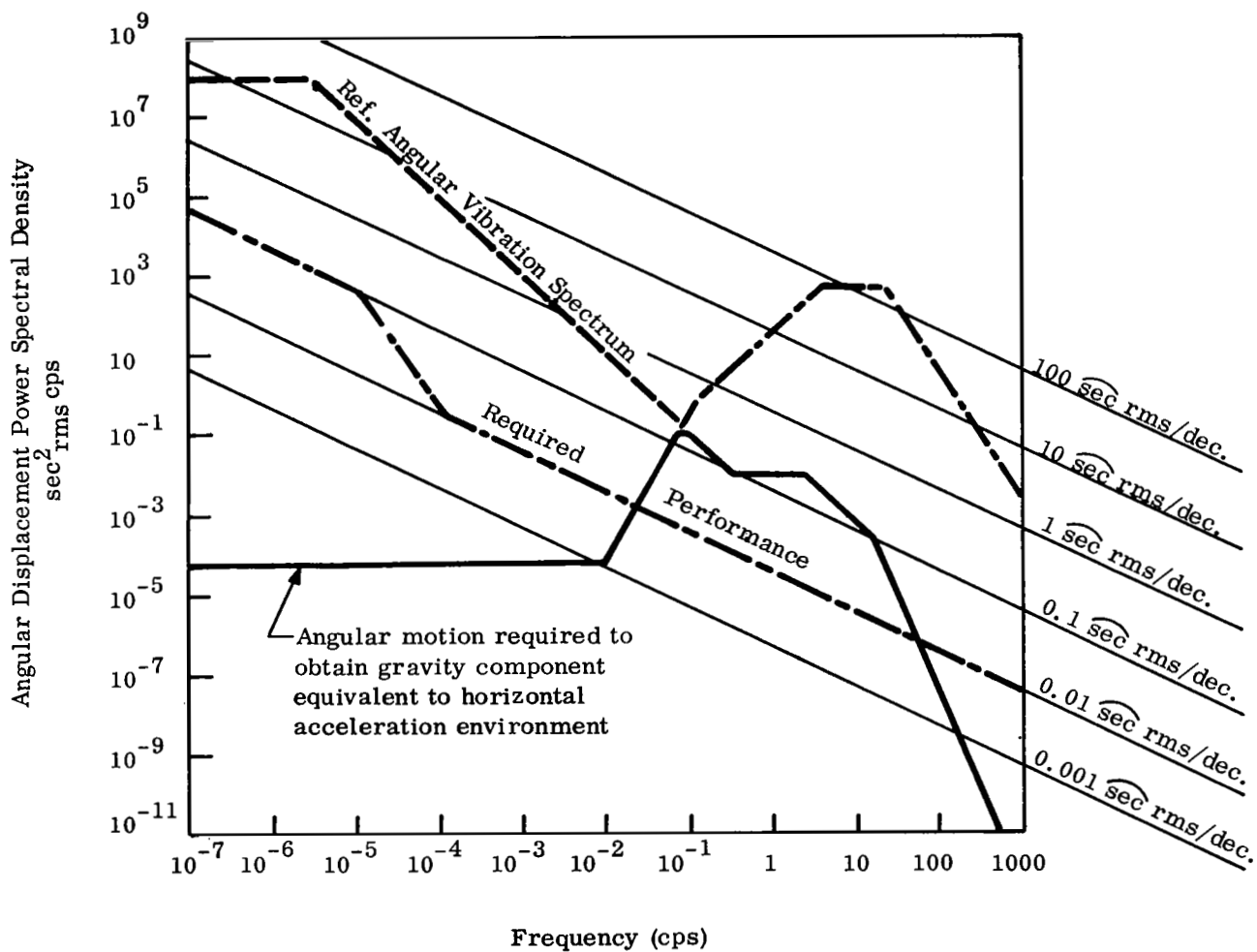
Figure 2-3. Best Conceivable Performance of Servo Levelled Platform in Reference Environment Using Only a Level Sensor for Control (Without Regard for Physical Realizability of System)

physically realizable system.

The best frequency characteristic that can be
obtained in a real system can be obtained from the Bode
and Shannon approach to the design of the optimum filter
(e.g., see Ref 10). This calculation is carried out in
Appendix A and the optimum characteristic is obtained as:

$$L (j\omega) = \frac{1 + \dfrac{j\omega}{0.628}}{\left(1 + \dfrac{j\omega}{0.438}\right)\left(\left(1 - \left(\dfrac{\omega}{0.523}\right)^2 + \dfrac{1.15\ j\omega}{0.523}\right)\right)} \tag{2-19}$$

The power spectral density of the error angle for
this frequency characteristic is calculated from Equation
(2-16) and is plotted as a function of frequency in
Figure 2-4. It is seen that the best possible servo-
mechanism system that uses only level transducers for
control fails to meet the specified requirements at all
frequencies above 0.0001 cps.

2.3 Servomechanism Levelling devices Using Both Level Sensors and Gyroscope Instruments

For a servomechanism to provide isolation at frequen-
cies above 0.08 cps and permit better low frequency isola-
tion characteristics a transducer is required that can
distinguish between angular rotations about a horizontal
axis and horizontal accelerations. This suggests the use
of an inertial grade gyroscope instrument. Gyroscope
instruments, however, have large low frequency random drift
rates. A plot of the experimentally obtained drift rate

28

The chart contains the following text labels:

Angular Displacement Power Spectrum sec^2 rms per cps

10^9
10^7
10^5
10^3
10
10^{-1}
10^{-3}
10^{-5}
10^{-7}
10^{-9}
10^{-11}

Angular Vibration Environment

Required Performance

"1 sec rms per decade"
Area under this line is 1 $\widehat{\text{sec}}^2$ rms
between 1 and 10 cps and for any
two frequencies separated by a factor
of 10 the area under the line corresponds
to 1 $\widehat{\text{sec}}$ rms

1 sec rms/dec.
0.5 sec rms/dec.
0.2 sec rms/dec.
0.1 sec rms/dec.
0.01 sec rms/dec.

10^{-7} 10^{-6} 10^{-5} 10^{-4} 10^{-3} 10^{-2} 10^{-1} 1 10 100 1000

Frequency (cps)

Figure 2-4. Best Possible Performance of Servo Levelling System Using a Level Sensor for Control

29

power spectral density of a typical gyroscope instrument is shown in Figure 2-5. It is seen that this spectral density is unbounded at zero frequency and any platform that was controlled by a gyroscope only would have a continuously growing drift angle. However, by combining a level sensor and a gyroscope instrument as indicated in Figure 2-6, it is conceivably possible to build a levelling servomechanism that will approach the required performance.

For computation purposes the power spectral density of the gyroscope drift rate is assumed to be given by:

$$\Phi_{gg}(f) = \frac{10^{-11}}{f^2} \ (1 + 1000 \ f^2) \ (1 + f^2) \ (^\circ/hr)^2/cps$$

$$(2-20)$$

The shape of this spectral density curve is consistent with the experimental results shown in Figure 2-5. The scale has been adjusted so that the expected rms drift rate in a 28 hour period as obtained in a standard constant orientation test would be 0.001 degree per hour rms. For purposes of this document, a nominal gyroscope figure of merit is defined as:

$$\text{Nominal Drift Rate} = \sqrt{\int_{10^{-5}}^{10^{-2}} \Phi_{gg}(f) \ df}$$

$$(2-21)$$

30
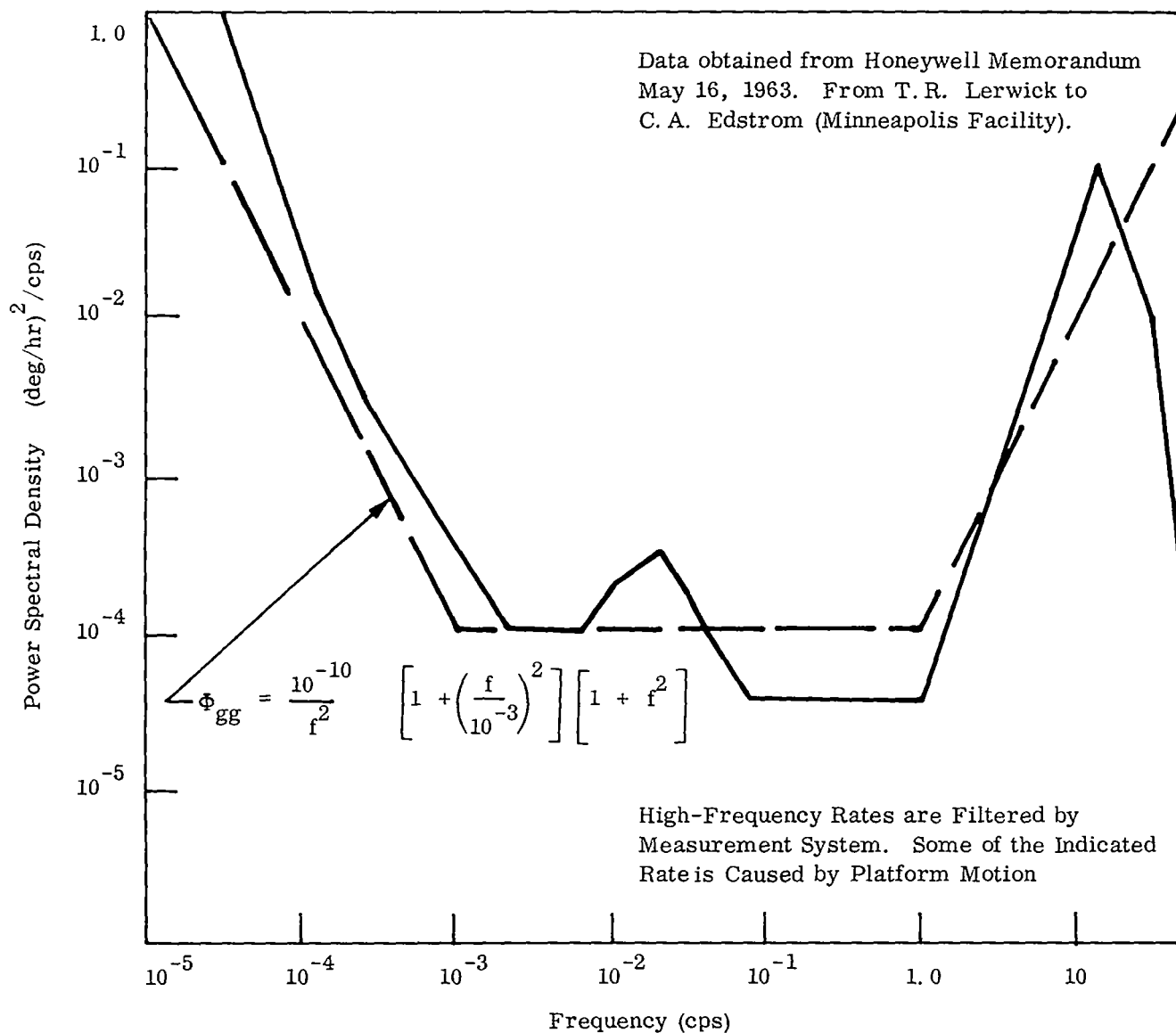
Figure 2-5. Estimated Power Spectral Density of Gyroscope Drift Rate
Honeywell Gyro Model #CG159 C1, Unit #5

31
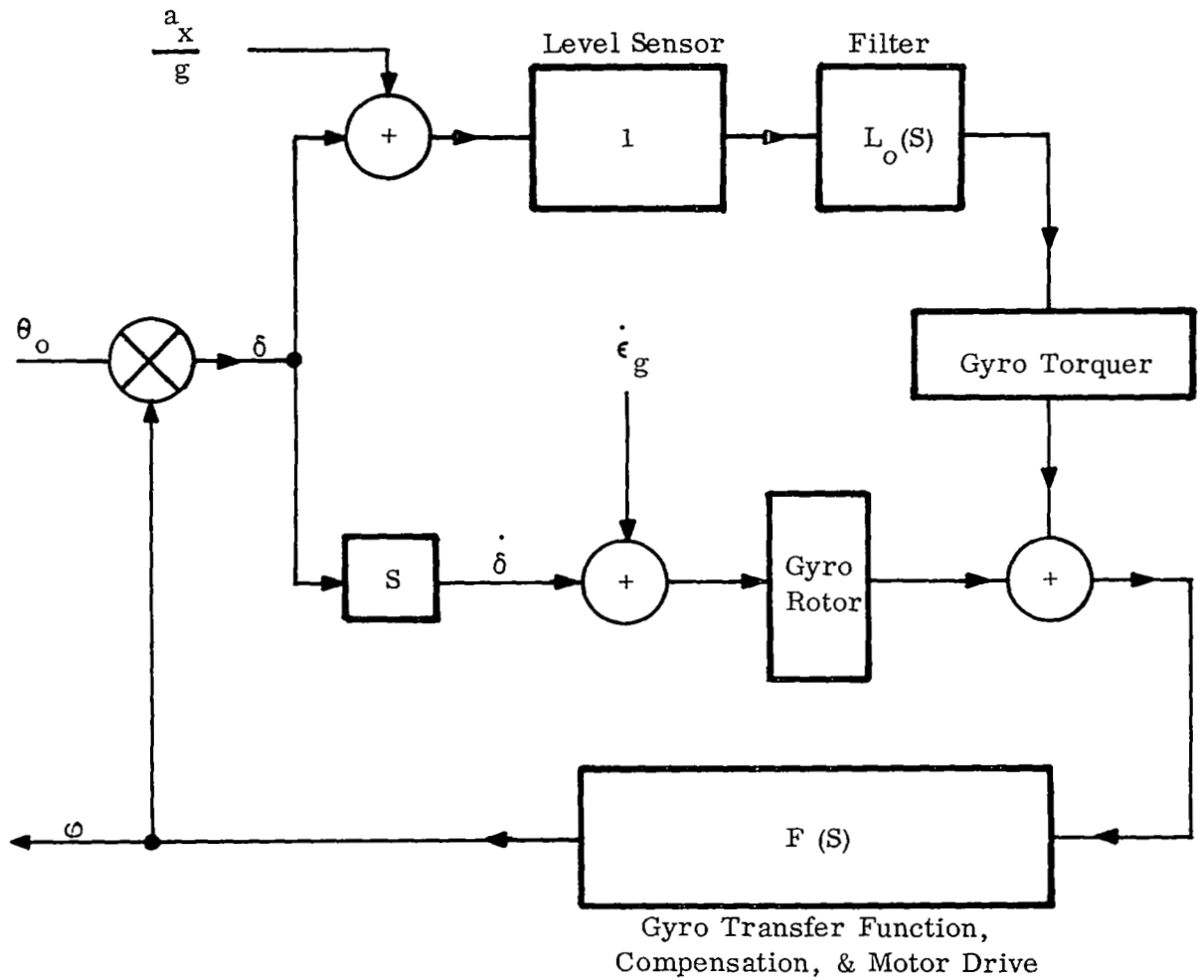
Figure 2-6. Schematic of Servomechanism Levelling System Using Gyroscope
and Level Sensor for Control

The lower limit of 10^{-5} cps is defined by the longest period that can be observed in a 28 hour test period and the upper limit of 0.01 cps represents the shortest period that is usually considered in such tests.

For the system indicated in Figure 2-6 the platform error angle is given by:

$$\delta(s) = \frac{\theta_o(s) + G(s)M(s)L_o(s)\dfrac{a_x(s)}{g} + G(s)M(s)\dot{\varepsilon}_g(s)}{1 + G(s)M(s)(L_o(s) + S)}$$

(2-22)

The substitutions:

$$L_1(s) = L_o/s, \quad \varepsilon_g = \int_0^t \dot{\varepsilon}_g(r)\, dr$$

$$F(s) = s\, G(s)M(s) \qquad\qquad (2\text{-}23)$$

permit Equation (2-13) to be rewritten as:

$$\delta(s) = \frac{\theta_o(s)}{F(s)\left[\dfrac{1}{F(s)} + (1+L_1(s))\right]} + \frac{L_1(s)\dfrac{a_x(s)}{g} + \varepsilon_g(s)}{\left[\dfrac{1}{F(s)} + (1 + L_1(s))\right]}$$

(2-24)

Figure 2-7 shows the power spectral densities of the rotational ground motions, the horizontal translational vibrations and the integral of the gyroscope drift rate power spectrum for an instrument having a nominal drift
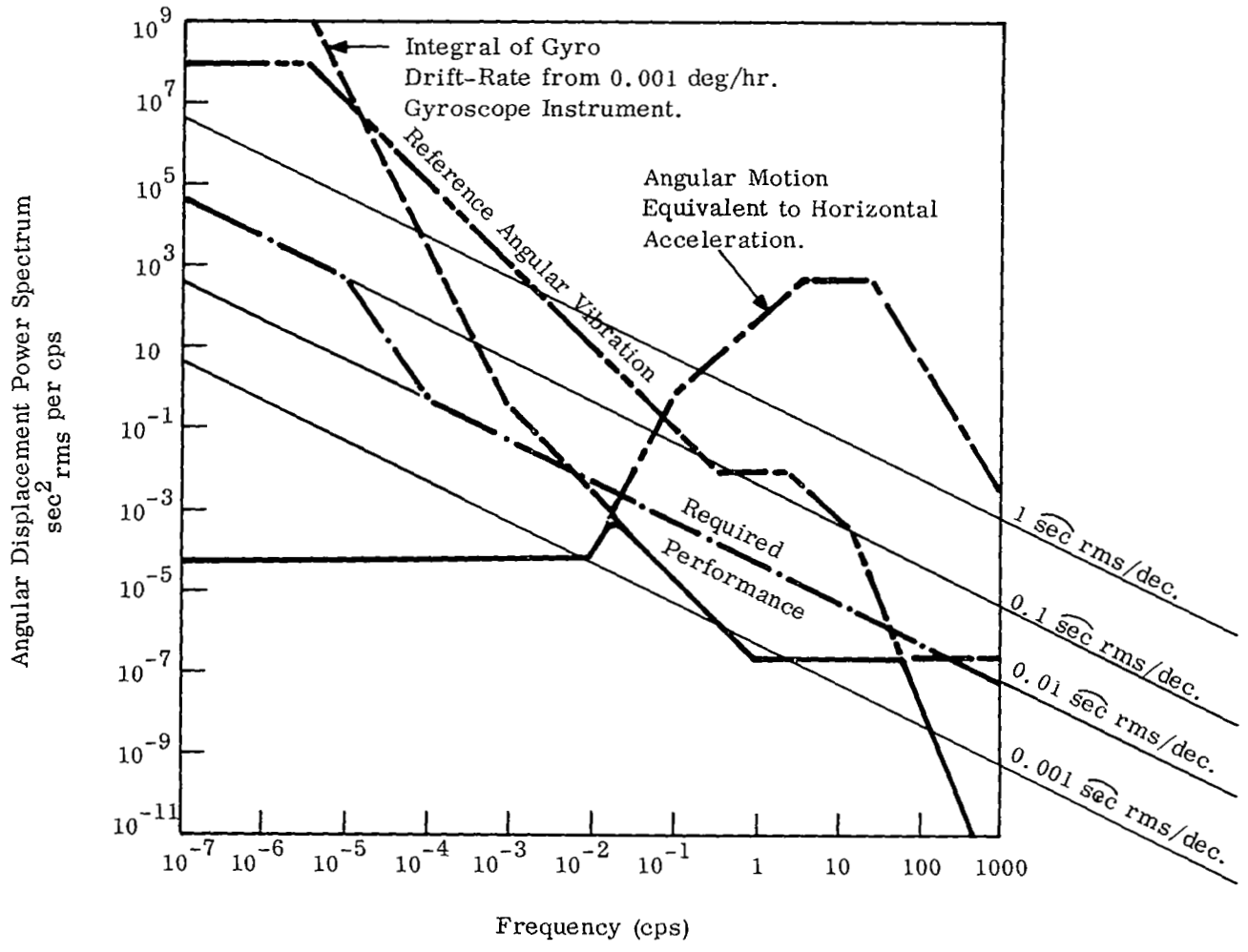
Figure 2-7. Best Conceivable Performance of Servo-Levelled Platform Using
Gyroscope and Level Sensor for Control (Employing No Passive Isolation and
without Regard for Physical Realizability)

rate of 0.001°/hr. It is seen that at frequencies below 0.012 cps the error that would be introduced by having the system follow the level signal exactly is several orders of magnitude less than the ground angular motion, θ_o. Similarly at frequencies between 0.012 cps and about 90 cps the error that would result from following the gyroscope instrument exactly is considerably smaller than the ground motion spectrum. Therefore, in a well designed system $F(s)$ would be quite large compared to 1 at frequencies below 1 cps. Similarly since the accelerations above 0.1 cps are quite large compared to the ground angular motions and the gyroscope drift angle spectrum $L_1(s)$ will be quite small compared to 1 at frequencies above 1 cps. These simplifications permit Equation (2-24) to be rewritten as:

For frequencies below 1 cps:

$$\delta(s) = \frac{L_1(s) \frac{a_x}{g}(s)}{1 + L_1(s)} + \frac{\epsilon_g(s)}{1 + L_1(s)} \qquad (2\text{-}25a)$$

and for frequencies above 1 cps:

$$\delta(s) = \frac{\theta_o(s)}{1 + F(s)} + \frac{F(s)\,\epsilon_g(s)}{1 + F(s)} \qquad (2\text{-}25b)$$

35

The substitutions:

$$L_2(s) = \frac{L_1(s)}{1 + L_1(s)}$$

$$L_3(s) = \frac{F(s)}{1 + F(s)}$$

(2-26a,b)

permit the error angle to be rewritten as:

For frequencies below 1 cps:

$$\delta(s) = L_2(s) \frac{a_x(s)}{g} + (1-L_2(s)) \varepsilon_g(s)$$

(2-27a)

and for frequencies above 1 cps:

$$\delta(s) = L_3(s) \varepsilon_g(s) + (1-L_3(s)) \theta_o(s)$$

(2-27b)

The form of these two equations is identical to Equation (2-15) of Section 2.2. The best conceivable performance of this system is obtained from the un-realizable optimum filter calculation given in Section 2.2. The power spectral density of the resulting error angle is plotted in Figure 2-7. As shown in Figure 2-8 the rms error angle of the best physically realizable system is within a factor of 2 of the result given in Figure 2-7.

36
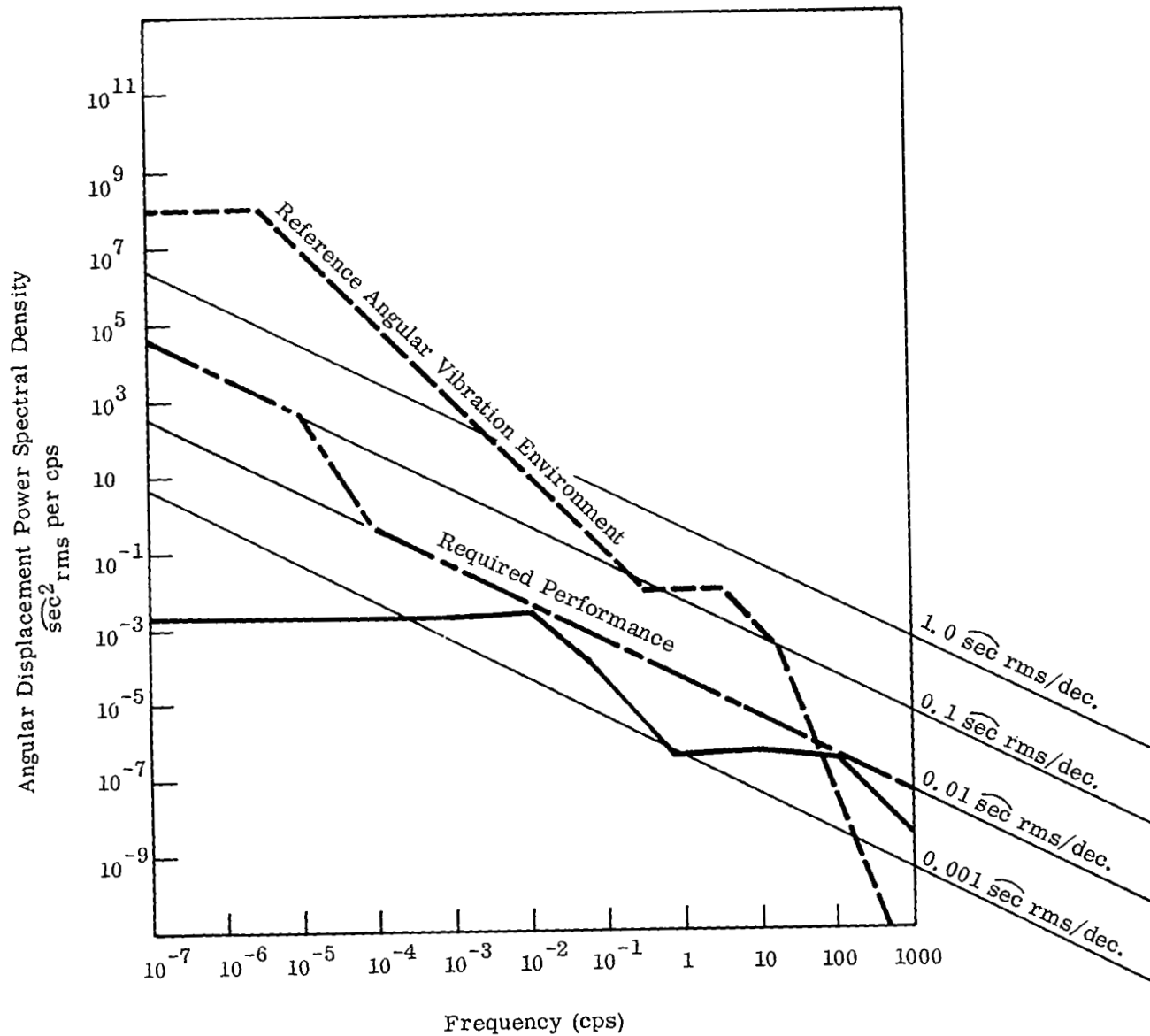
Figure 2-8. Best Possible Performance of Servo-Levelled Platform Using Gyroscope and Level Sensor for Control (No Passive Isolation)

37

The form of Equations (2-27) is amenable to the Bode and Shannon approach for the optimum linear (Wiener) filter. The optimum frequency characteristics are obtained in Appendix A as:

$$L_o(s) = \frac{0.0735 \left[1 + \frac{0.00575}{S}\right]}{(1 + 8.6S + 33.3S^2)} \qquad (2\text{-}28a)$$

$$L_3(s) = \frac{\left(1 + 1.28 \left(\frac{S}{556}\right)\right)}{(1 + 1.41 \, S/556 + S^2/(556)^2)} \qquad (2\text{-}28b)$$

or in terms of frequency as:

$$L_o'(f) = \frac{0.0735 \left[1 - j \, \frac{9.15 \times 10^{-4}}{f}\right]}{\left(1 - \frac{f^2}{(.0275)^2}\right) + 1.5j \, \frac{f}{.0275}} \qquad (2\text{-}29a)$$

$$L_3'(f) = \frac{1 + 1.28j \left(\frac{f}{88.5}\right)}{\left(1 - \frac{f^2}{(88.5)^2}\right) + 1.41 \, j \, \frac{f}{88.5}} \qquad (2\text{-}29b)$$

The performance of this optimum servomechanism operating in the reference environment is shown in Figure 2-8. This system meets the basic performance requirements given in Section I with the exception that it amplifies the input angular vibrations at high frequencies. However, the required system natural frequency of 88.5 cps demands that the structural natural frequencies

of the platform be well above 100 cps. This represents
an unreasonable requirement for a platform supporting a
5,000 lb. load contained in a 5 ft by 5 ft by 5 ft volume.

2.4 Active Vibration Isolation Systems

Active vibration isolation systems improve the
performance of conventional spring-mass-dashpot vibra-
tion isolators by the application of forces and/or
torques to the mass that are a function of the un-
desired motion of the mass. Such a system is shown
schematically in Figure 2-9. The error angle of this
platform is given by:

$$\delta(s) = \frac{\left(1 + 2\frac{\beta S}{\omega_n}\right)\Theta_o(s) + \frac{T(s)}{K} + \frac{B(s)n(s)}{K}}{\frac{B(s)}{K} + \left(1 + 2\frac{\beta S}{\omega_n} + s^2/\omega_n^2\right)} \qquad (2\text{-}30)$$

If the operation $B(s)$ is equivalent to taking the second
derivative of δ with respect to time (feedback torque
proportional to acceleration) the result is an increase
in the apparent inertia of the platform and a correspond-
ing decrease in the system natural frequency. If the
feedback torque is proportional to the angular rate of
the platform, the effect is the same as damping relative
to inertial space and if the feedback torque is proportion-
al to the angular displacement, an effective stiffness
relative to inertial space is introduced. The most common
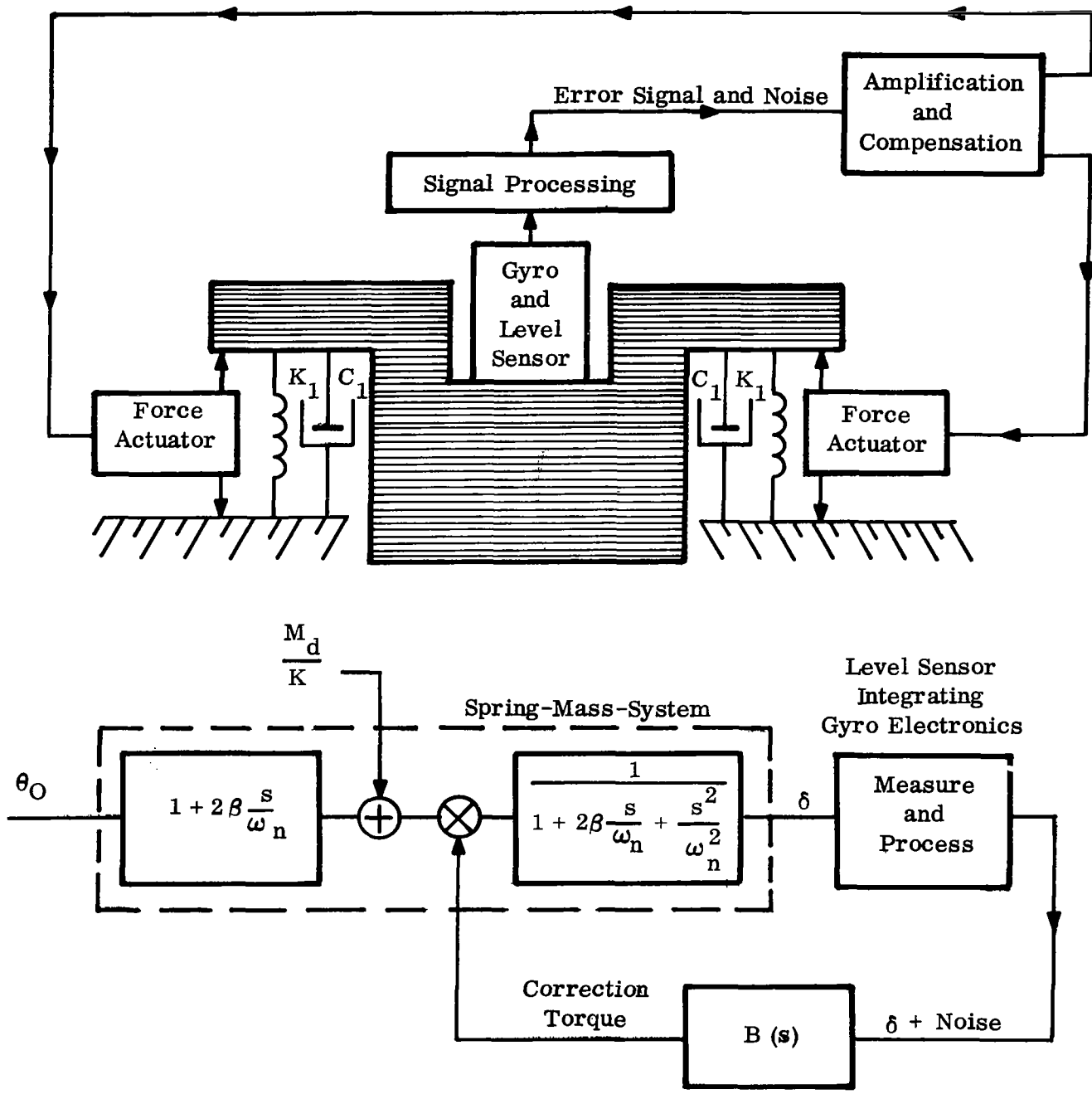
Figure 2-9. Schematic of Active Isolation System Using Gyro
and Level Sensor for Control

form of active isolation system makes use of a feedback torque which is proportional to the integral of the relative displacement between the mass and the system foundation. This permits the design of very low natural frequency (about 1 cps) vibration isolators that do not require large static deflections and are capable of resisting disturbance forces and torques at frequencies below the system natural frequency. This type of system is discussed in more detail in the following sections. To provide isolation of very low frequency angular displacements of the base, the error angle δ must be measured relative to the average position of the gravity vector as in the system of Figure 2-9. The substitutions:

$$B(s) = \frac{B(s)}{K \left(1 + 2 \frac{\beta s}{\omega_n} + s^2/\omega_n^2\right)} \tag{2-31}$$

$$e(s) = \frac{\left(1 + \frac{2\beta s}{\omega_n}\right) \Theta_o(s) + \frac{T(s)}{K}}{\left(1 + \frac{2\beta s}{\omega_n} + s^2/\omega_n^2\right)} \tag{2-32}$$

permit Equation (2-23) (the performance equation of the system of Figure 2-9) to be written as:

$$\delta(s) = \frac{e(s)}{B_1(s) + 1} + \frac{B_1(s)n(s)}{B_1(s) + 1} \tag{2-33}$$

41

If the error signal for control of the system is provided by the gyroscope and level sensor combination discussed in the section on servomechanism systems, the noise may be represented as:

$$n(s) = L_2(s) \frac{a_x(s)}{g} + (1 - L_2(s)) \epsilon_g(s) \tag{2-34}$$

The power spectral densities of the quantities e(t) and n(t) for a 1 cps spring mass system with a damping ratio of 0.5 and a 20,000 lb-ft-sec^2 moment of inertia are plotted in Figure 2-10 as functions of frequency. The torque disturbances at low frequency are taken as 250 lb-ft rms per decade for frequencies below 0.001 cps, and the disturbance pressure of 10^{-5} psi rms per decade is assumed to produce a disturbance torque of 0.09 lb-ft rms per decade. The performance obtainable from the second order system characteristics:

$$\frac{B_1(s)}{1 + B_1(s)} = \frac{1}{1 + s/\omega_a + s^2/\omega_a^2} \tag{2-35}$$

$$\frac{1}{1 + B_1(s)} = \frac{s/\omega_a + s^2/\omega_a^2}{1 + s/\omega_a + s^2/\omega_a^2} \tag{2-36}$$

42
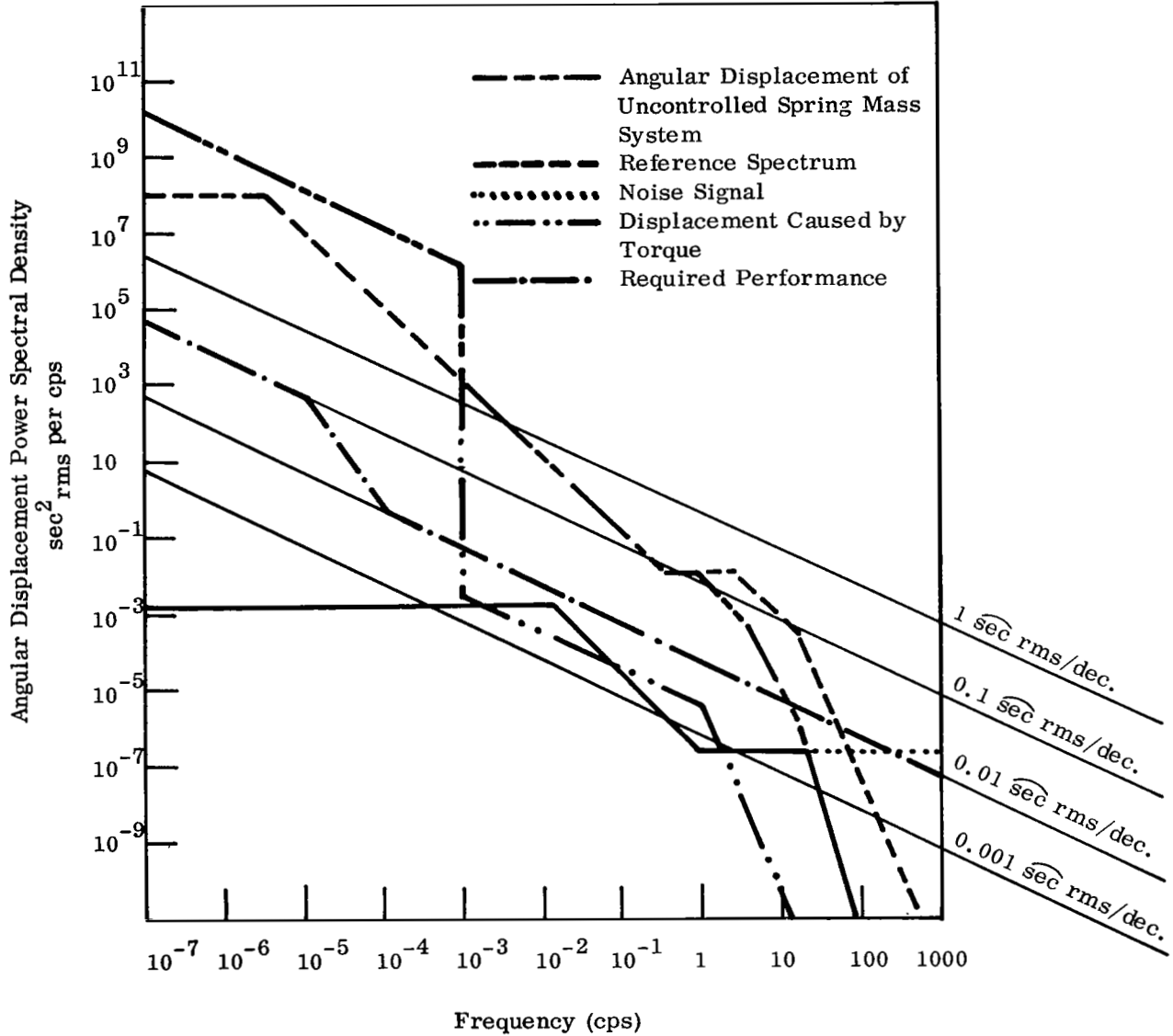
Figure 2-10. Best Conceivable Performance of Active Vibration Isolation System
Using Gyroscope and Level Sensor for Control

is plotted in Figure 2-11 for $\omega_a = 2\Pi f_a$, $f_a = 25$ cps.
This platform meets all of the performance requirements
given in Section I.

The characteristics of the feedback networks required
to provide this performance are given by:

$$B(s) = \frac{K \omega_a \left(1 + \frac{s}{\omega_n} + \frac{s^2}{\omega_n^2}\right)}{s \left(1 + \frac{s}{\omega_a}\right)} \qquad (2-37)$$

At frequencies below the spring mass natural frequency,
$f_n = \omega_n/2\Pi$, of the suspension the feedback torque is
basically proportional to the integral of the error angle.
At frequencies between the natural frequency and the sys-
tem cutoff frequency, $f_a = \omega_a/2\Pi$, the feedback torque is
proportional to the rate of the error angle and provides
damping relative to inertial space.

The drive motor for this system must be capable of
resisting torques of 250 lb-ft rms per decade for frequen-
cies between 10^{-7} cps and 0.001 cps which implies a torque
capacity of the order of 500 lb-ft. If there is a noise
input to the system other than those considered above that
causes the motor to produce a torque of 0.25 lb-ft.
(0.05% of the rated torque) at 2 cps the system will be
forced into oscillation at an amplitude of:

44
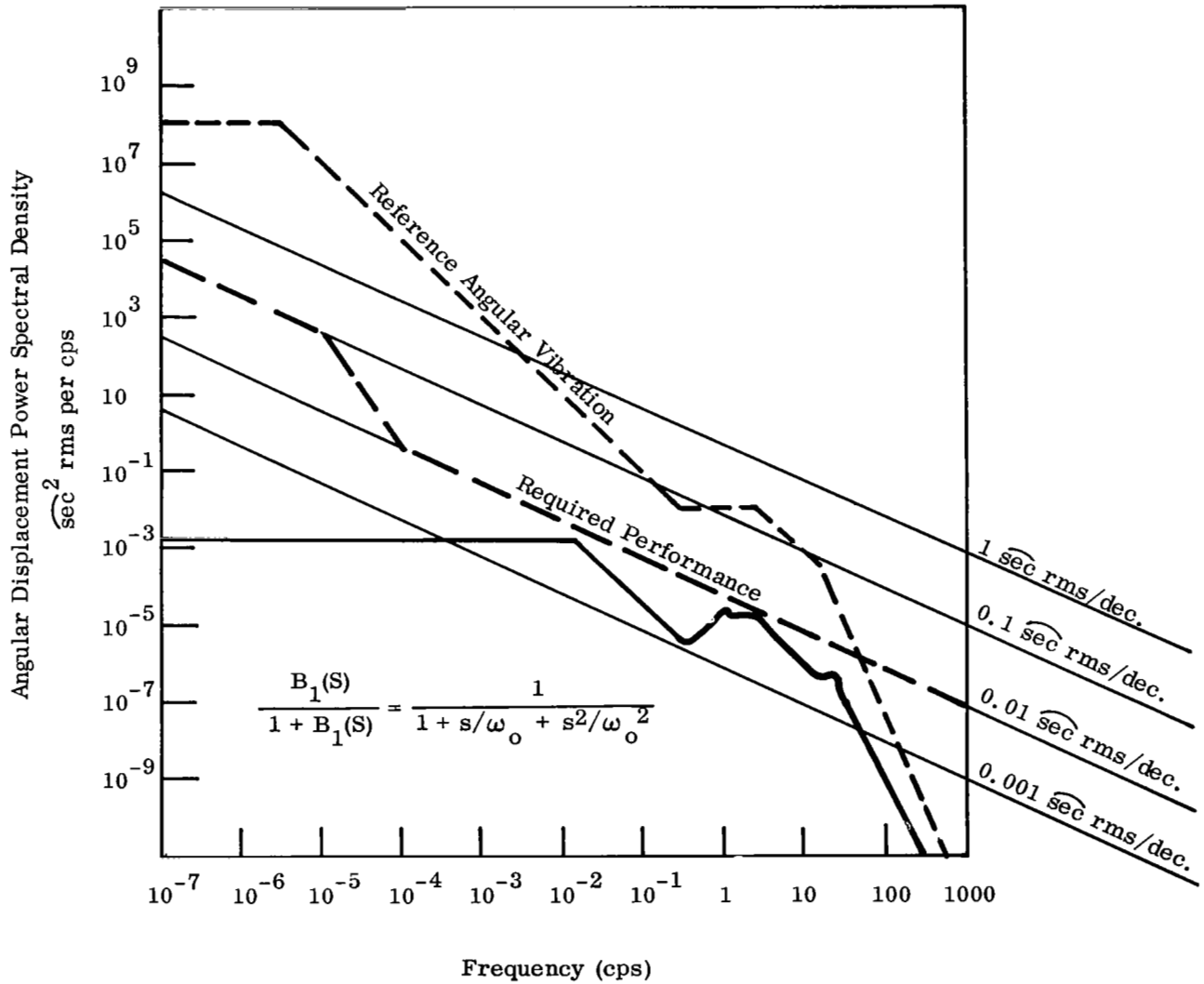
Figure 2-11. Performance of Active Isolation System Using Gyroscope and Level Sensor for Control

$$\delta_n = \frac{M_n}{I\,\omega^2} \times 2.06 \times 10^5 \; \widehat{\sec} = \frac{.25 \times 2.06 \times 10^5}{2 \times 10^4 \, (4\pi)^2} = 0.06 \; \widehat{\sec}$$

The strong lead compensation required by Equation (2-29) tends to amplify noise inputs at frequencies above the suspension natural frequency. This would make a high frequency noise input quite likely. These considerations would require considerable care in the design of this system. Although a good deal of effort would be required in the design and fabrication of a system having the characteristics given above the system is basically feasible and represents a design alternative. However, the use of the two stage active vibration isolation system described in the following paragraphs permits a simpler design that can take advantage of existing hardware and produce identical performance characteristics.

2.5 Two Stage Active Vibration Isolation System

A system meeting the requirements given in Section I can be built using the two stage active vibration isolation system represented by Figure 2-12. The first stage consists of a conventional active vibration isolator of the type built by Barry-Wright Corporation of Watertown, Mass. This system makes use of feedback forces which are proportional to the integral of the relative displacement between the suspended mass and the ground to provide resistance to low

46

8 ft

Test Table
(5000 lb.)

Laboratory Floor

Laboratory Floor

Steel frame passive
system inertia
20,000 lb.-ft.-sec.^{2}
35,000 lb.

3 ft

Active System Pivot

Concrete Base

Active System Drive

Air Spring Barry Servo Level
1 cps Natural Frequency
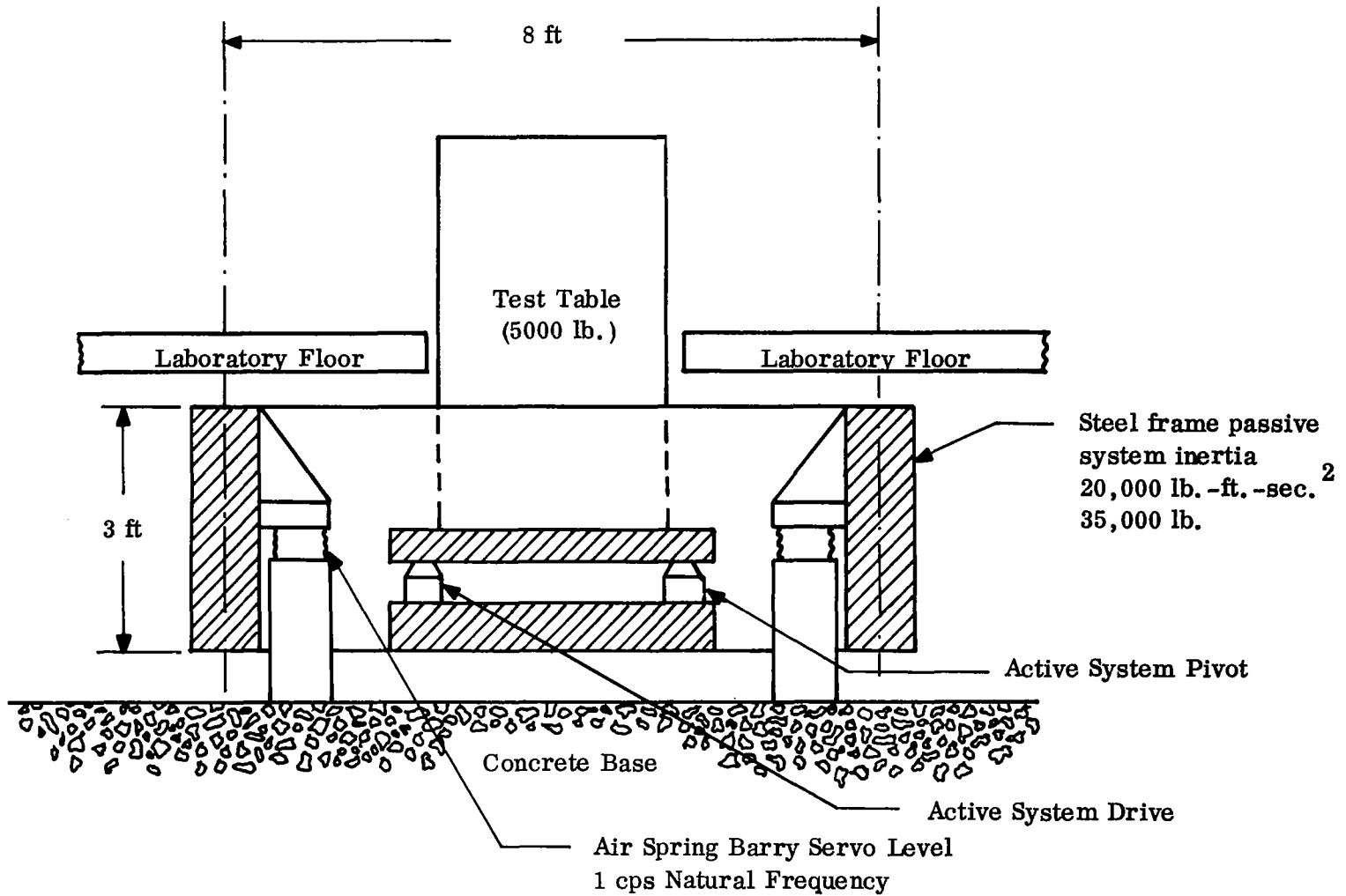
Figure 2-12. Active (Servo-Controlled) Base Motion Isolation System Mounted on
Low-Frequency Air Spring Isolation System

frequency disturbance torques and forces and still provide the isolation characteristics of a low natural frequency spring mass system. The response of this type of system to angular displacements and disturbance torques is given by:

$$\theta_1(s) = \frac{\left(\frac{\alpha\omega_\theta}{s} + 1 + \frac{2\beta s}{\omega_\theta}\right)\theta_0(s) + \frac{Md(s)}{K}}{\left(\frac{\alpha\omega_\theta}{s} + 1 + \frac{2\beta s}{\omega_\theta} + s^2/\omega_\theta^2\right)} \tag{2-38}$$

The requirement for stability of this system is:

$\alpha < 2\beta$

The spectral density of the response θ_1 of this first stage to the reference vibration spectrum and the specified torques of 250 lb-ft rms per decade for frequencies less than 0.001 cps and 0.09 lb-ft rms per decade for frequencies above 0.001 cps is plotted in Figure 2-13 for a system having a 20,000 lb-ft-sec^2 moment of inertia, a 1 cps natural frequency, a damping ratio of 0.5 and a feedback parameter α of 0.1. It is seen that this system has the effect of filtering the angular vibrations at frequencies above 1.5 cps with a negligible increase in the low frequency angular displacements. The second stage of the isolation system is a servomechanism system identical to that discussed in Section 2.3. However, the high frequency angular vibration environment is reduced sufficiently to permit the

48
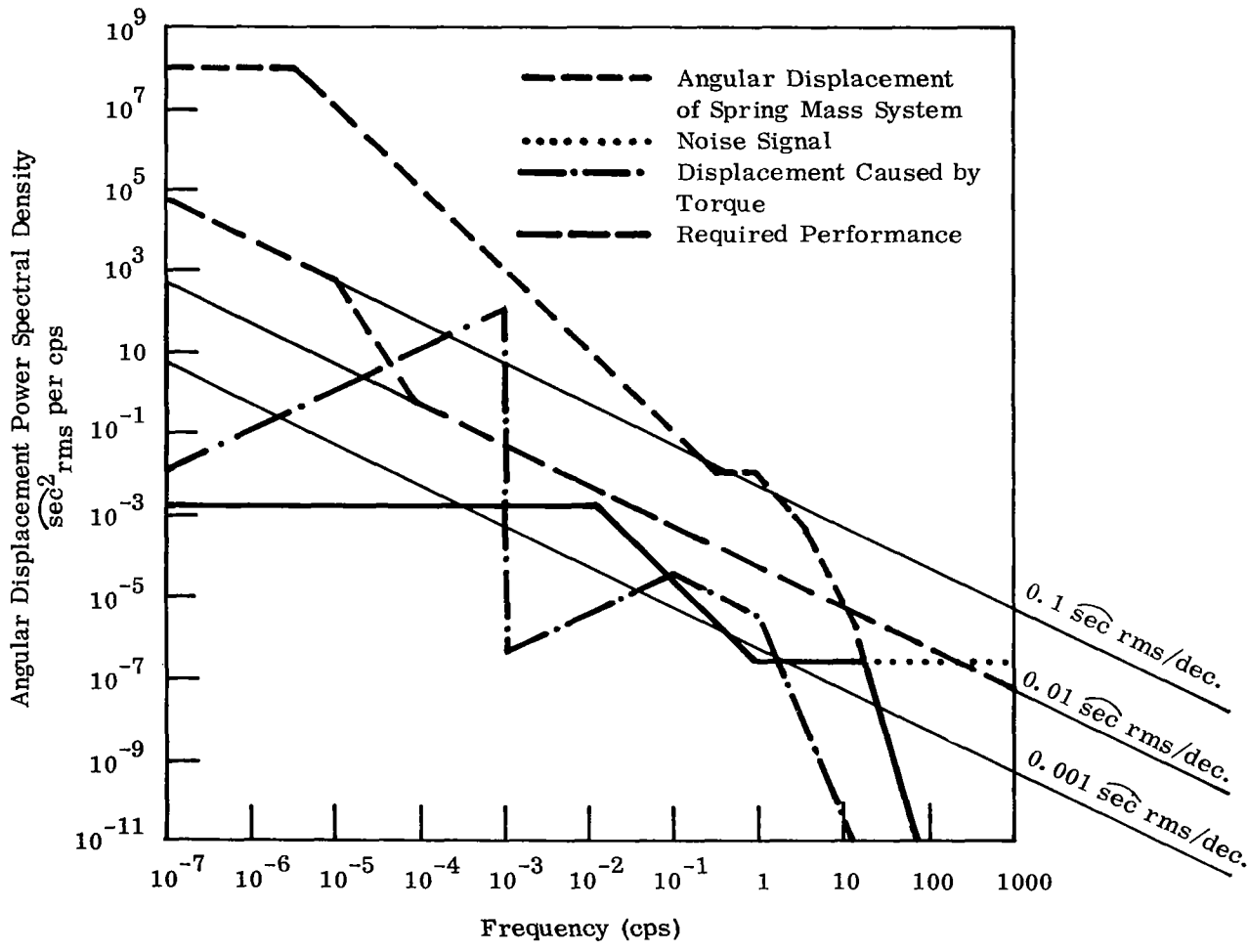
Figure 2-13. Best Conceivable Performance of Two-Stage Active Isolation Using Gyroscope and Level Sensor for Control and 1-cps Passive Isolation

use of a 25 cps servomechanism cut off frequency. The
ultimate performance of this system is identical to that
shown in Figure 2-10 for the active vibration isolation
system. This is seen by comparing the plots of the
spectral densities of the noise inputs and the angular
motion inputs to this servomechanism as shown in
Figure 2-13 with those given in Figure 2-7 and Figure
2-10.

The optimum frequency characteristic for this
system is calculated in Appendix A as:

$$L(s) = \frac{1 + \frac{1.7s}{108} + \frac{s^2}{(108)^2}}{\left(1 + \frac{s}{134}\right)\left(1 + \frac{1.11s}{120} + \frac{s^2}{(120)^2}\right)} \qquad (2\text{-}39)$$

The performance achievable with this frequency
characteristic is shown in Figure 2-14. It is seen
that the system can meet the specification given in
Section I for all frequencies below 100 cps. At
frequencies above 100 cps the response to gyroscope
noise is such that the ratio of the platform motion
to the existing ground motion is greater than 1.
Should this represent a serious difficulty, better
high frequency performance can be obtained by com-
promising the performance at lower frequencies. For
example, the characteristic:

50
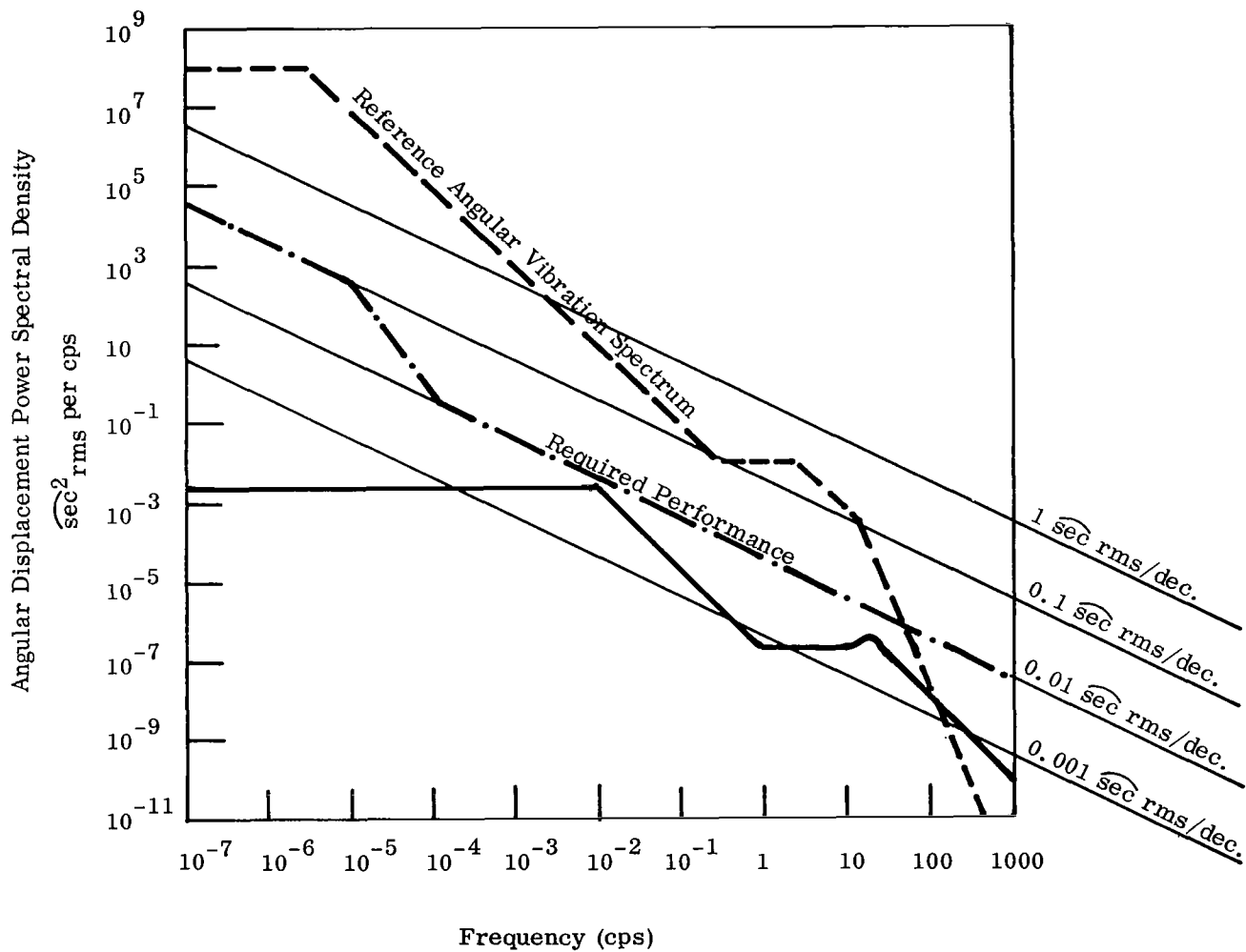
Figure 2-14. Performance Achievable with Two Stage Active Isolation System
Using Gyro and Level Sensor for Control and 1-cps Passive Isolation System

$$L(s) = \frac{1}{1 + s/\omega_a + s^2/\omega_a^2}$$

considered in Section 2.4 will meet all the require-
ments to a calculated 1000 cps.

The final parameters of the frequency characteristics
of an isolation system would be tailored to the environ-
ment of that particular location and the particular instru-
ments to be used in the system.

2.6 Stability of Two Stage Active Vibration Isolation System

The calculations given above assume no interaction
between the servomechanism system and the passive isola-
tion system. In order to maintain the platform at level
the servomechanism drive must exert torques on the plat-
form which must be reacted by the passive isolation sys-
tem as indicated in Figure 2-15. The torque exerted on
the inertia mass of the passive system is:

$$T = - I_a \ddot{\delta} \qquad (2-40)$$

which is taken by the stiffness, damping and inertia of
the passive system:

$$T = K (\theta-\theta_0) + c (\dot{\theta}-\dot{\theta}_0) + I_0 \ddot{\theta} \qquad (2-41)$$

for zero inputs and with the substitutions indicated in

52
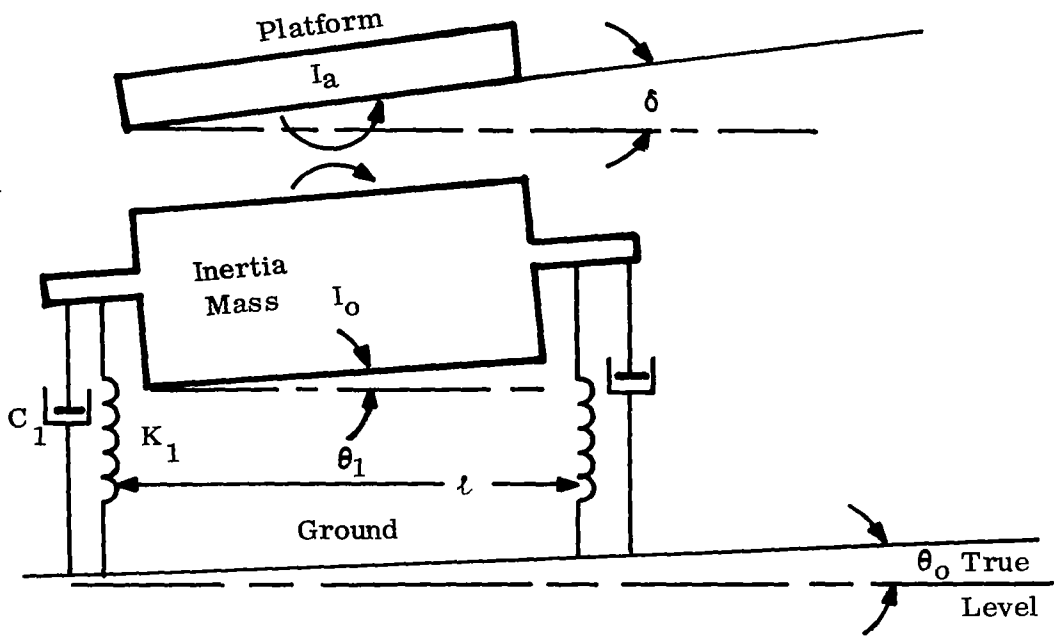
$$K = \frac{K_1 \ell^2}{2} = \text{Rotational Stiffness}$$

$$C = \frac{C_1 \ell^2}{2} = \text{Rotational Damping}$$

$$\omega_n{}^2 = \sqrt{\frac{K}{I_o}} \qquad r = \frac{I_a}{I_o}$$

$$\beta_2 = \frac{1}{2} \frac{C}{I_o \omega_n}$$

Figure 2-15. Interaction between Passive Isolation System and Servomechanism System

53

Figure 2-15, the response of the system is governed by:

$$0 = (\omega_n^2 + 2\beta_2 s\, \omega_n + s^2)\, \theta + r\, s^2\, \delta \qquad (2\text{-}42)$$

Taking the second order system characteristic of Equation (2-27) the error angle is related to the displacement of the inertia mass by:

$$\frac{\delta(s)}{\theta(s)} = \frac{\dfrac{2\beta_1 s}{\omega_a} + \dfrac{s^2}{\omega_a^2}}{1 + 2\,\dfrac{\beta_1 s}{\omega_a} + \dfrac{s^2}{\omega_a^2}} \qquad (2\text{-}43)$$

so that the system transient response is governed by:

$$0 = \left[\left(1 + \frac{2\beta_2 s}{\omega_n} + \frac{s^2}{\omega_n^2}\right) + \frac{\dfrac{r\, s^2}{\omega_n^2}\left(\dfrac{2\beta_1 s}{\omega_a} + \dfrac{s^2}{\omega_a^2}\right)}{1 + \dfrac{2\beta_1 s}{\omega_a} + \dfrac{s^2}{\omega_a^2}}\right]\theta$$

$$(2\text{-}44)$$

The criteria for stability are obtained from the Routh-Hurwitz conditions (e.g. see Reference 11) as:

$$\frac{\omega_a}{\omega_n} + \frac{\omega_n}{\omega_a} + 4\beta_1\beta_2 > \frac{(1 + r)(\beta_1\dfrac{\omega_n}{\omega_a} + \beta_2)}{(1 + r)\,\beta_1 + \beta_2\dfrac{\omega_n}{\omega_a}} \qquad (2\text{-}45)$$

54

$$\left(1 + \frac{\omega_n^2}{\omega_a^2} + \frac{4\beta_1\beta_2\omega_n}{\omega_a}\right) > \frac{(1 + r)\left(\beta_2 + \beta_1\frac{\omega_n}{\omega_a}\right)^2 \left(\beta_2\frac{\omega_n}{\omega_a} + \beta_1\left(1 + r\right)\right)}{\left(\beta_1 + \beta_2\frac{\omega_a}{\omega_n}\right)} \tag{2-46}$$

both of these criterion are easily satisfied for:

$$\frac{\omega_a}{\omega_n} \geq 10; \quad r \leq 0.1; \quad \beta_1 \simeq \beta_2 \simeq 0.5$$

so that the total system is stable. The large ratio of
the inertia of the passive system to the servomechanism
inertia and the large ratio of the servomechanism natural
frequency to the passive natural frequency thus justifies
the assumption that the passive system response may be
treated independently of the servomechanism dynamics
for the parameters of interest.

2.7 Two Axis Crosscoupling

The above discussions have been restricted to systems
which maintain level about a single axis. In order to
maintain a plane at level, it is necessary to control
the platform about two non parallel axes. If the two
axes are orthogonal as indicated in Figure 2-16 and the
system is insensitive to load variations there is no
coupling between axes and the analyses given above may
be applied directly. However, if a rotational accelera-
tion exists on one axis inertia coupling produces a
torque that acts about the second axis which tends to

55
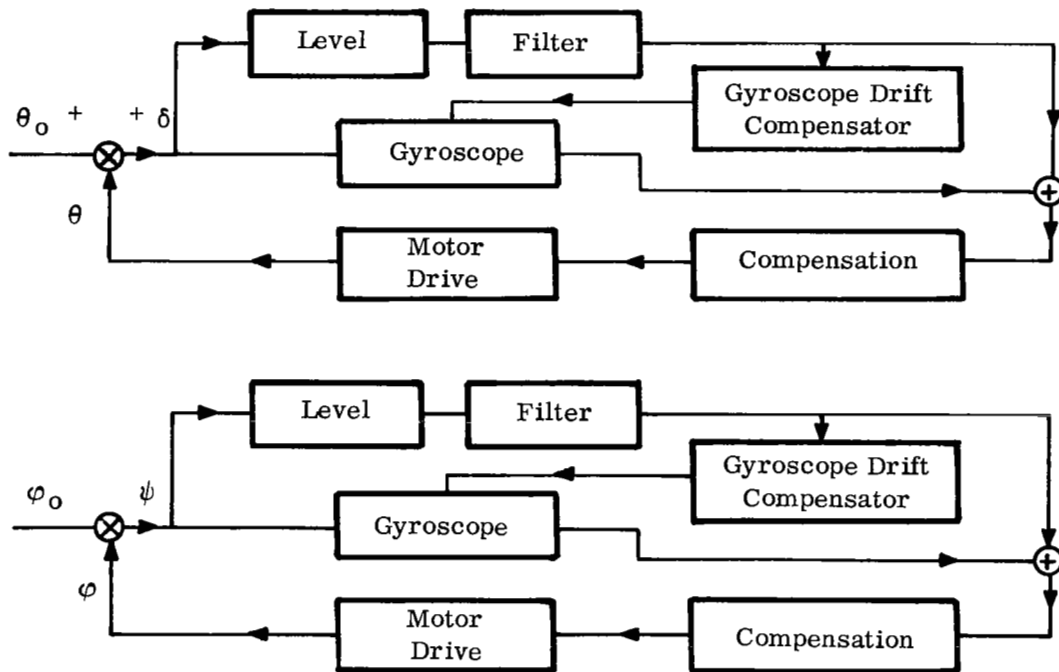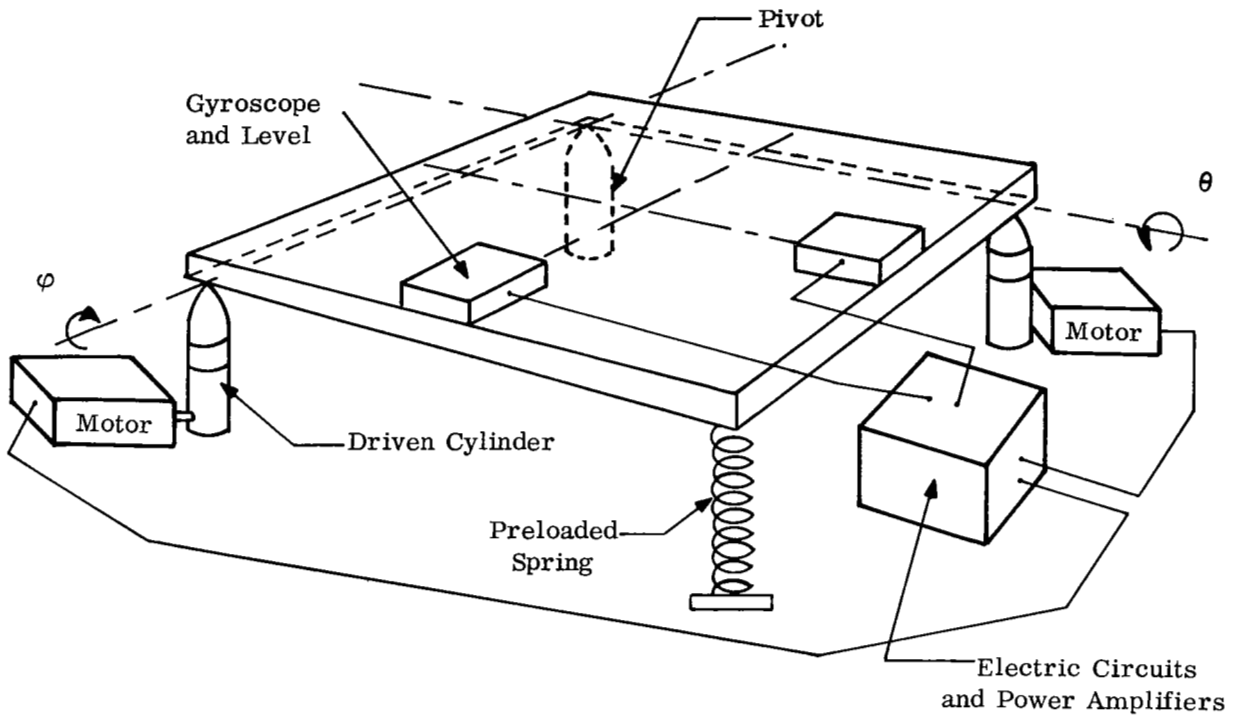
Figure 2-16. Orthogonal Drives for Servomechanism System

couple the two axes in practical applications. The
redundancy of the support can also introduce difficulties
in the assembly and initial levelling of the system.
The more conventional approach would mount the system
on three points spaced on an equilateral triangle as
indicated in Figure 2-17. However, if the platform is
rotated through an angle θ about the axis 1 by moving
the jack 1 thru a distance of y_1 there is a motion about
the axis 2 of $\Phi = \dfrac{-\theta}{2}$. If this coupling effect was
ignored the servomechanism system would demand:

$$y_1(s) = F_1(s)\ \delta(s) \qquad\qquad\qquad (2\text{-}47a)$$

$$y_2(s) = F_1(s)\ \Psi(s) \qquad\qquad\qquad (2\text{-}47b)$$

since

$$L\theta = y_1 - \frac{y_2}{2} \qquad\qquad\qquad (2\text{-}48a)$$

$$L\Phi = y_2 - \frac{y_1}{2} \qquad\qquad\qquad (2\text{-}48b)$$

and $\quad \theta = \theta_o - \delta \qquad\qquad\qquad\qquad\quad (2\text{-}49a)$

$$\Phi = \Phi_o - \Psi \qquad\qquad\qquad\qquad (2\text{-}49b)$$

resulting in the system performance equations:

57

$$\theta_1 = \frac{y_1 - y_a}{\ell}, \qquad \varphi_1 = \frac{y_2 - y_b}{\ell}$$

$$y_a = \frac{y_2 + y_3}{2}, \qquad y_b = \frac{y_1 + y_3}{2}, \qquad y_3 = 0$$

$$\ell\theta_1 = y_1 - \frac{y_2}{2}, \qquad \ell\varphi_1 = y_2 - \frac{y_1}{2}$$

View along Axis 2

View along Axis 1
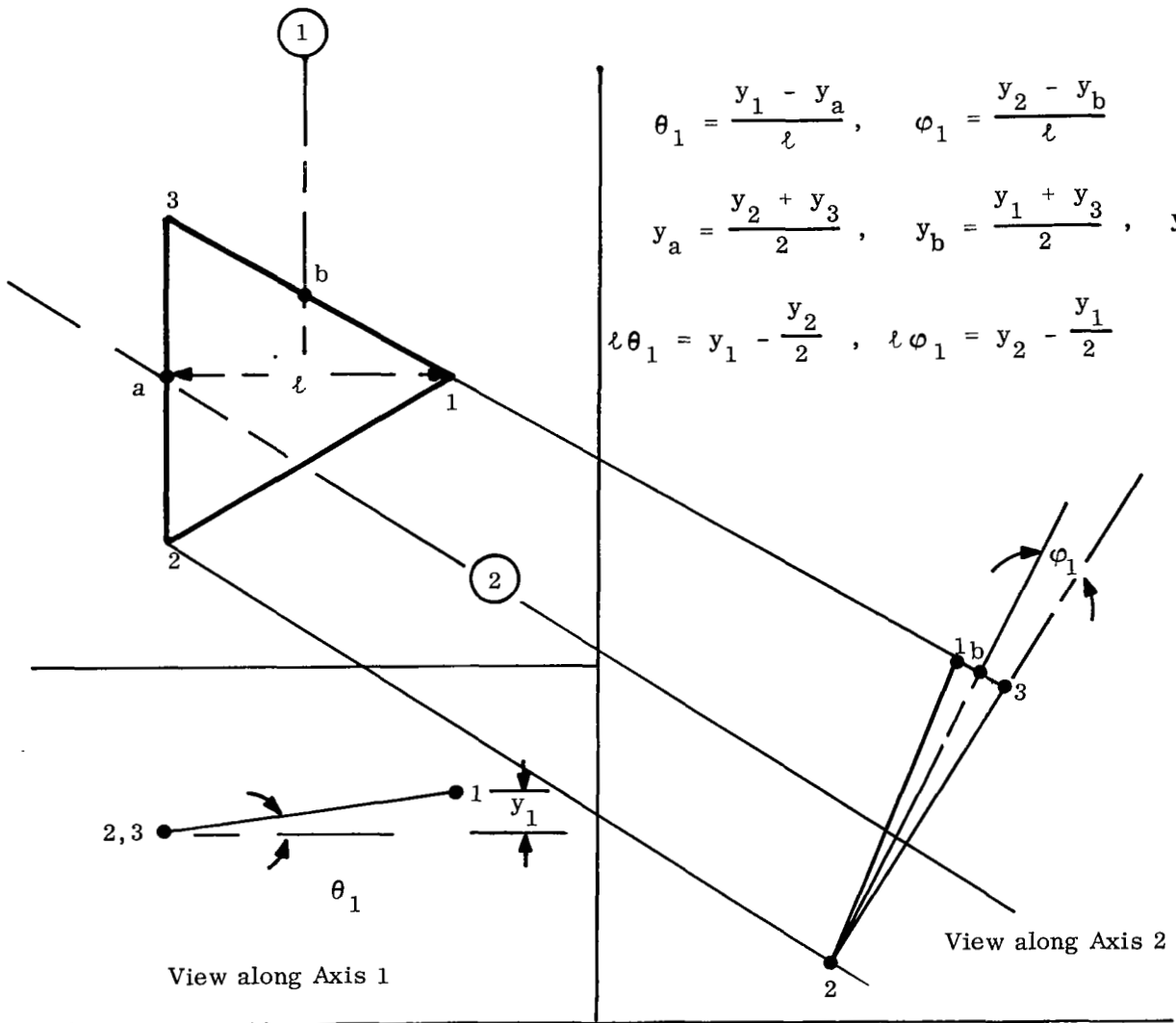
Figure 2-17. Coupling of Three Point Levelling System

$$\Theta_o(s) = (1 + F(s)) \, \delta(s) - \frac{F(s)}{2} \, \Psi(s) \tag{2-50a}$$

$$\Phi_o(s) = (1 + F(s)) \, \Psi(s) - \frac{F(s)}{2} \, \delta(s) \tag{2-50b}$$

The system errors are thus:

$$\delta(s) = \frac{4}{3} \, \frac{(1 + F(s)) \, \Theta_o(s) - \frac{F(s)}{2} \, \Phi_o(s)}{(2 + F(s)) \, (\frac{2}{3} + F(s))} \tag{2-51}$$

For a single axis motion about the 1 axis $\Phi_o = \frac{1}{2} \Theta_o$ and

$$\delta(s) = \frac{5}{3} \, \frac{(\frac{4}{5} + F(s)) \, \Theta_o(s)}{(2 + F(s)) (\frac{2}{3} + F(s))} \tag{2-52}$$

The frequency response of the error angle for a simple integration $F(s) = A/S$ is shown in Figure 2-18. It is seen that the effects of the crosscoupling are to reduce the effective gain at low frequencies to 60% of the low frequency gain of the single axis system and to extend the bandwidth of the system. This increased bandwidth coupled with resonance effects can eliminate the stability of the system. Improvement of the low frequency characteristic would require a still larger gain and a corresponding increase in the bandpass of the required
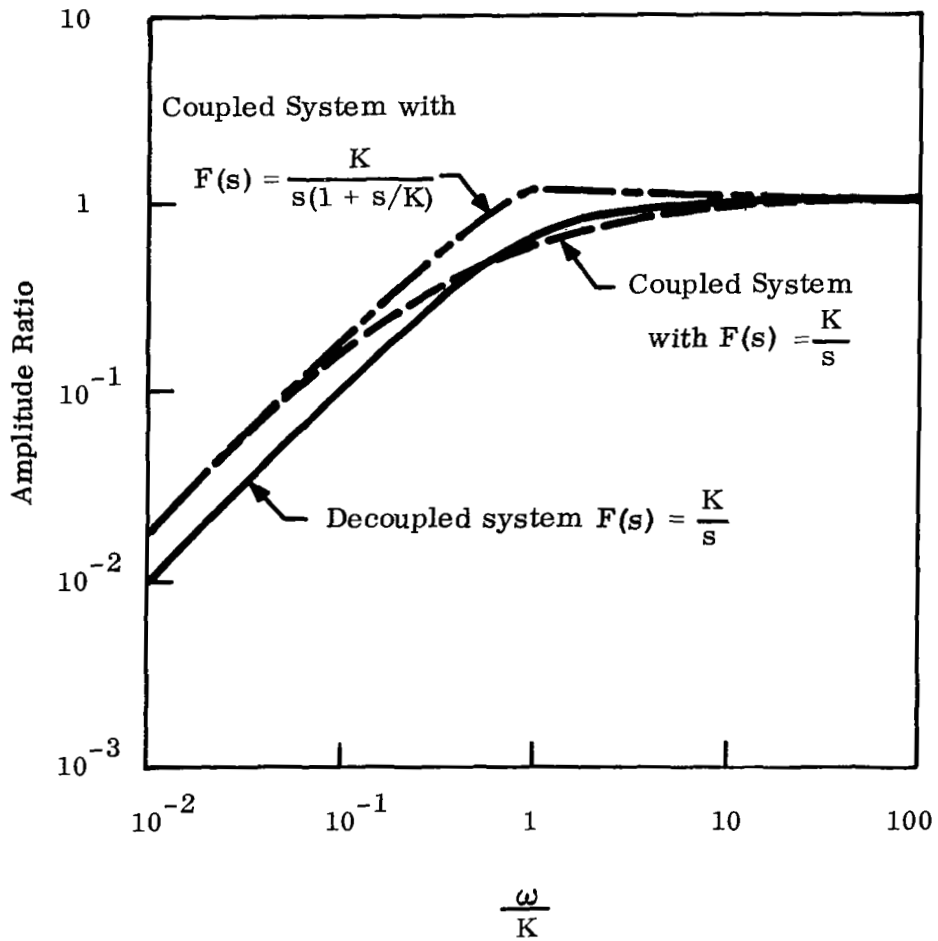
Figure 2-18. Response of Coupled System to Ground Motions

system. Although it is possible to design and construct
a coupled system of this type, a better solution is to
effectively decouple the two axes by using the error
signals from both axes to calculate the appropriate
drive motions as shown in Figure 2-19.

For the decoupled system the servomechanism demands:

$$y_1(s) = F_1(s) \left(\delta(s) + \frac{\Psi(s)}{2} \right) \tag{2-53a}$$

$$y_2(s) = F_1(s) \left(\Psi(s) + \frac{\delta(s)}{2} \right) \tag{2-53b}$$

and Equations (2-48) become:

$$L\Theta = F_1(s) \left[\delta(s) + \frac{\Psi(s)}{2} - \frac{\Psi(s)}{2} - \frac{\delta(s)}{4} \right] \tag{2-54a}$$

$$= \frac{3}{4} F_1(s) \; \delta(s)$$

$$L\Phi = F_1(s) \left[\Psi(s) + \frac{\delta(s)}{2} - \frac{\delta(s)}{2} - \frac{\Psi(s)}{4} \right] \tag{2-54b}$$

$$L\Phi = \frac{3}{4} F_1(s) \; \Psi(s)$$

which results in a decoupled system about the two axes.
If the gains of the drive motors are increased by a factor
of 4/3 the analyses of the preceding sections may be
applied directly.
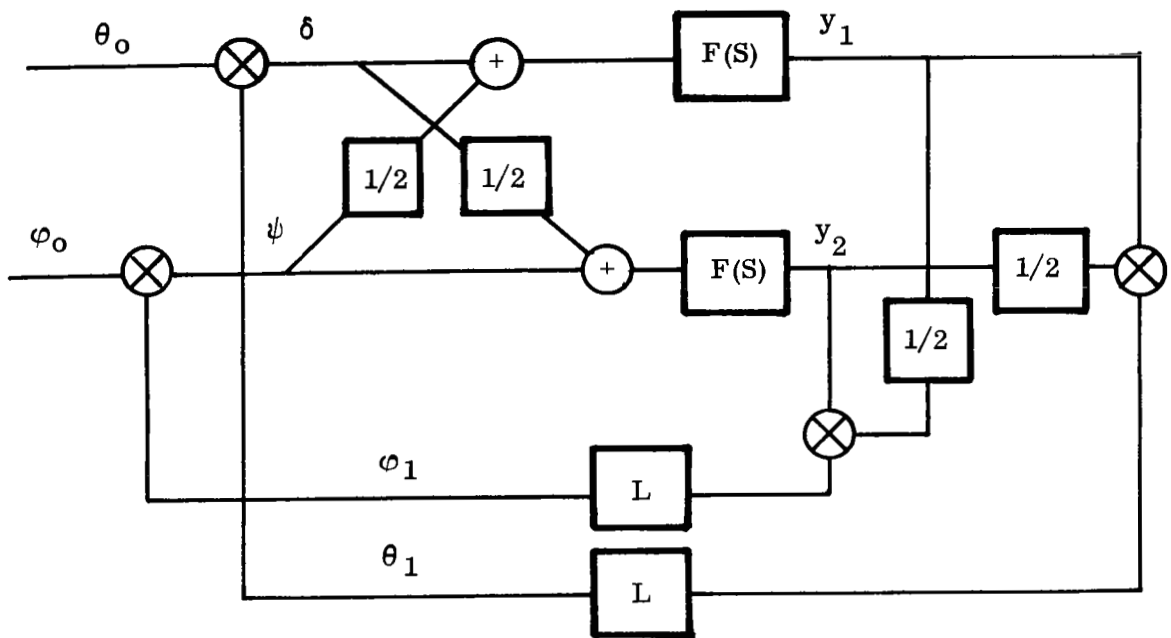
Figure 2-19. Block Diagram of Decoupling Calculation for Three Point Levelling

SECTION III

ISOLATION SYSTEM DESIGN

3.0 Introduction

The previous section outlines in general terms
the overall configuration of the system and the op-
timum design parameters. This section is concerned
with the physical realization of the system and the
specific components and configuration to be employed
in construction of the final system. For purposes of
discussion the system is broken down into the follow-
ing elements: control sensors, drive motors, loop
compensation and passive isolation system. The func-
tions of each of these elements and their components
are reviewed and their parameters are specified to
permit preparation of detailed drawings for fabrica-
tion of the system.

3.1 Control Sensors

The function of the control sensors (level sensor
and gyroscope) is to measure the angular motions of
the platform and to generate voltages which are accu-
rately known functions of these angular motions. The
level sensor is basically a low level accelerometer
which measures the component of specific force (gravity
and acceleration) in the plane of the controlled plat-
form. Several different types of level sensors have

63

been used for control of low frequency tilts in plat-
forms that use servomechanisms to maintain accurate
level. The M.I.T. Instrumentation Laboratory and the
Stanford University systems both use bubble levels that
have been provided with electrical readouts of the
bubble position. No long term drift data on the M.I.T.
sensor is available at this date. The level used in
the Stanford system exhibited drifts as large 0.5 arc
second in a 12 hr. period. The Barry Wright system
described in Reference 7 used a specially built pen-
dulum with an air gauge readout which contends an
accuracy of ± 0.25 arc seconds for a 72 hour period in
a quiet environment. The tiltmeter used in the experi-
mental platform described in Section IV is a dual cistern
tiltmeter made by Ideal Aerosmith Inc. of Cheyenne,
Wyoming which contends resolution and accuracy of better
than 0.02 arc second. This device is shown schematically
in Figure 3-1. The device consists of a stainless steel
bar with two shallow interconnected pools of mercury. A
capacitance plate is rigidly mounted to each of the top
plates with a nominal air gap of 0.025 inches. At low
frequencies the mercury surface is normal to the direc-
tion of the specific force and the difference in capaci-
tance is proportional to the tilt of the steel base.
With the electronics provided with the instrument the
nominal sensitivity is 2 volts/sec. Hughes Research

64
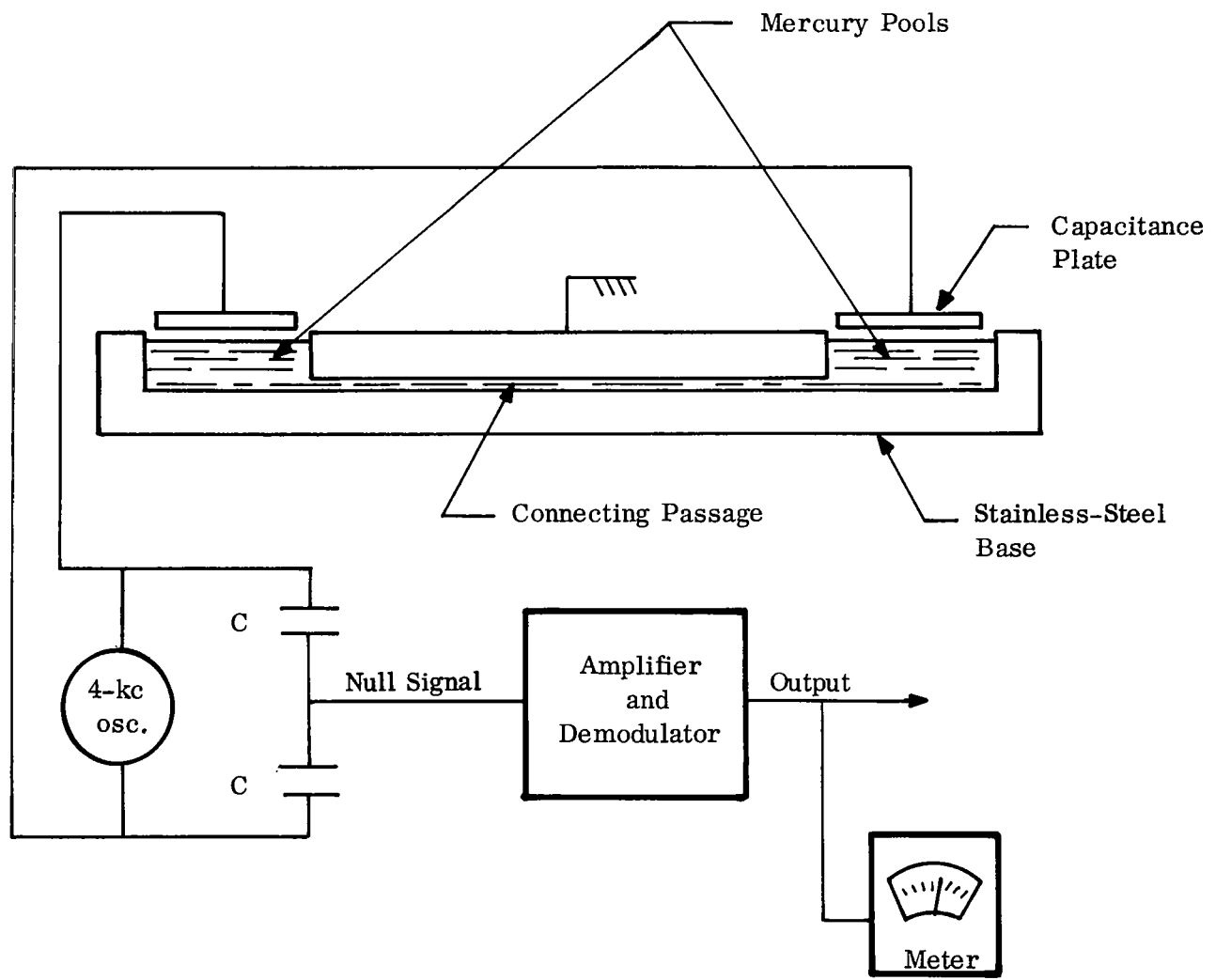
Figure 3-1. Schematic of Ideal-Aerosmith Tiltmeter

Laboratories of Malibu, California and Varian Associates
of Palo Alto, California have recently announced develop-
ment of instruments having accuracies and resolutions
of 10^{-8} radians. Similar accuracies have been claimed
for several accelerometers designed for extremely low
level measurement in space applications (e.g. Autonetics,
Division of North American Aviation, Inc., Anaheim,
California and Bell Aircraft Corporation, Buffalo, N. Y.).
These instruments being accelerometers can only be used
for control at low frequencies. As indicated in Section
II, if the accelerometer was used for high frequency
control the platform would be forced into oscillation
in response to horizontal vibratory accelerations.
Therefore at high frequencies the platform motions are
measured by an inertial grade gyroscope. Available un-
classified data indicates that the best resolution and
accuracy is obtainable from single degree of freedom
integrating gyroscopes of the general type originally
designed by the M.I.T. Instrumentation Laboratory. This
type of gyroscope instrument is shown schematically in
Figure 3-2. The instrument consists of a rotor rotating
at a high angular velocity which is rigidly mounted in a
cylindrical shell called the float gimbal which is
supported by a dense viscous fluid whose density is
adjusted to provide neutral buoyancy. At the ends of
the float the rotors of the signal generator and the

Figure 3-2. Gyroscope Single Degree of Freedom Schematic

torque generator are rigidly mounted. The signal
generator provides an a-c electrical signal which is
proportional to the angular motion of the float gimbal
about the output axis. The torque generator is used to
apply command torques to the float gimbal which may be
used to compensate gyro drift rates or command an
attitude of a gimballed inertial navigation system or
in strapdown navigation application to act with the
signal generator to produce the equivalent of a rate gyro.
When an angular velocity is applied about the instrument
input axis a gyroscopic inertia torque of $-H\omega_{IA}$ about
the output axis is produced, this torque must be reacted
by the damping about the output axis C_d, the elastic
restraint of the power leads and electromagnetic elements
k_g and the inertia of the rotor and float about the out-
put axis I_{OA}.

$$k_g\, A_{OA} + C_d\, \dot{A}_{OA} + I_O\, \ddot{A}_{OA} = H\omega_{IA} \qquad (3-1)$$

which results in the performance equation:

$$A_{OA} = \frac{H/C_d \quad \omega_{IA}}{\dfrac{k_g}{C_d} + s\left(1 + \dfrac{I_{OA}}{C_d}\, s\right)} \qquad (3-2)$$

In integrating gyroscope instruments the elastic

restraint is designed to be quite small compared to the damping of the instrument and at low frequencies the gyroscope output signal is proportional to the integral of the rate about the input axis. The bandwidth of the instrument is controlled by the gyroscope time constant $\tau = \dfrac{I_{OA}}{C_d}$ and the resolution is controlled by the gyroscope gain $h = \dfrac{H}{C_d}$ and mechanical and electrical noise considerations. The ratio of the gain to the time constant is:

$$\frac{h}{\tau} = \frac{H}{I_{OA}} = \frac{I_{spin}\ \omega_{spin}}{I_{OA}} \tag{3-3}$$

which for a given wheel speed tends to be approximately constant for most single degree of freedom gyroscope designs. A rule of thumb is that the gyroscope gain is about 1500 times the gyroscope time constant. For the required bandwidth of 25 cps the gyro time constant should be less than 0.0064 sec which implies a maximum gain of about 9.6. This implies that in order to sense an angular motion of 0.01 arc seconds the gyro signal generator must be capable of resolution of 0.096 sec which is within the capabilities of these transducers. A gyroscope instrument with a longer time constant could be used with compensation by a lead network but with the electrical noise penalties

69

associated with these schemes.

Both ball and gas bearings are currently used in gyroscope designs. Ball bearing instruments, however, are known to have large mechanical noise properties at frequencies above 0.1 cps. This would force the control system to oscillate in response to the bearing noise.

On the basis of unclassified published data, the instrument that best meets the above requirements is the KING II gas bearing gyroscope instrument, made by General Precision, Inc. of New Jersey. The parameters of this instrument of interest to this discussion are given in Figure 3-3.

Section II finds that the optimum performance for a gyroscope instrument having a nominal drift rate of 0.001 degree per hour is achieved if the characteristic of the filter L_O indicated in Figure 2-6 is:

$$L_O = \frac{0.0735 \left[1 + \frac{0.00575}{s} \right]}{\left[1 + 8.6s + 33.3s^2 \right]} \qquad (2\text{-}28a)$$

The response of the tiltmeter to horizontal vibrations may be amplified at frequencies above 1 cps due to resonance of the mercury pools. In addition, electrical noise from the tiltmeter electronics may introduce higher frequency noise signals. It is therefore desirable to introduce a second filter to

70

Figure 3-3. Parameters of King II Gas Bearing Gyroscope

The block diagram shows: Input Rate → H (Gyro Rotor) → (+) → $\dfrac{1}{cs\,(1 + \tau_g\, s)}$ → Signal Generator → Output Voltage, with Command Torque entering through the Torquer into the summing junction.
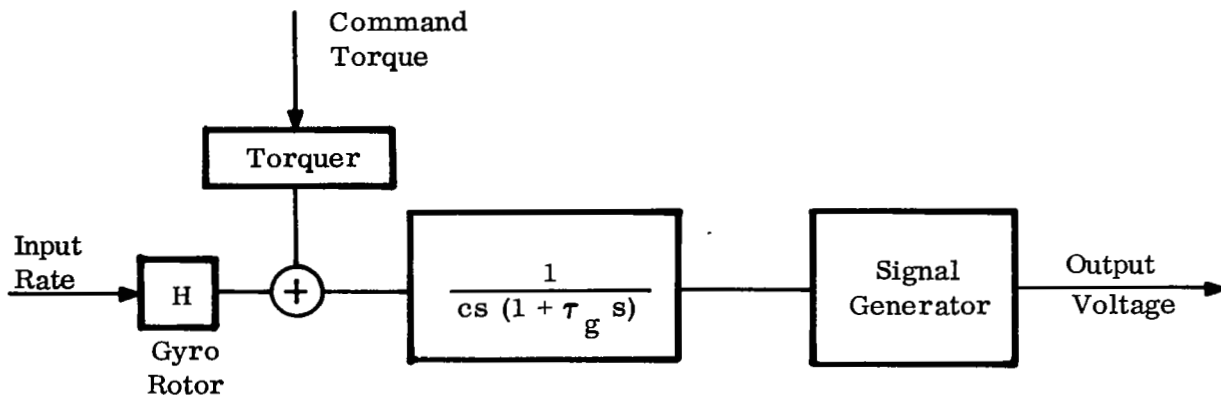
Angular Momentum (H)	350,000 dyne-cm - sec/rad.
Damping (c)	48,000 dyne-cm - sec/rad.
Wheel Speed	24,000 rpm = 400 rps
Time Constant (τ_g)	0.0066 sec
Gain (h)	8.8
Signal Generator Sensitivity	620 mv/deg
Torque Scale Factor	50 deg/hr/ma.
Elastic Restraint	0.14 deg/hr/deg of float motion
Bias Rate	±0.5 deg/hr
Life	40,000 hrs = 4.5 years
Random Drift Rate (Fixed Attitude) 10 hours	0.001 deg/hr* rms

*Measured Random Drift Rate for 108 Hours on Selected Unit: 0.0013 deg/hr.

attenuate the higher frequency noise. An electrical
network that produces the desired frequency response
characteristics is shown in Figure 3-4. The ampli-
fiers A1, A2 and A3 are standard operational ampli-
fiers having an open loop gain of 10^6 and outputs of
20 ma at $\pm$ 10 volt output voltages. The D.C. drift
of the amplifiers is critical since the servo loop
can not distinguish between amplifier drift and level
sensor output variations. The equivalent drift to
produce an indicated error of 0.01 sec is 20 mv
referred to the input of the amplifier network. If
the drift is slow (effective periods greater than 10
minutes) the drift of amplifiers A1 and A3 will be com-
pensated by the integration circuit of A2 in closed
loop operation. The drift of A2 however is critical
and in closed loop operation can produce steady state
errors. Analog Devices Operation Amplifier Model 301
has an input voltage offset drift of 100 $\mu v/^oC$ of tem-
perature change and a current offset drift of less than
10^{-9} ma which should be within the drift requirements.
To act as a true integrator the 1μF capacitor in the
circuit of A2 must have a high leakage resistance.
1μF capacitors having leakage resistances of between
10^{11} and 10^{12} ohms are commercially available. The
Model 301 amplifier is capable of using feedback
resistors as large as 10^{12} ohms, It is therefore
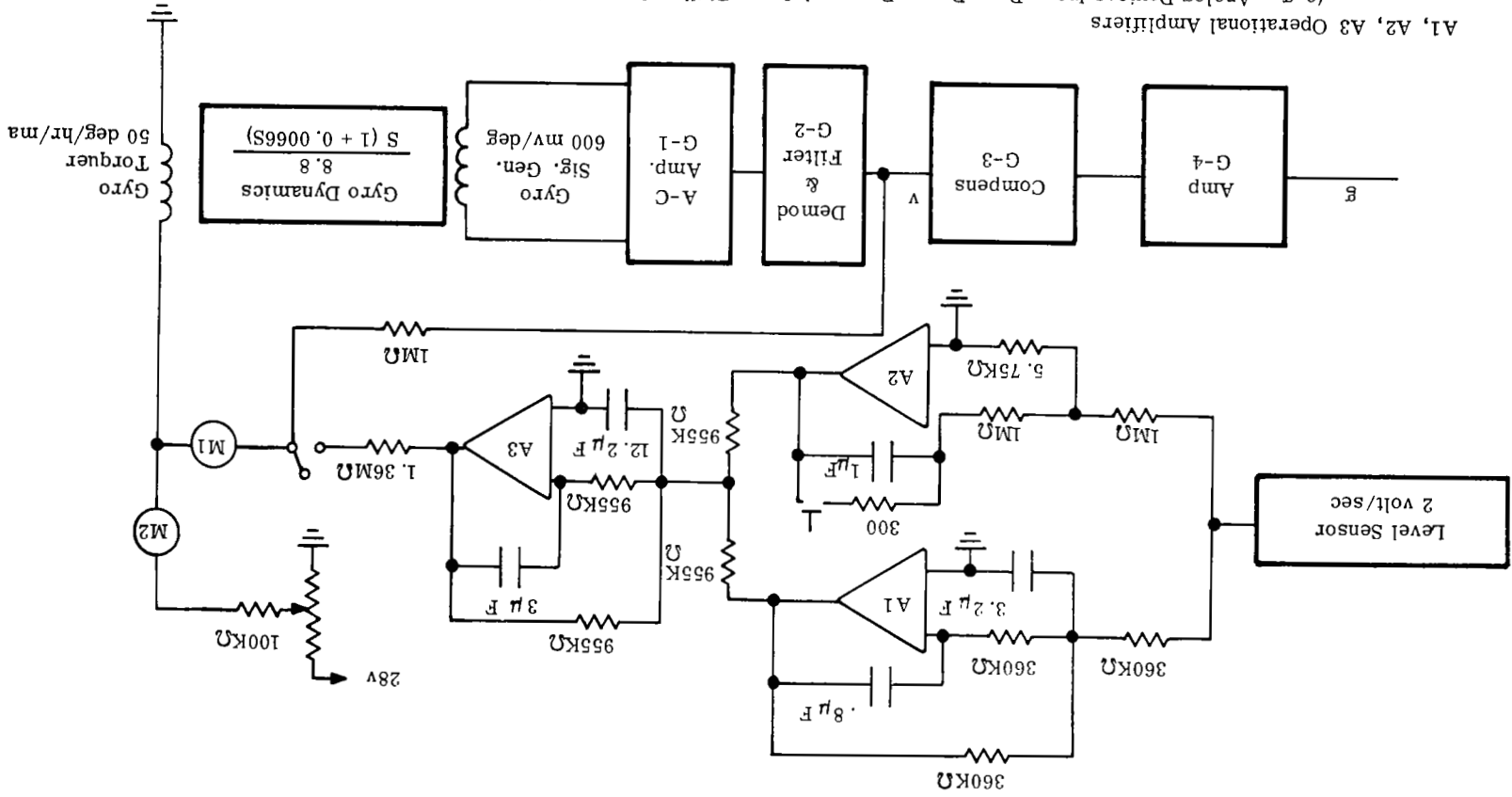
72

reasonable to assume a leakage resistance of 10^{11} ohms. The circuit should therefore act as an integrator for periods shorter than 6.28×10^5 sec = 7.25 days. At lower frequencies it will act as an amplifier having a gain of 575.

In closed loop operation the system can be considered as a gyro controlled platform where the gyro drift rate is compensated by the level sensor through the electrical circuits before the gyroscope torquer. The maximum drift rate that can be compensated is limited by the 10 volt saturation voltage of amplifier A3. With the parameters given in Figure 3-4 the maximum rate that can be compensated by the level sensor is 0.367^O/hr. which is well above the 0.001^O/hr. random drift rate of the gyroscope instrument. However, the instrument will measure the horizontal component of Earth Rate which depending on the platform azimuth orientation may be as large as 10.5^O/hr. at a 45° latitude. The 28 volt supply shown in Figure 3-5 is intended to provide a constant current to compensate for this rate. To remain consistent with the 0.001^O/hr. random drift rate of the gyro, this supply voltage must be constant to within about 10 parts per million (.001%).

The feedback loop produced by the 1 megohm resistor from the d.c. gyro output signal to the gyro torquer is

intended to keep the float of the gyroscope near null

when the servo system is not in operation and to assist

in establishing the current required to compensate for

earth rate and any other fixed torques. The meter M1

provides the change in gyro drift rate since the last

manual compensation. This change in drift rate in closed

loop operation is compensated for by the integration

circuit.

The output of the gyroscope signal generator is a

20 kc amplitude modulated signal which must be demodu-

lated and filtered to obtain a D.C. signal. This is

accomplished in standard "servo-amplifiers" used in

gyroscope test turntables. These "servo-amplifiers"

also provide capability of introducing several forms

of compensation in the servo loop. For discussion

purposes the gain of the AC preamplifier and the

demodulator is set at 1000 and constant for gyro

error signals between 0 and 200 cps.

The voltage v to be used for control of the

system is related to the platform error angle by the

transfer function:

$$\frac{v\ (s)}{\delta\ (s)} = 1.47 \frac{\left[\dfrac{0.0735 \left(\dfrac{0.00575}{s+10^{-5}} + \dfrac{1}{1+0.86s+.333s^2}\right)}{1 + 8.6s + 33.3s^2} + s\right] \dfrac{\text{volt}}{\text{sec}}}{0.0735 + s\ (1 + 0.0066s)}$$

(3-4)

This transfer function is closely approximated by:

$$\frac{v_{\ddot{\alpha}}(s)}{\delta(s)} \approx \frac{1.47 \left(1 + \dfrac{0.00575}{s+10^{-5}}\right)}{1 + 0.0066s} \quad \frac{\text{volt}}{\widehat{\text{sec}}} \tag{3-5}$$

The sensitivity to horizontal accelerations is given by:

$$\frac{v(s)}{\varepsilon_a(s)} = \frac{1.47 \left(\dfrac{.00575}{s+10^{-5}} + \dfrac{1}{1 + 0.86s + .333s^2}\right) \quad \dfrac{\text{volts}}{\widehat{\text{sec}}}}{(1 + 8.6s + 33.3s^2)(1 + 13.6s(1 + .0066s))} \tag{3-6}$$

which is approximated by:

$$\frac{1.47 \left(1 + \dfrac{0.00575}{s+10^{-5}}\right) \qquad\qquad \dfrac{\text{volts}}{\widehat{\text{sec}}}}{(1+0.86s+.333s^2)(1+8.6s + 33.3s^2)(1+13.6s)(1+.0066s))} \tag{3-7}$$

The sensitivity to gyroscope drift rate is:

$$\frac{v(s)}{\dot{\varepsilon}_g(s)} \approx \frac{1.47}{0.0735 + s(1 + .00666s)} \qquad \frac{\text{volts}}{^\circ/\text{hr.}} \tag{3-8}$$

which is approximated by:

$$\frac{v(s)}{\dot{\varepsilon}_g(s)} = \frac{1.47(13.6)}{(1 + 13.6s)(1 + 0.0066s)} \tag{3-9}$$

76

The ratio of the response to horizontal accelerations to that due to angular motions is:

$$\frac{v_a(s)}{v_\delta(s)} = \frac{1}{(1+13.6s)(1+8.6s+33.3s^2)(1+0.86s+0.333s^2)}$$

(3-10)

and the ratio of the response to gyro drift rate to that due to angular motions is:

$$\frac{v_g(s)}{v_\delta(s)} = \frac{13.6}{(1+13.6s)\left(1+\dfrac{0.00575}{s+10^{-5}}\right)}$$

(3-11)

Thus at frequencies below 0.012 cps, the system will essentially follow the level sensor and at higher frequencies, within the system bandpass, the system will follow the integral of the gyroscope drift rate.

3.2 Servomechanism Drive and Compensation

The servomechanism drive must perform the following functions:

1. Support the dead weight of the platform (5,000 lb).

2. Resist externally applied disturbance torques (250 lb-ft rms per decade for frequencies below 0.001 cps).

3. Provide relative displacement between the equipment mounting surface and the base of the

77

servomechanism system to compensate for base motions.

4. Respond to noise signals generated by the control sensors and electronics within the bandpass of the system.

In order to resist disturbance torques of 250 lb-ft rms per decade for frequencies between 10^{-7} cps and 10^{-3} cps, the drive system must be capable of applying a torque of 500 lb-ft rms. The relative velocity spectrum, as obtained from differentiation of the reference angular displacement spectrum that the drive must generate if the control system were perfect is shown in Figure 3-5 . It is seen that the relative velocity required with a 1 cps passive isolation is approximately 1.5 $\overset{\frown}{\text{sec}}$/sec rms $\approx 7.5 \times 10^{-6}$ rad/sec. The relative acceleration required is approximately 4×10^{-4} rad/sec^2 rms. For an electrical motor the relative velocity is proportional to the applied voltage and the torque is proportional to the current. The supply power to the motor should therefore be capable of supplying:

$$500 \times 7.5 \times 10^{-6} = 3.75 \times 10^{-3} \frac{\text{lb-ft}}{\text{sec}}$$

$$= 0.0051 \text{ volt-amp}$$

which is a very small useful power requirement. As discussed in Section II , if the torque applied by the

78
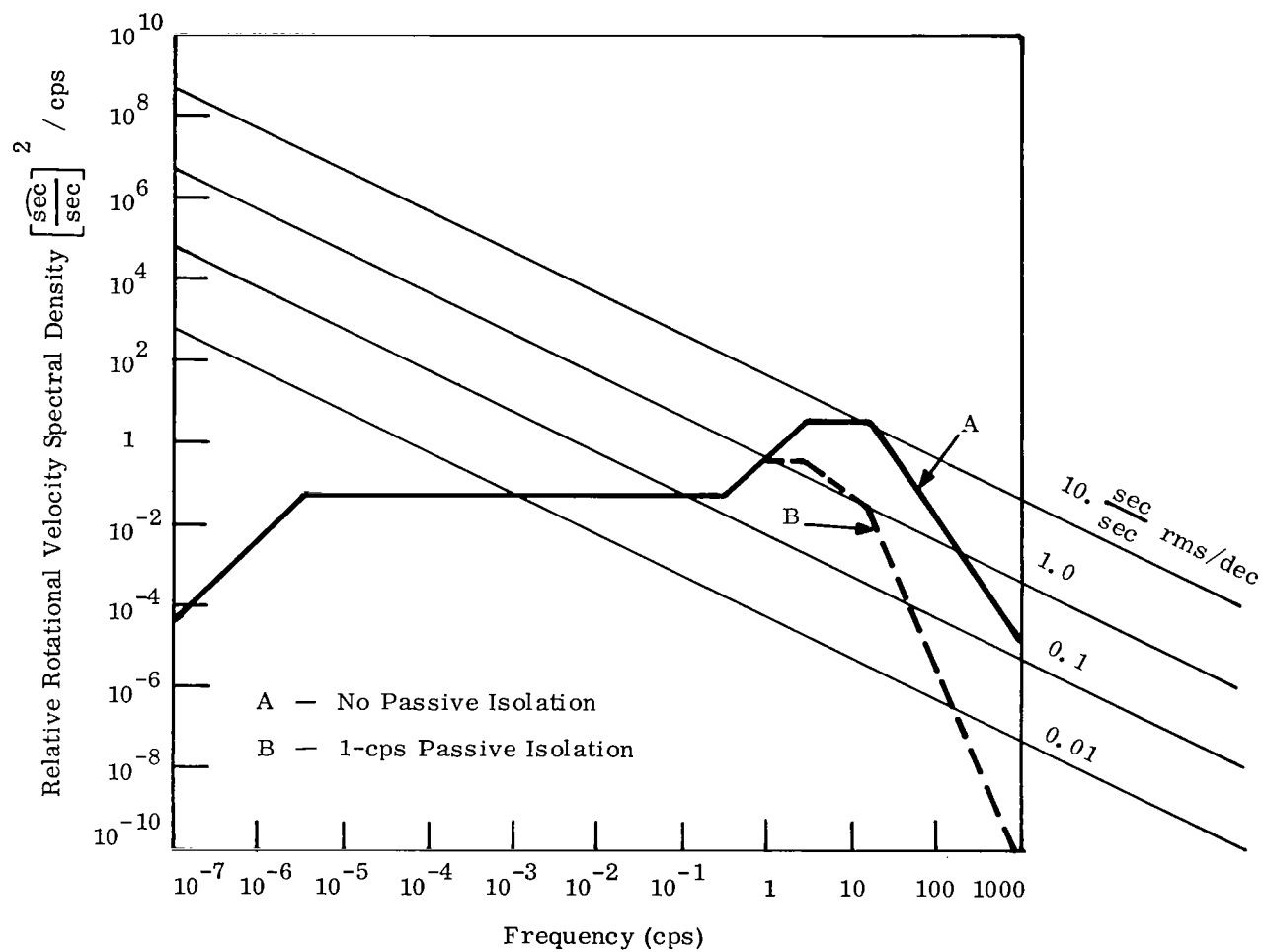
Figure 3-5a. Angular Velocity (φ) Required of Servo Drive for Perfect Isolation with Perfect Control Sensors
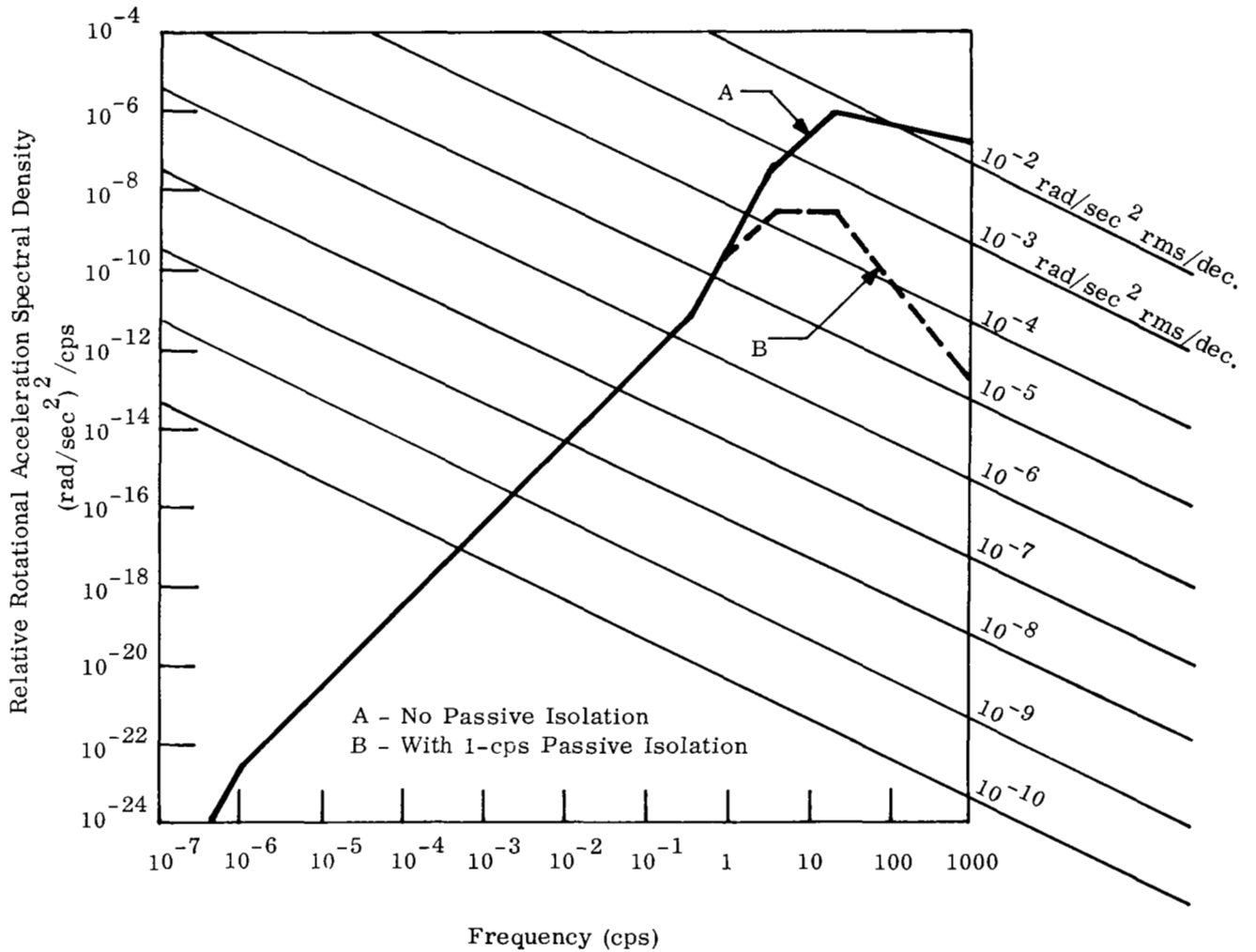
Figure 3-5b. Acceleration ($\ddot{\varphi}$) Required of Servo System Drive for Perfect Isolation with Perfect Control Sensors

drive motor is resisted only by the platform inertia

small torque variations will result in large platform

motions. Both of these considerations imply the

desirability of a large mechanical advantage for

the system to permit resolution of the very small

angular motions that are required. Since electrical

torquers are limited to accelerations of about 2,500

rad/sec^2 the maximum mechanical advantage that can be

used is 6.25 x 10^6. A mechanical advantage of this

magnitude can be obtained by modification of the

micromotion drive used in the M.I.T. Instrumentation

Laboratory isolation system. This drive is shown in

Figure 3-6 . As used in the M.I.T. Instrumentation

Laboratory system the drive has a mechanical advantage

of 2.3 x 10^8 with the 50" lever arm used in this plat-

form. This mechanical advantage is reduced to 2.25 x

10^5 by removing the gear train (which is a potential

source of backlash problems at high frequencies and

friction problems) and using a direct drive motor.

The metal to metal contact of the drive nut and

threaded shaft and of the drive nut and the unit

housing, however, results in a measured friction

torque of about 0.3 lb-in per 100 pounds of load.

For the 5,000 lb equipment weight the load on the

drive is 1,666 lb which would result in a friction

torque of 5 lb-in that varies with the position of

SPHERICAL DRIVING HEAD

BELLOWS (A)

DRIVE SCREW

SERVO MOTOR

HYDRAULIC FLUID

MAIN HOUSING

BELLOWS (B)

THRUST NUT

BELLOWS (C)

BASE
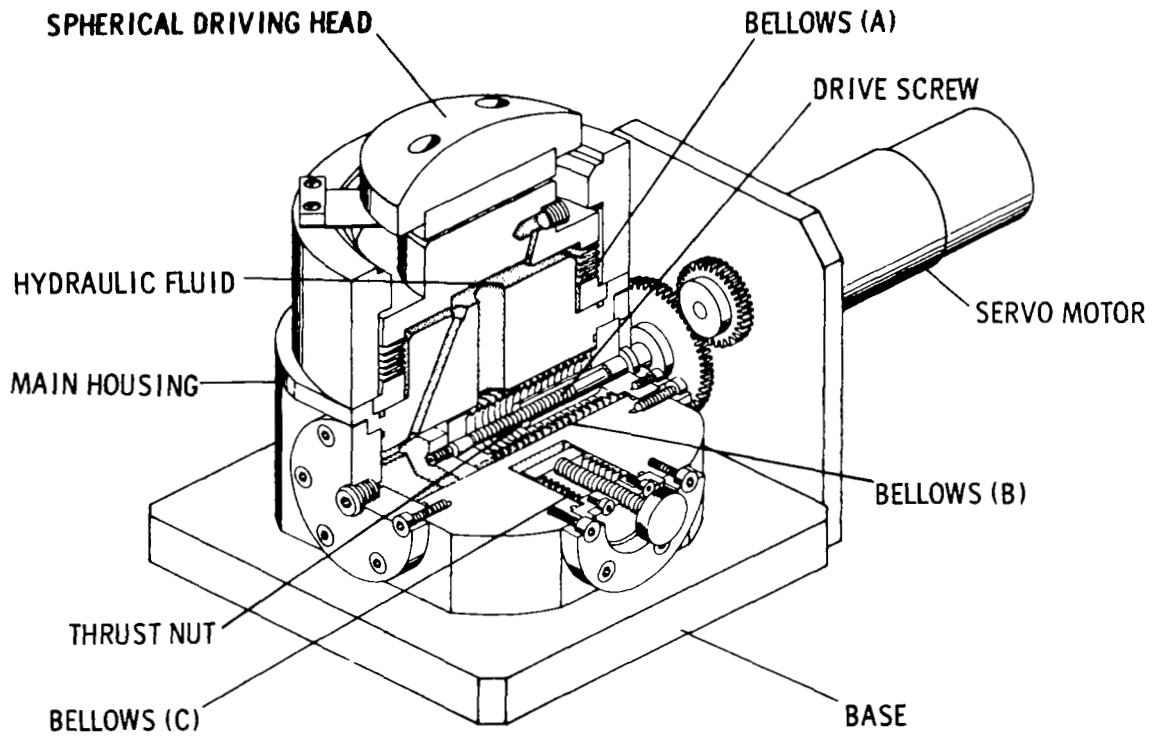
Figure 3-6. Photo of Micromotion Drive Assembly

82

the drive. This friction torque is considerably
larger than any other of the torque requirements and
would result in selection of a larger torque motor
than is actually required. By removing the thrust
bearing and using a ball nut and lead screw drive
as shown in Figure 3-7 , the friction torque is
reduced to a measured friction range of 0.05 to
0.5 lb-in depending on drive position at a 1000 lb
load. The use of the ball nut and lead screw reduces
the mechanical advantage to $0.56 \times 10^{+5}$ since ball
nut threads finer than 10 threads per inch can not
readily be obtained. For the 60 inch lever arm of
the final system the mechanical advantage is 0.67 x
10^5 the motor requirements for the drive are:

    a.   Steady State Torque due to platform
        weight - 1.5 lb-in.

    b.   Resistance to disturbance torques - 0.045 lb-in.

    c.   Acceleration required - 24.8 rad/sec^2.

    d.   Range - $\pm$10 revolutions

               $\approx \pm$ 125 $\widehat{sec}$ platform rotation.

These requirements are readily met by the 0.85 lb-ft
Inland Motors torquer specified in Figure 3-7 . The
tachometer shown in Figure 3-7 is used to provide
effective damping to the drive by the electrical
networks discussed in the following paragraphs.

Figure 3-7. Drive Motor for Modified Micromotion Drive Assembly

In order to drive the platform at frequencies up to 25 cps the stiffness of the drive should be high enough to provide a natural frequency that is higher than 75 cps. The most compliant parts of the drive are the large bellows and the fluid and air volume contained in the unit. For the SAE30 oil used in the drive the compliance of the fluid volume is:

$$C_f = \frac{\delta}{\Delta P} = \frac{1}{\Delta P}\left(\frac{\Delta P}{A_o}\frac{V_o}{K}\right)\frac{1}{A_o} = \frac{V_o}{A_o^2 K} \qquad (3\text{-}12)$$

where C_f = fluid compliance (inch/lb)

P = applied load (lb)

V_o = fluid volume (in ^{3})

K = bulk modulus of fluid (psi)

A_o = effective piston area so that:

$$C_f = \frac{4.4}{(10.6)^2(350,000)} = 0.11 \times 10^{-6} \text{ in/lb}$$

The compliance of the air trapped in the unit is:

$$C_a = \frac{\delta}{\Delta P} = \frac{1}{\Delta P}\left(\frac{\Delta P}{A_o}\right)\left(\frac{\alpha\, V_o}{P/A_o + 15}\right)\frac{.1}{A_o}$$

$$= \frac{\alpha\, V_o}{(P + 15A_o)\, A_o} \qquad (3\text{-}13)$$

where α = ratio of volume of

air at load P to total

volume.

For P = 1,667 lb and α = 0.01

$$C_a = \frac{0.01 \times 4.4}{(1,667 + 15. \ 10.6)(10.6)} = 1.83 \times 10^{-6} \ in/lb$$

Since α is inversely proportional to the pressure in the
unit, the compliance of the air is inversely proportional
to the square of the pressure in the unit. Thus at a
load of 1000 lb the air compliance would be 4.54×10^{-6}
in/lb and at a **200** lb load it would be 47.3×10^{-6} in/lb.

The bellows are fabricated by welding slightly
conical disks together as indicated in Figure 3-8.
When the ends of the bellows are sealed and a load is
applied there is a change in the volume of the bellows
produced by a bulging of the disks. The deflection
produced by a pressure loading on a disk of the given
dimensions can be approximately obtained from the
deflection of a fixed-fixed beam of constant cross-
section having a length equal to the difference in
radii of the disk. Reference 17 gives this beam deflec-
tion as:

$$y = \frac{p}{24EI} \ \frac{x^2}{\ell} \ (2\ell x - \ell^2 - x^2)$$

(3-14)

86

P
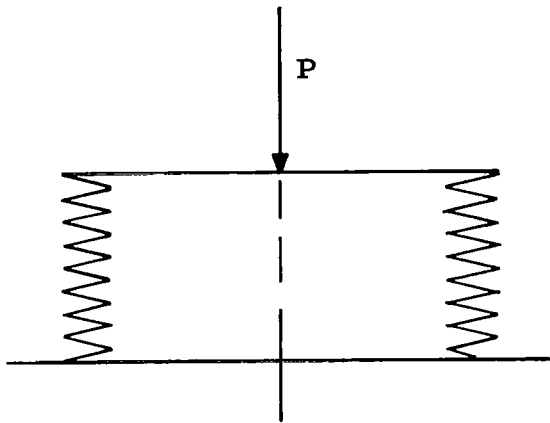
Outer Diameter   4.00 in.
Inner Diameter   3.34 in.
Effective Area   10.7 in.^{2}
No. of Convolutions   8
Max. Deflection
per Convolution   0.026 in.
Spring Constant   183 lb/in.
Material –   Stainless steel
Thickness –   .006 inch

From M. I. T. Instrumentation
Laboratory Drawing 55C–51652

r_o

ℓ r_i

p
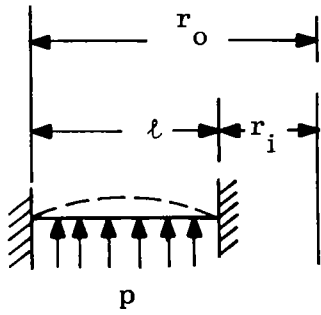
Disc under Pressure
Loading

p

ℓ

x

p
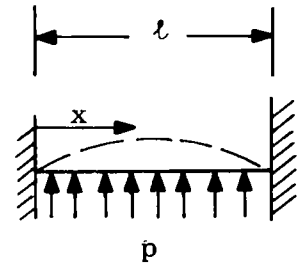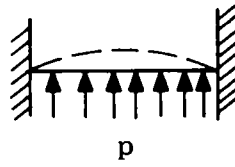
Fixed – Fixed
Beam under
pressure loading

Disc and beam are equivalent for $\dfrac{r_i}{r_o} \rightarrow 1$

Figure 3-8. Calculation of Compliance of Large Bellows

where x = length along the beam

ℓ = length of the beam

δ = deflection

E = modulus of elasticity

I = moment of inertia of the section

The change in volume of the disk produced by this deflection is:

$$\Delta V_1 = 2\pi R_o \int_0^\ell y\,dx = \frac{p\ell^4(2\pi R_o)}{720EI} \qquad (3-15)$$

where R_o is the radius of the disk. The total change in volume for an applied force P is:

$$\Delta V = \frac{P\pi R_o \ell^4 N}{60t^3 A_o E} \qquad (3-16)$$

where N = number of convolutions (2 disks per convolution) resulting in a deflection per unit load of:

$$\frac{\delta}{P} = \frac{N\pi R_o \ell^4}{60\, A_o^2 t^3} \qquad (3-17)$$

For the bellows used by the micromotion drive as used in the M.I.T. Instrumentation Laboratory system the bellows compliance is estimated as:

$$C_b = \frac{\delta}{P} = \frac{8\Pi(1.836)(0.3)^4}{60(10.6)^2 \text{x} 30\text{x} 10^6 \text{x}(0.006)^3}$$

$$= 8.57 \text{ x } 10^{-6} \text{ in/lb}$$

The total compliance is therefore estimated as:

$$C = C_f + C_a + C_b \approx 10.5 \text{ x } 10^{-6} \text{ in/lb}$$

The measured compliance of the drive is $13 \text{ x } 10^{-6}$ in/lb at a 1000 lb load which is in agreement with the air compliance estimated above.

If the compliance of all three of the support points were equal the vertical natural frequency corresponding to this compliance is:

$$f_v = \frac{1}{2\Pi}\sqrt{\frac{g}{CW}} = \frac{1}{2\Pi}\sqrt{\frac{386 \text{ x } 10^6}{10.5 \text{x} 1667}} \qquad (3\text{-}18)$$

$$= 23.6 \text{ cps}$$

The rotational natural frequency will have approximately the same magnitude. This natural frequency can be increased to 42 cps by decreasing the number of bellows convolutions to 2½ from the 8 convolutions currently used. This would reduce the allowable stroke to 0.065 inches which is consistent with the 0.060 inch travel

that is required by the stroke of the small bellows. Decreasing the number of convolutions increases the spring constant of the bellows from 183 lb/in to 586 lb/in which is reflected at the drive smaller bellows as a stiffness of $\left(\dfrac{0.46}{10.6}\right)^2$ (586) = 1.1 lb/in which is negligible compared to the small bellows stiffness (to pressure changes) of 15 lb/in. A further increase in stiffness of the drive can be obtained by increasing the effective area of the bellows while maintaining the same difference in the disk radii. An increase of the nominal bellows diameter to 6 inches from the 4 inch nominal diameter given above results (from Equation 3-17) in a factor of $(1.5)^3$ = 3.38 increase in drive stiffness resulting in a natural frequency of 77 cps. The spring constant of the bellows as a result of this change in radius is increased by a factor of 1.5 and becomes approximately 850 lb/inch which is reflected at the drive smaller bellows as a stiffness of $\left(\dfrac{0.46}{10.6 \times 1.5^2}\right)^2$ (850) = 0.316 lb/in which is again negligible compared to the small bellows stiffness of 15 lb/in. Modification of the bellows to 2½ convolutions and to a 6 inch nominal diameter increases the mechanical advantage of the drive to 1.51×10^5. The accompanying decrease in working pressure also results in a decrease in the

working stress of the bellows. This decrease in work-
ing pressure and the overall stiffness requirement,
however, requires greater care in filling the unit with
oil to avoid compliance due to trapped air bubbles. To
prevent an air volume of 0.5% at the 75 psi working
pressure, the unit should be filled under a vacuum having
an absolute pressure of 0.45 psia (about 29 inches of
mercury). The above modifications to the large bellows
should result in a compliance of approximately one micro-
inch per lb. Assuming equal stiffnesses at each of the
three support points the rotational stiffness of the
drive is obtained from Figure 3-9 as:

$$K_\theta = 6K_\ell \left(\frac{\ell}{3}\right)^2 = 6\times10^6 \times 20^2$$

$$K_\theta = 2.4\times10^9 \;\frac{\text{lb-in}}{\text{radian}}$$

In order to allow for other compliances in the structure,
however, for calculation purposes the rotational stiffness
is taken as $10^9 \;\frac{\text{lb-in}}{\text{rad.}}$. Assuming a radius of gyration of
20 inches for the 5,000 lb test equipment, the rotational
natural frequency is:

$$K_\theta = 6K \left(\frac{\ell}{3}\right)^2$$

about 2 orthogonal axes.
Therefore equal rotational
stiffness about all horizontal
axes through elastic center.

$$K_\theta = 2K \left(\frac{\ell}{3}\right)^2 + K \left(\frac{2\ell}{3}\right)^2$$

$$= 6K \left(\frac{\ell}{3}\right)^2$$
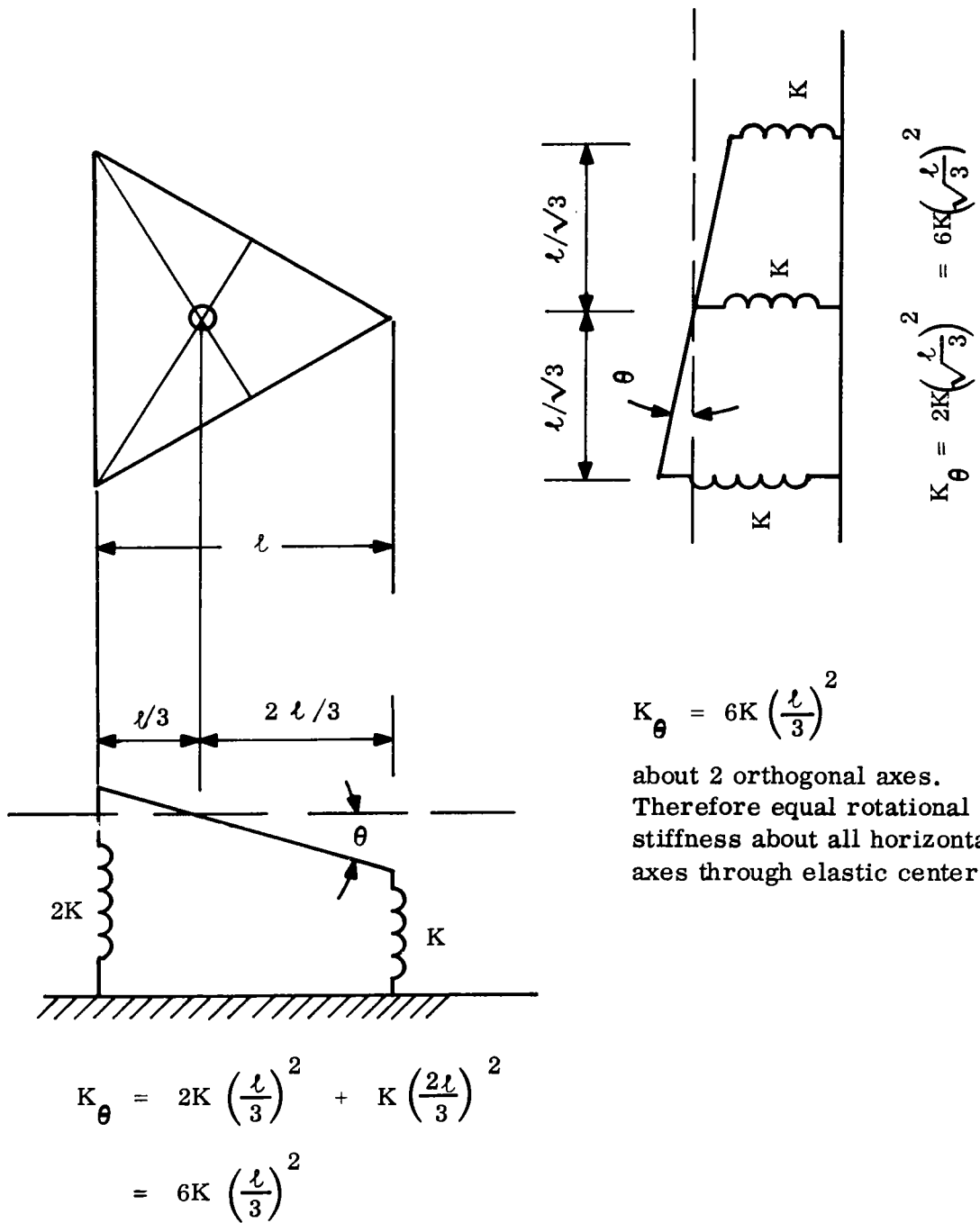
Figure 3-9. Calculation of Drive Rotational Stiffness

$$f_\theta = \frac{1}{2\pi} \sqrt{\frac{10^9 \times 386}{5,000 \times 20^2}}$$

$$= \frac{440}{2\pi} = 70 \text{ cps}$$

The drive sections of the system are completed by providing a current amplifier to supply power for the torque motor and the tachometer and operational amplifier to provide rate feedback to the drive section. A block diagram of the drive system characteristics is shown in Figure 3-10 .

The transfer function of the drive is given by:

$$\frac{\Phi(s)}{v(s)} = \frac{K_3}{QK_2 s} \left(\frac{1}{1 + \dfrac{Js}{K_1 K_2} + \dfrac{k_1}{K_1 K_2 s}} \right) \left(\frac{1 + 2\beta \dfrac{s}{\omega_n}}{1 + 2\beta \dfrac{s}{\omega_n} + \dfrac{s^2}{\omega_n^2}} \right)$$

$$(3-19)$$

The response to disturbance torques is:

$$\frac{\Phi(s)}{M_d(s)} = \frac{1}{K_\theta} \frac{1}{\left(1 + 2\beta \dfrac{s}{\omega_n} + \dfrac{s^2}{\omega_n^2}\right)} + \frac{1}{K_1 Q} \frac{\Phi(s)}{v(s)}$$

$$(3-20)$$
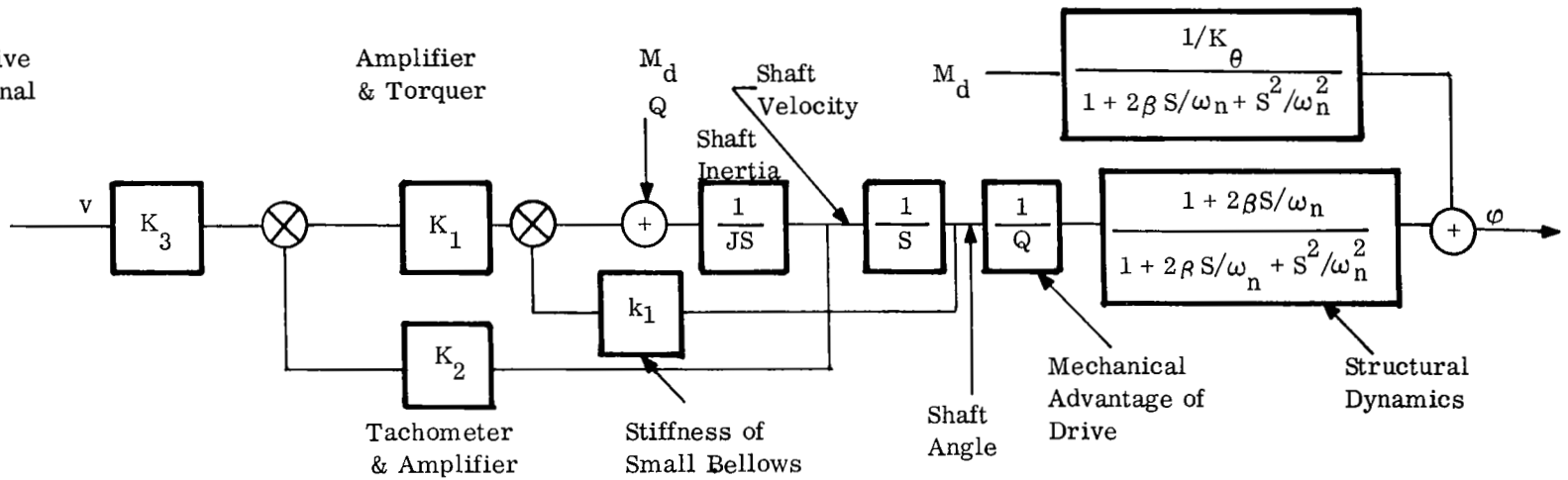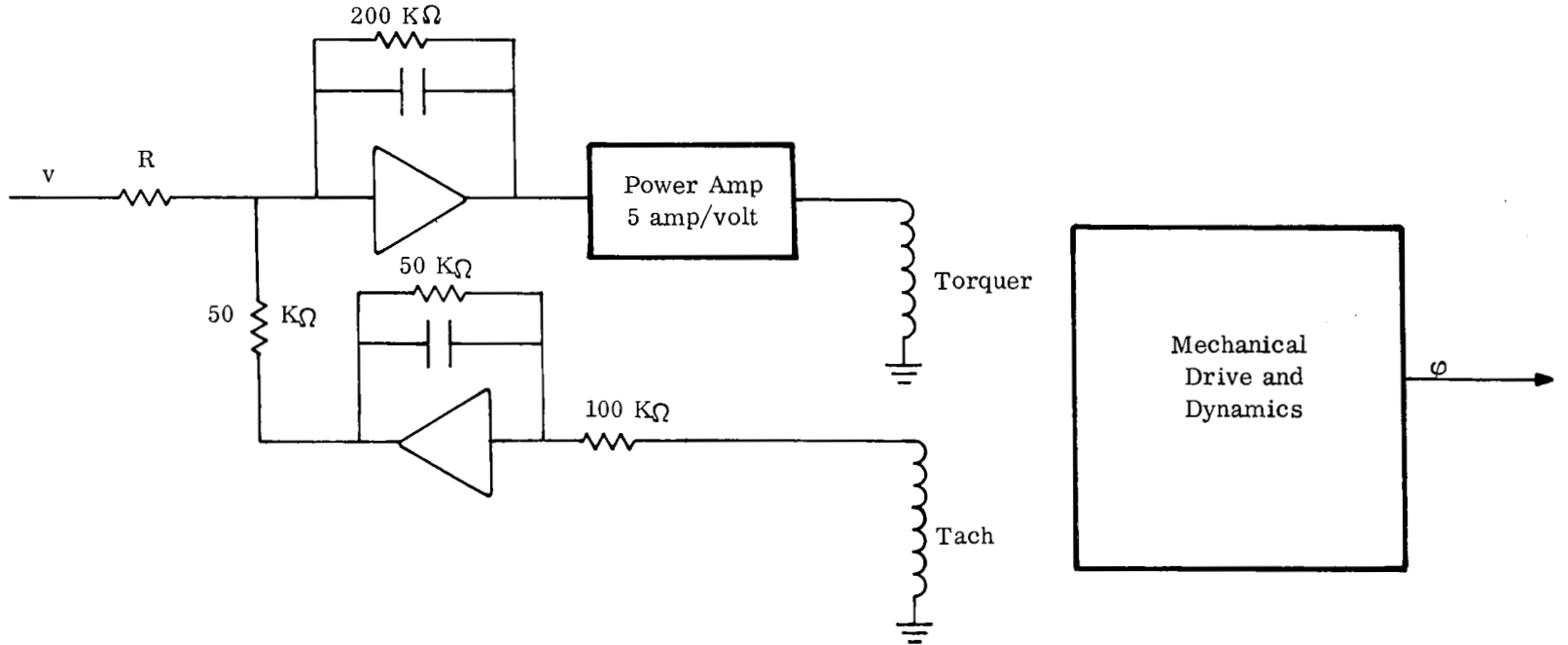
Figure 3-10. Schematic of Drive System Dynamics

For the drive motor assembly shown in Figure 3-7 with the modified large bellows described above, the mechanical and electrical constants are:

J = Shaft Moment of Inertia = 5×10^{-4} lb-ft-sec^2

Q = Mechanical Advantage = 1.51×10^5

C_{TQ} = Torque Motor Constant = $0.125 \dfrac{\text{lb-ft}}{\text{amp}}$

C_{TCH} = Tachometer Sensitivity = $1.2 \dfrac{\text{volt}}{\text{rad/sec}}$

I_o = Platform Moment of Inertia = 5200 lb-in-sec^2

K_Θ = Drive Rotational Stiffness = $10^9 \dfrac{\text{lb-in}}{\text{rad}}$

ω_n = Rotational Natural Frequency = 440 rad/sec

= 70 cps

k_1 = Bellows stiffness as seen by torque motor

= $4 \times 10^{-3} \dfrac{\text{lb-in}}{\text{rad}}$

β = Ratio of damping in rotational spring mass system to critical damping = 0.05 (estimated)

For the gains given in Figure 3-10 , K_1 = 5 $\dfrac{\text{lb-ft}}{\text{volt}},$

K_2 = 0.6 $\dfrac{\text{volts}}{\text{radian}},$ so that Equation 3-19 becomes:

$$\frac{\Phi}{v(s)} = \frac{K_3}{QK_2s} \left(\frac{1}{1 + \dfrac{5 \times 10^{-4}s}{3} + \dfrac{4 \times 10^{-3}}{3s}} \right) \left(\frac{1 + 2\beta \dfrac{s}{\omega_n}}{1 + 2\beta \dfrac{s}{\omega_n} + \dfrac{s^2}{\omega_n^2}} \right)$$

(3-21)

95

$$\frac{\phi}{v(s)} \simeq \frac{K_3}{QK_2 s} \quad \frac{1}{(1+0.00017s)(1+\frac{0.00133}{s})} \left(\frac{1+2\beta \frac{s}{\omega_n}}{1+2\beta \frac{s}{\omega_n} + \frac{s^2}{\omega_n^2}} \right)$$

$$(3-22)$$

Current amplifiers having "gains" of 5 amp/volt are readily available commercially (e.g. Inland Motors Co., Radford, Va., Goerz Optical Co., etc.). The other required gains can readily be obtained with operational amplifiers as indicated in Figure 3-10.

If the gyroscope instrument had an infinitely fast response characteristic ($\tau_g = 0$) and no compensation networks were used in the system, the open loop transfer function for frequencies above 1 cps would be:

$$\frac{\phi(s)}{\delta(s)} = \frac{G}{s} \quad \frac{(1+\frac{2\beta s}{\omega_n})}{(1+\frac{2\beta s}{\omega_n} + \frac{s^2}{\omega_n^2})}$$

$$(3-23)$$

This system is unstable if:

$$G > 2\beta \omega_n = 0.1 \times 440 = 44 \frac{rad}{sec}$$

so that with no compensation and an infinitely fast gyroscope instrument the maximum system bandpass that could be

achieved would be 7 cps due to the amplification resulting from the drive system resonance.

For a gyroscope having a time constant of 0.0066 seconds as specified in the section on control sensors the open loop transfer function for frequencies above 1 cps is:

$$\frac{\Phi(s)}{\delta(s)} = \frac{G}{s} \frac{\left(1 + \frac{2\beta s}{\omega_n}\right)}{\left(1 + \frac{2\beta s}{\omega_n} + \frac{s^2}{\omega_n^2}\right)(1 + 0.0066s)}$$

(3-24)

The criteria for stability is approximately given as:

$$G < 0.0066(2\beta\omega_n) \quad \omega_n = 129 \frac{rad}{sec}$$

This implies a maximum system bandwidth of 20.6 cps with a marginally stable system.

If compensation networks were introduced which resulted in a system open loop transfer function of:

$$\frac{\Phi(s)}{\delta(s)} = \frac{G\left(1 + \frac{2\beta s}{\omega_n}\right)}{S\left(1 + \frac{2\beta s}{\omega_n} + \frac{s^2}{\omega_n^2}\right)(1 + 0.003s)^2}$$

(3-25)

97

the criterion for stability (gain less than one at 180° phase shift) is approximately:

$$G < \left(1 - \frac{1}{(.003\omega_n)2}\right) \left(\frac{0.006}{0.003}\right) \left(\frac{1}{0.003}\right)$$

$$G < 284 \; \frac{rad}{sec} = 45 \; cps$$

For this transfer function the closed loop response to ground motions is:

$$\frac{\delta(s)}{\theta_o(s)} = \frac{\frac{s}{G}(1 + 0.003s)^2 \left(1 + \frac{2\beta s}{\omega_n}\right)}{1 + \frac{2\beta s}{\omega_n} + \frac{s}{G}(1 + 0.003s)^2 \left(1 + \frac{2\beta s}{\omega_n} + \frac{s^2}{\omega_n^2}\right)}$$

$$(3-26)$$

The system response to noise signals is given by:

$$\frac{\delta(s)}{n(s)} = \frac{1 + \frac{2\beta s}{\omega_n}}{1 + \frac{2\beta s}{\omega_n} + \frac{s}{G}(1 + 0.003s)^2 \left(1 + \frac{2\beta s}{\omega_n} + \frac{s^2}{\omega_n^2}\right)}$$

$$(3-27)$$

The frequency response functions corresponding to these transfer functions for $G = 157 \; \frac{rad}{sec}$ (25 cps) are compared to a simple second order system having a natural frequency of 25 cps and a 0.5 damping ratio in Figure 3-11.
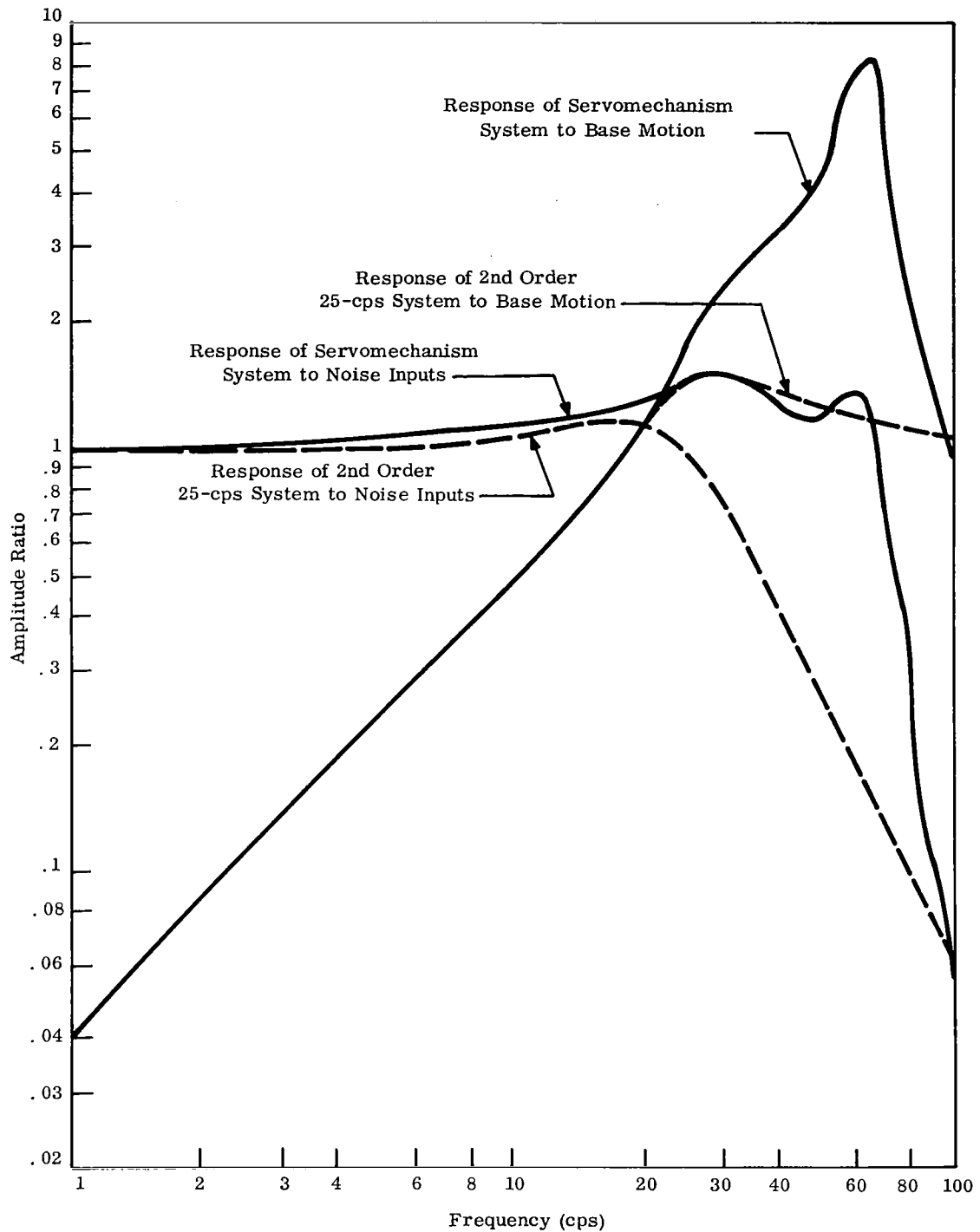
Figure 3-11. Servomechanism System Frequency Response Characteristics

It is seen that the behaviour of this system is approximately the same as a 25 cps second order system for frequencies below 20 cps. The structural resonance and form of compensation selected, however, result in an amplification of the base motion for frequencies between 20 and 100 cps and an extension of the response to noise signals to about 70 cps. These amplifications are not exceptionally serious since the passive isolation system strongly attenuates ground motions at these frequencies and there is no known source for large gyro noise signals in this frequency range. Although for computation purposes gyroscope drift rate and noise has been represented as a continuous spectrum, the major gyro noise contributions for a gas bearing instrument occur at the wheel frequency of 400 cps and the half wheel speed frequency of 200 cps which is outside the range where the system amplifies gyro noise.

The shaft angle angular velocity and acceleration that the drive shaft must move through in response to the noise signal are given by:

$$\frac{\alpha(s)}{n(s)} = Q\left(\frac{\delta(s)}{n(s)}\right)\frac{\left(1 + \frac{2\beta s}{\omega_n} + \frac{s^2}{\omega_n^2}\right)}{\left(1 + \frac{2\beta s}{\omega_n}\right)}$$

(3-28a)

$$\frac{\dot\alpha(s)}{n(s)} = s \frac{\alpha(s)}{n(s)} \tag{3-28b}$$

$$\frac{\ddot\alpha(s)}{n(s)} = s^2 \frac{\alpha(s)}{n(s)} \tag{3-28c}$$

The velocity and acceleration spectral densities that are implied by this transfer function and the noise spectral density given in Section II are plotted in Figure 3-12 and indicate an rms angular velocity of about .007 rad/sec and an rms angular acceleration of about 200 rad/sec^2 in response to sensor noise inputs. These motions are within the capabilities of the drive mechanism.

An alternate compensation scheme for increasing the system bandpass is to introduce a second order lead network that will cancel the amplification produced by the mechanical resonance. This would result in an open loop transfer function of:

$$\frac{\Phi(s)}{\delta(s)} = \frac{G}{s(1 + \tau_g s)} \tag{3-29}$$

the resulting closed loop response to base motions would be:

101
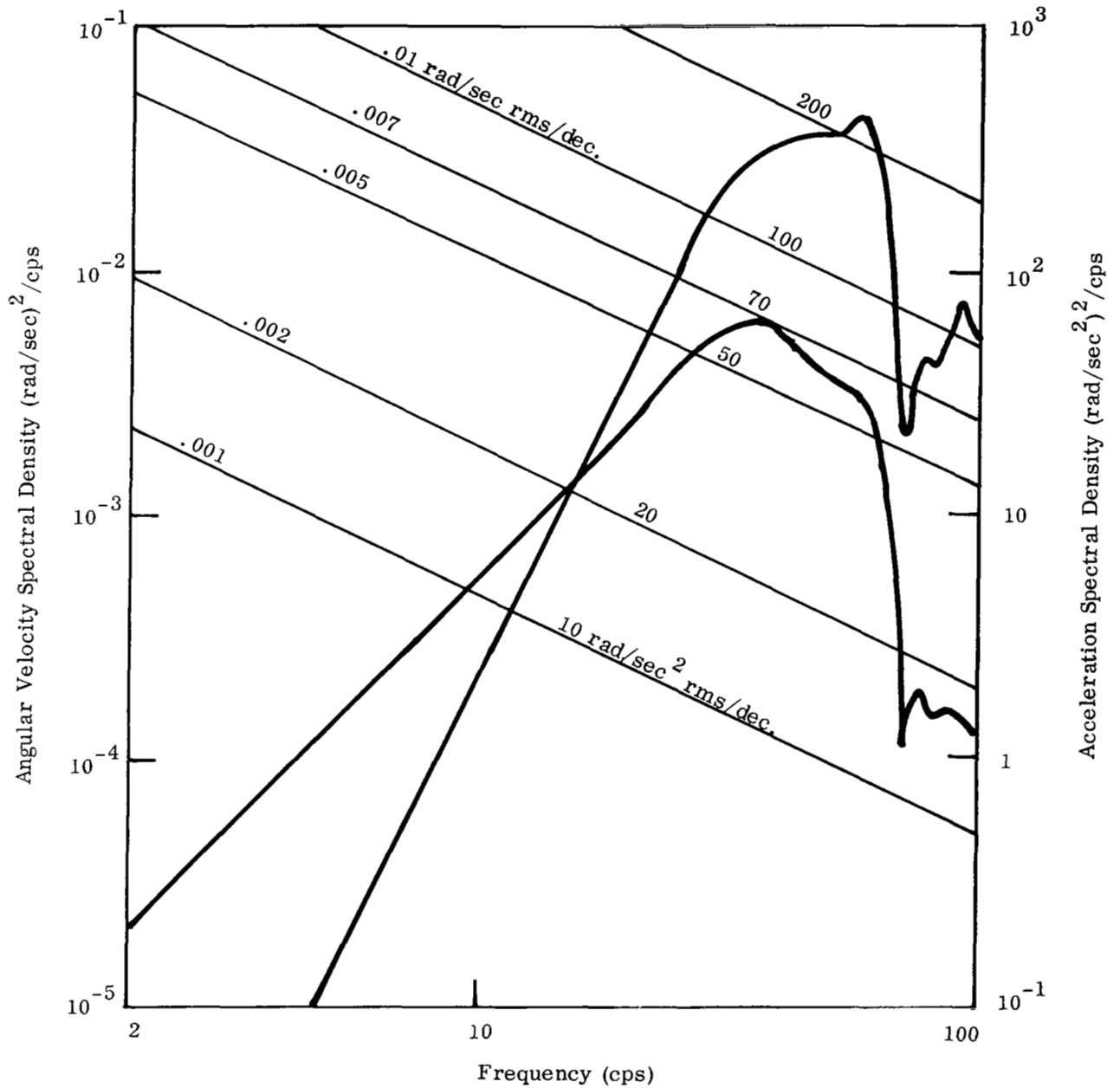
Figure 3-12. Shaft Angular Velocity and Acceleration Required by Gyro Noise

102

$$\frac{\delta(s)}{\theta_o(s)} = \frac{\left[\frac{s}{G}(1 + \tau_g s)\right](1 + \frac{2\beta s}{\omega_n})}{\left[1 + \frac{s}{G}(1 + \tau_g s)\right](1 + \frac{2\beta s}{\omega_n} + \frac{s^2}{\omega_n^2})} \qquad (3-30)$$

the response to control sensor noise would be:

$$\frac{\delta(s)}{n(s)} = \frac{1}{1 + \frac{s}{G}(1 + \tau_g s)} \qquad (3-31)$$

The shaft angle required to respond to the gyro noise is given by:

$$\frac{\alpha(s)}{n(s)} = \frac{Q(1 + \frac{2\beta s}{\omega_n} + \frac{s^2}{\omega_n^2})}{\left[1 + \frac{s}{G}(1 + \tau_g s)\right](1 + \frac{2\beta s}{\omega_n})} \qquad (3-32)$$

To approximate a 25 cps second order system with $\tau_g = 0.006$ sec., $G = 157$ rad/sec.

This compensation scheme results in a higher amplification of the base motion at the mechanical natural frequency and a smaller platform response to gyro noise. The shaft angular velocity and acceleration required for this type of compensation becomes quite large for noise inputs at higher frequencies. For the noise spectrum given in Section II infinite shaft angular velocities and accelerations are required. Since the principal noise inputs occur at 200 and 400 cps,

103

this type of compensation is not recommended in the initial construction of the system. The "optimum" frequency characteristic given in Section II also implies lead compensation of this type and larger platform and shaft angle noise responses than discussed here. Therefore in the initial construction of the system, based on the above considerations and the estimates of instrument noise and environmental ground motions, it is recommended that the compensation be of the form represented by Equation 3-25 . Once the actual noise inputs of the instruments and electronics are determined and the base motions transmitted by the passive system measured at the final system location, it would be desirable to **reevaluate** the form of compensation to be used to obtain the best overall system performance.

3.3 Inertia Isolation System

As discussed above the servomechanism system does not provide any isolation at frequencies between 20 and 100 cps and amplifies any motions of its base in this frequency range. To attenuate the transmission of these base motions from the ground a massive

conventional spring-mass isolation system is employed.
The mass and inertia of the isolation system are
obtained from an 8 foot steel weldment having a six
foot square mounting surface for the servomechanism
system. This frame is supported at the four corners
by air springs of the type used in the Barry Wright
serva level isolation system. These air springs are
shown schematically in Figure 3-13 and are discussed
in considerable detail in Reference 8. The change
in force due to a change in deflection of these air
springs is given in Reference 8 as:

$$\frac{F(s)}{x(s)} = \frac{nP_oA^2}{V_c} \left[\frac{1 + c_1s}{N + 1 + c_1s} \right] + \frac{G_1}{s}$$

$$= \frac{K_T}{N+1} \left[\frac{1 + T\,c_1\,s}{1 + \dfrac{c_1s}{N+1}} \right] + \frac{G_1}{s} \tag{3-33}$$

The first portion of this transfer function is equivalent
to the spring dashpot arrangement (filtered damper) shown
in Figure 3-13 where the force due to a change in dis-
placement is given by:

$$\frac{F_1(s)}{x(s)} = k_1 + Nk_1 \left(\frac{cs}{Nk_1 + cs} \right) \tag{3-34}$$

105
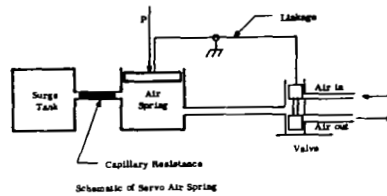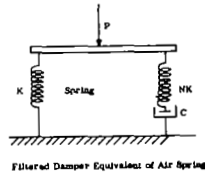
Figure 3-13a.   Schematic of Air Springs Used in Isolation System
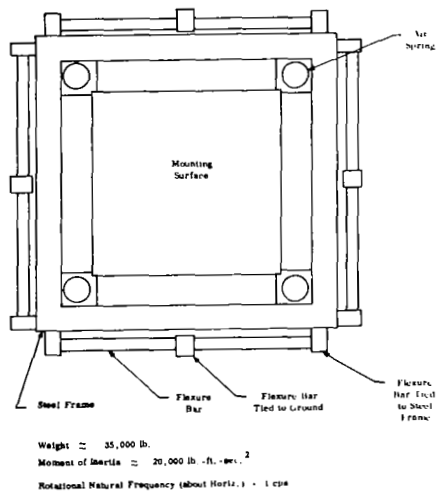
Figure 3-13b.   Inertia Isolation System

$$= k_1 \left[\frac{1 + \frac{N+1}{N}\ cs}{1 + \frac{cs}{N}} \right]$$

$$= k_1 \left[\frac{1 + c_1 s}{1 + \frac{c_1 s}{N+1}} \right]$$

At very low frequencies the filtered damper (first portion of the transfer function) behaves as a simple spring damper arrangement having a stiffness k_1 and viscous damping of $k_1\ c_1$. At high frequencies the dashpot effectively becomes locked (the capillary resistance is effectively sealed) and the function behaves as a spring having a stiffness of $(n+1) k_1$. The characteristics of vibration isolation systems employing filtered dampers are discussed in some detail in Reference 18.

The torque exerted by the four air springs due to rotation θ about a horizontal axis is:

$$\frac{M(s)}{\Theta(s)} = 4 \left[\frac{F(s)}{x(s)} \right] \frac{\ell^2}{4} = \left[\frac{F(s)}{x(s)} \right] \ell^2$$

$$= \frac{K_\theta}{N+1} \left[\frac{1 + c_1 s}{1 + \frac{c_1 s}{N+1}} \right] + \frac{G}{s} \tag{3-35}$$

107

The response of the platform to ground motions is given by:

$$\frac{\Theta_1(s)}{\Theta_o(s)} = \frac{\dfrac{K_\Theta}{N+1}\left[\dfrac{1 + c_1 s}{1 + \dfrac{c_1 s}{N+1}}\right] + \dfrac{G}{s}}{\dfrac{K_\Theta}{N+1}\left[\dfrac{1 + c_1 s}{1 + \dfrac{c_1 s}{N+1}}\right] + \dfrac{G}{s} + Is^2}$$

(3-36)

and the response to external torques is:

$$\frac{\Theta_1(s)}{M(s)} = \frac{1}{\dfrac{K_\Theta}{N+1}\left[\dfrac{1 + c_1 s}{1 + \dfrac{c_1 s}{N+1}}\right] + \dfrac{G}{s} + Is^2}$$

(3-37)

the substitutions:

$$\alpha = \frac{(N+1)G}{K_\Theta \, \omega_n}$$

$$\beta = \frac{1}{2} c_1 \omega_n$$

$$\omega_n = 2\pi f_n = \sqrt{\frac{K_\Theta}{I(N+1)}}$$

permit the above transfer functions to be rewritten as:

$$\frac{\Theta_1(s)}{\Theta_0(s)} = \frac{\left[\dfrac{1 + \dfrac{2\beta s}{\omega_n}}{1 + \dfrac{2\beta}{N+1}\dfrac{s}{\omega_n}}\right] + \dfrac{\alpha\,\omega_n}{s}}{\dfrac{s^2}{\omega_n^2} + \left[\dfrac{1 + \dfrac{2\beta s}{\omega_n}}{1 + \dfrac{2\beta}{N+1}\dfrac{s}{\omega_n}}\right] + \dfrac{\alpha\,\omega_n}{s}} \qquad (3\text{-}38)$$

$$\frac{\Theta_1(s)}{M(s)} = \frac{1/K_\Theta}{\dfrac{s^2}{\omega_n^2} + \left[\dfrac{1 + \dfrac{2\beta s}{\omega_n}}{1 + \dfrac{2\beta}{N+1}\dfrac{s}{\omega_n}}\right] + \dfrac{\alpha\,\omega_n}{s}} \qquad (3\text{-}39)$$

The frequency response characteristics correspond-
ing to these transfer functions for $\beta = 0.5$, $N = 8$,
$\alpha = 0.1$ and a natural frequency of 1 cps are plotted
in Figure 3-14 . It is seen that these response
functions closely approximate the transfer functions
given in Section II for frequencies below 10 cps and
behave as an undamped 3 cps natural frequency system
for frequencies above 10 cps. In Reference 19
Barry Wright Corporation states that a system having
the transfer functions given above can be built by
simple modifications of existing designs for the
masses and inertias considered. The Heath isolation
system (Reference 7) has a 40,000 lb mass and a 0.6 cps
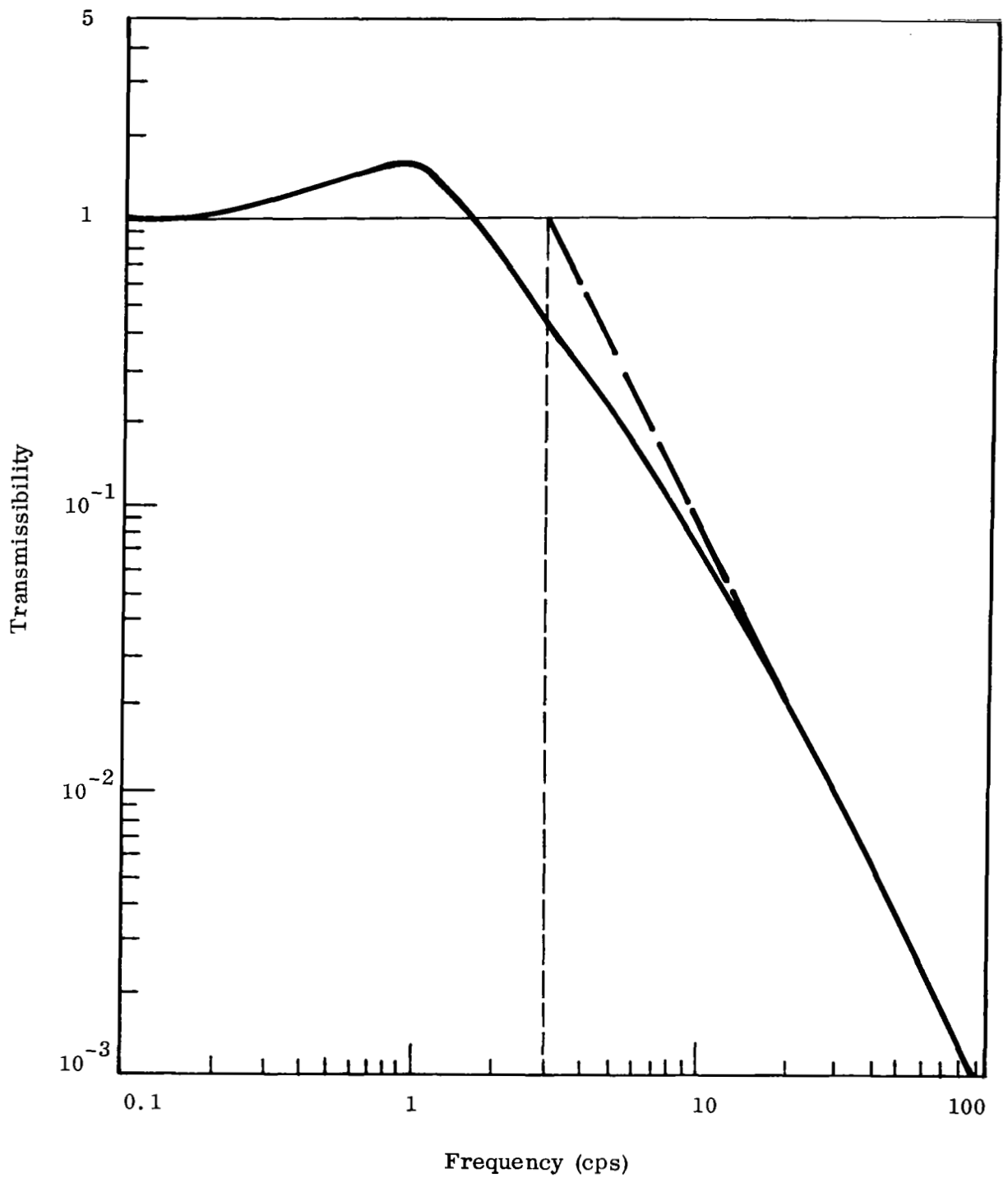
Figure 3-14. Response of Inertia Isolation System to Ground Motions

vertical natural frequency which represents a more difficult design than considered here. The damping required may, however, make it desirable to use viscous dampers to complement the damping provided by the air springs.

The air springs are to be located inside the weldment to provide a higher vertical than rotational natural frequencies. To avoid coupling between translational and rotational motions the centers of horizontal and vertical stiffnesses shall coincide with the gravity center.

Since the air springs usually have poor lateral stability the flexure bars shown in Figure 3-13 are included to provide a large horizontal stiffness and rotational stiffness about a vertical axis while maintaining a low vertical natural frequency and low rotational natural frequencies about the horizontal axes.

The transient response to step torque inputs is obtained from the inverse Laplace transform of the transfer function:

$$\theta_1(t) = M_d L^{-1} \frac{1}{s} \left[\frac{\theta_1(s)}{M(s)} \right]$$

(3-40)

$$\theta_1(t) = \frac{M_d}{K_\theta} \left[1.2e^{-0.111\omega_n t} - 1.2e^{-0.435\omega_n t} \cos.911\omega_n t \right.$$

$$\left. - 0.44e^{-0.435\omega_n t} \sin.911\omega_n t \right]$$

$$(3-41)$$

This transient is plotted in Figure 3-15 for a 250 lb-ft torque load.

3.4 Total System Performance

As discussed in Section II, the large ratio of the inertia of the inertia isolation system to the inertia of the servomechanism system permits independent treatment of the two systems. Therefore the total system response to ground rotations is given by:

$$\frac{\delta(s)}{\theta_o(s)} = \left(\frac{\delta(s)}{\theta_1(s)}\right)\left(\frac{\theta_1(s)}{\theta_o(s)}\right) \qquad (3-42)$$

The response of the system to accelerations (assuming direct transmission by the inertia system) is:

$$\frac{\delta(s)}{\varepsilon_a(s)} = \frac{v_a(s)}{v_\delta(s)} \quad \frac{\delta(s)}{n(s)} \qquad (3-43)$$

and the response to the gyro drift angle is:

$$\frac{\delta(s)}{\varepsilon_g(s)} = \frac{v_g(s)}{v_\delta(s)} \quad \frac{\delta(s)}{n(s)} \qquad (3-44)$$

112
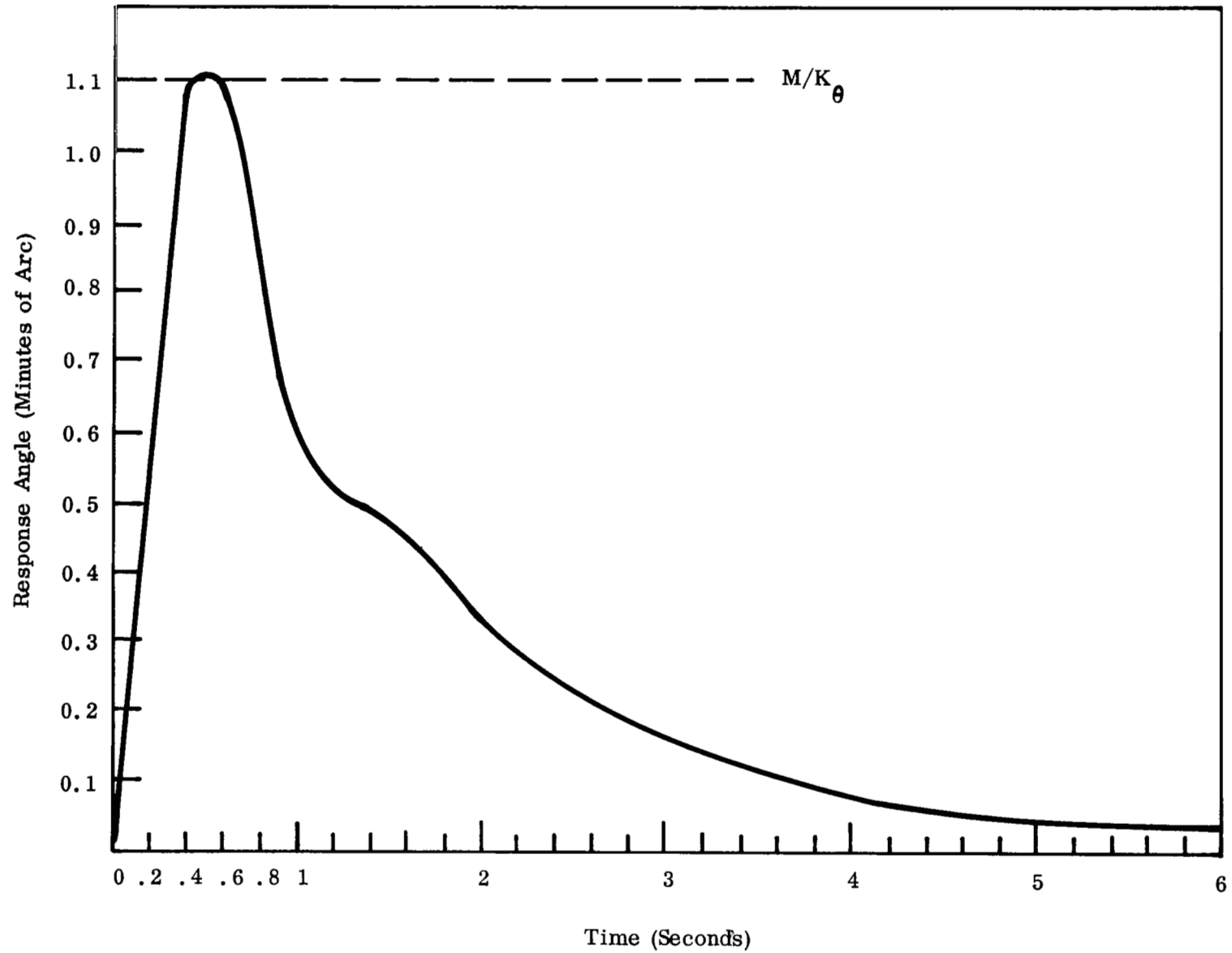
Figure 3-15.   Transient Response of Inertia Isolation System to Step Torque of 250 lb-ft.

The frequency response characteristics of these transfer functions are shown in Figure 3-16 The spectral densities of the responses to the reference environmental motions and the gyroscope noise spectrum are plotted in Figure 3-17 and indicate compliance with the design requirements given in Section I.

The response to the transient motion of the inertia isolation system is obtained from the inverse Laplace transform as:

$$\delta(t) = L^{-1}\theta_1(s)\left[\frac{\delta(s)}{\theta_1(s)}\right] \tag{3-45}$$

$$\frac{K_\theta \delta(t)}{M} = 0.054e^{-0.437\omega_n t}\sin 0.911\omega_n t$$

$$+ 0.0049e^{-0.437\omega_n t}\cos 0.911\omega_n t$$

$$- 0.0054e^{-0.111\omega_n t} + \text{small terms at 25}$$

$$\text{and 70 cps.}$$

For the torque of 250 lb-ft and a moment of inertia of 2×10^4 lb-ft-sec^2 $M/K_\theta = 65.3$ $\widehat{\text{sec}}$ resulting in a maximum platform error of about 2 $\widehat{\text{sec}}$. After a two second period the platform error due to the base motion is less than 0.01 $\widehat{\text{sec}}$.
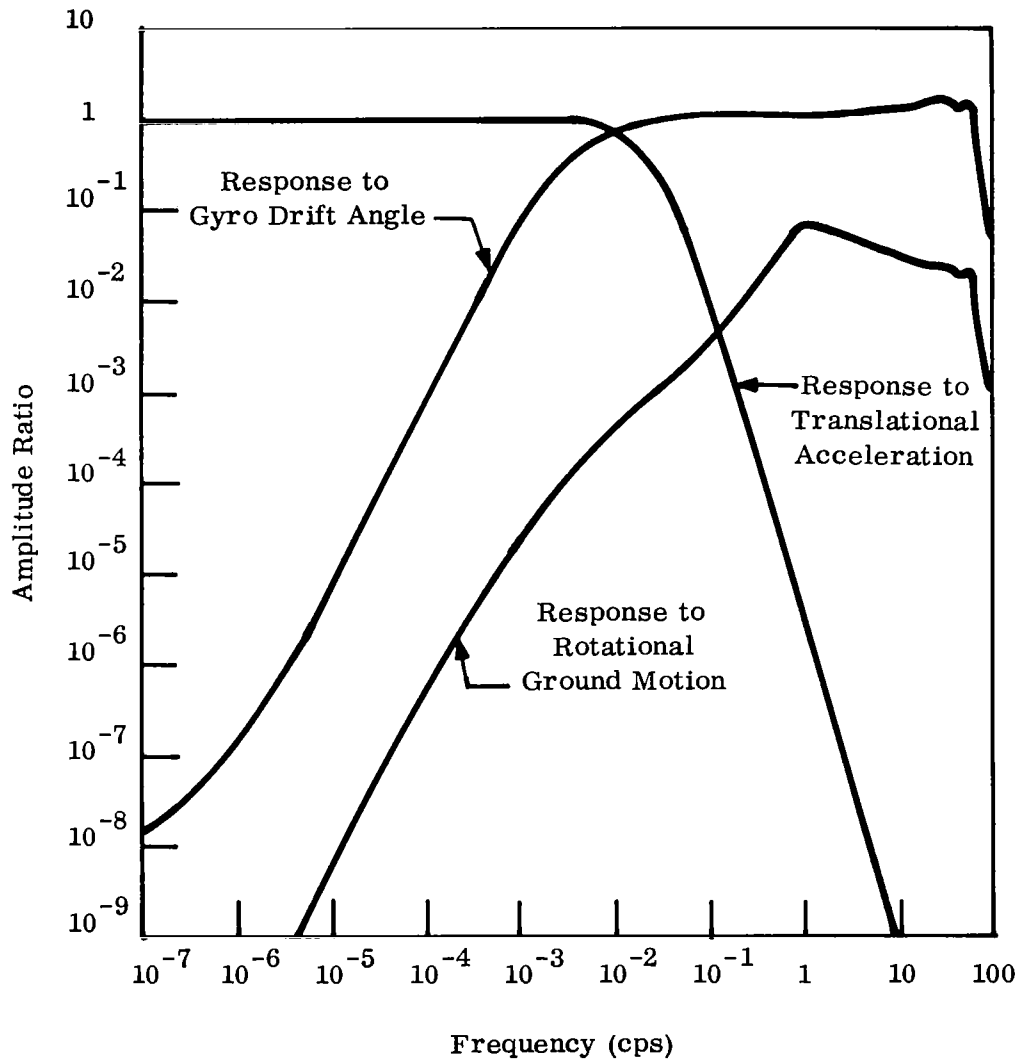
Figure 3-16. Frequency Response Characteristics of Completed Isolation System

"1 sec rms per decade"
Area under this line is 1 sec^2 rms
between 1 and 10 cps and for any
two frequencies separated by a
factor of 10 the area under the
line corresponds to 1 sec rms.
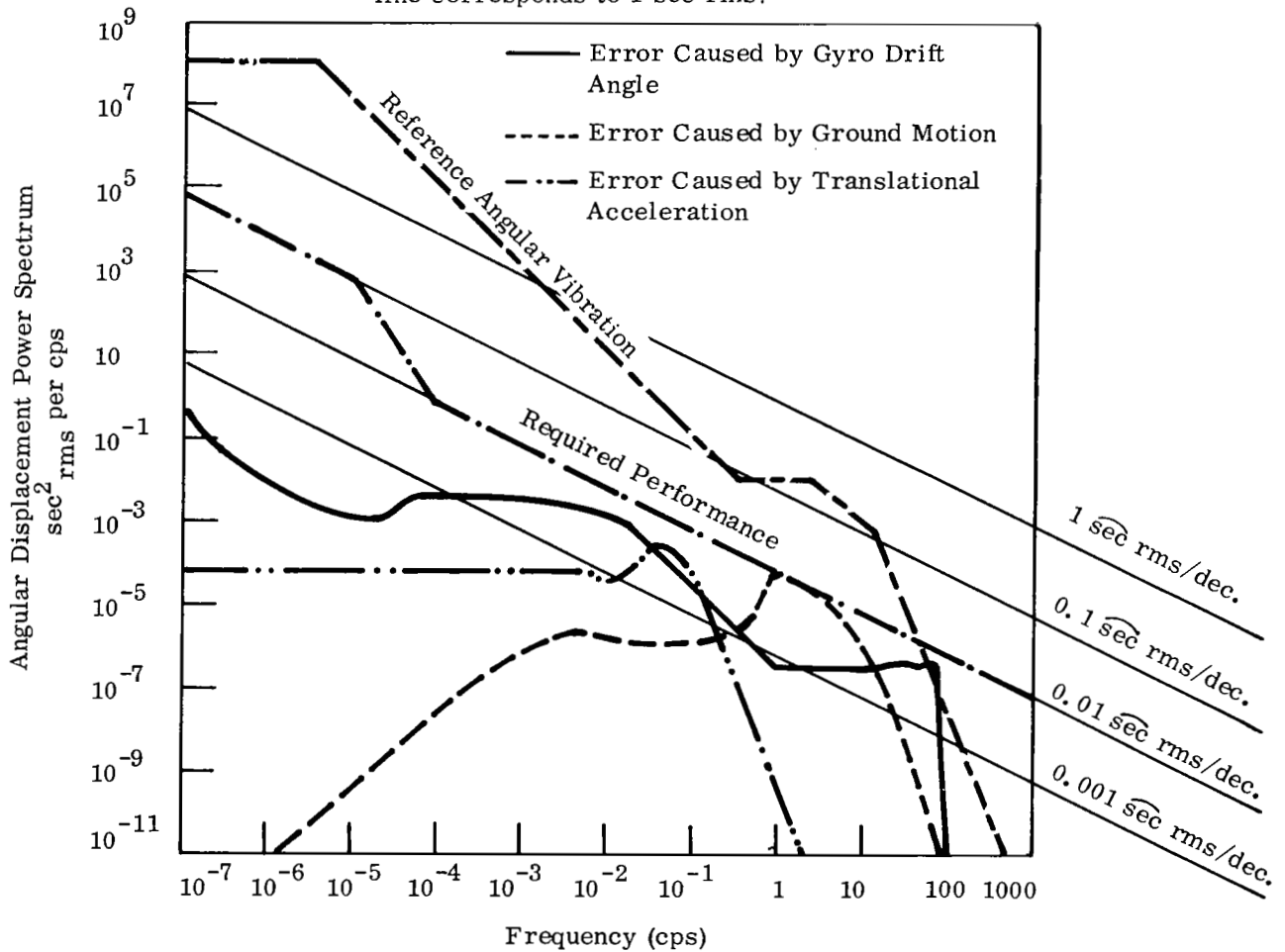
Figure 3-17. Spectral Density of Complete Isolation System
in Reference Environment

In addition to compensating for the motions of the inertia isolation system, the servomechanism system must compensate for the angular deflection of the drive due to its own compliance. When a 250 lb-ft load is applied the drive compliance implies a static deflection of the drive of about 0.4 arc seconds which, with no servo system, would be accompanied by a 70 cps oscillation having an amplitude of 0.4 arc seconds. decaying exponentially with a time constant of $1/(0.05 \times 2\pi \times 70) = .045$ sec. The maximum excursion of the system is therefore estimated at about 2.8 arc seconds which is again in compliance with the design requirements given in Section I.

SECTION IV

EXPERIMENTAL MODEL OF SERVOMECHANISM ISOLATION SYSTEM

4.0 Introduction

An experimental model of the servomechanism portion of the tilt and rotational vibration isolation system described in this document has been constructed. This model serves to provide a test base for evaluation of control sensors to be used in the final isolation system and to permit experimental verification of the dynamics and performance predicted in this document. The model consists of a 5 3/4 foot steel triangular weldment which is pivoted on two points and driven at the third point of the triangle by an M.I.T. Instrumentation Laboratory micromotion drive modified as indicated in Figure 3-7. The platform is loaded by 2,100 lb. of lead weight to provide a total load of 3,000 lb. The level used to command the gyroscope instrument is a dual cistern Ideal Aerosmith Company Tiltmeter described in Section III.

High frequency control for the platform was initially obtained from the gas bearing King II gyroscope described in Section III. A failure of a power lead in the course of the test program required replacement of the gas bearing instrument with a King II ball bearing gyroscope having similar electrical characteristics for continuation of the experimental work. A photograph of the experimental system is shown as Figure 4-1. A schematic drawing of the
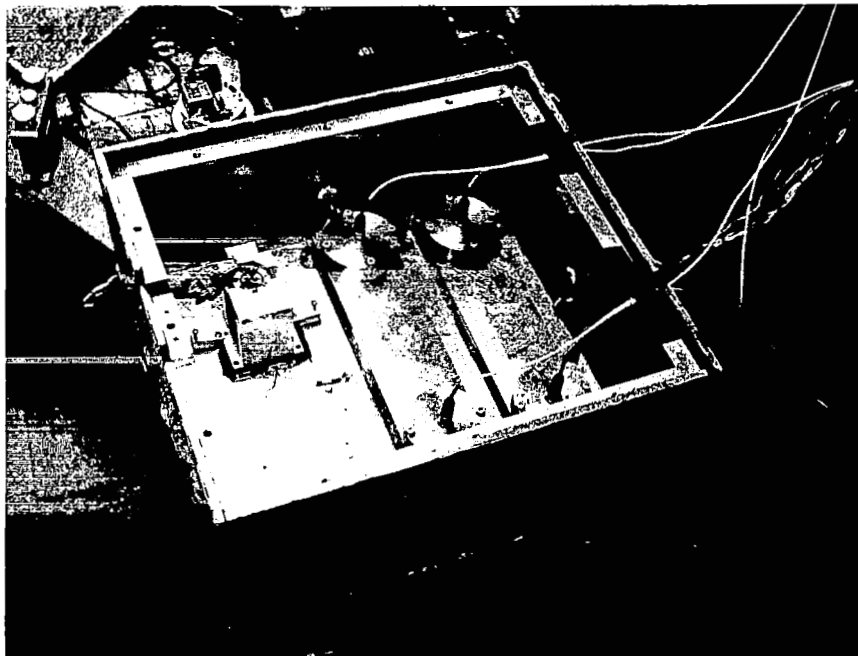
Figure 4-1. Overall View of Experimental System (top) and Closeup View Showing Control and Monitor Tiltmeter and Control Gyroscope (left)

119

electronics used to close the control loop is shown in Figure 4-2. A block diagram of the experimental system is shown in Figure 4-3. The dynamics of the experimental system and its electronics are similar to those discussed in Section III with the exceptions that the ball bearing instrument has a nominal gain of 4 and a time constant of 0.003 seconds and flexibility has been included to permit varying the frequency at which the gyroscope instrument assumes control and the response to signals from the level falls off. Provision is also included for using only the level for control of the system and for using only the gyroscope instrument for control. The drive compliance of 13 microinches per lb and other flexibilities in the floor and structure result in a 27 cps mechanical resonant frequency limiting the system response to that of a 9 cps system. The tests conducted on the experimental system are described in the following paragraphs:

4.1 Level Calibration

Long term tests were conducted using the level loop of the experimental system. The system gain was adjusted to produce a damped natural frequency of about 0.05 cps to avoid oscillations as a result of translational accelerations. The system response was also limited by the tiltmeter dynamics. The tiltmeter has an apparent time constant of about 3 seconds and a sloshing natural
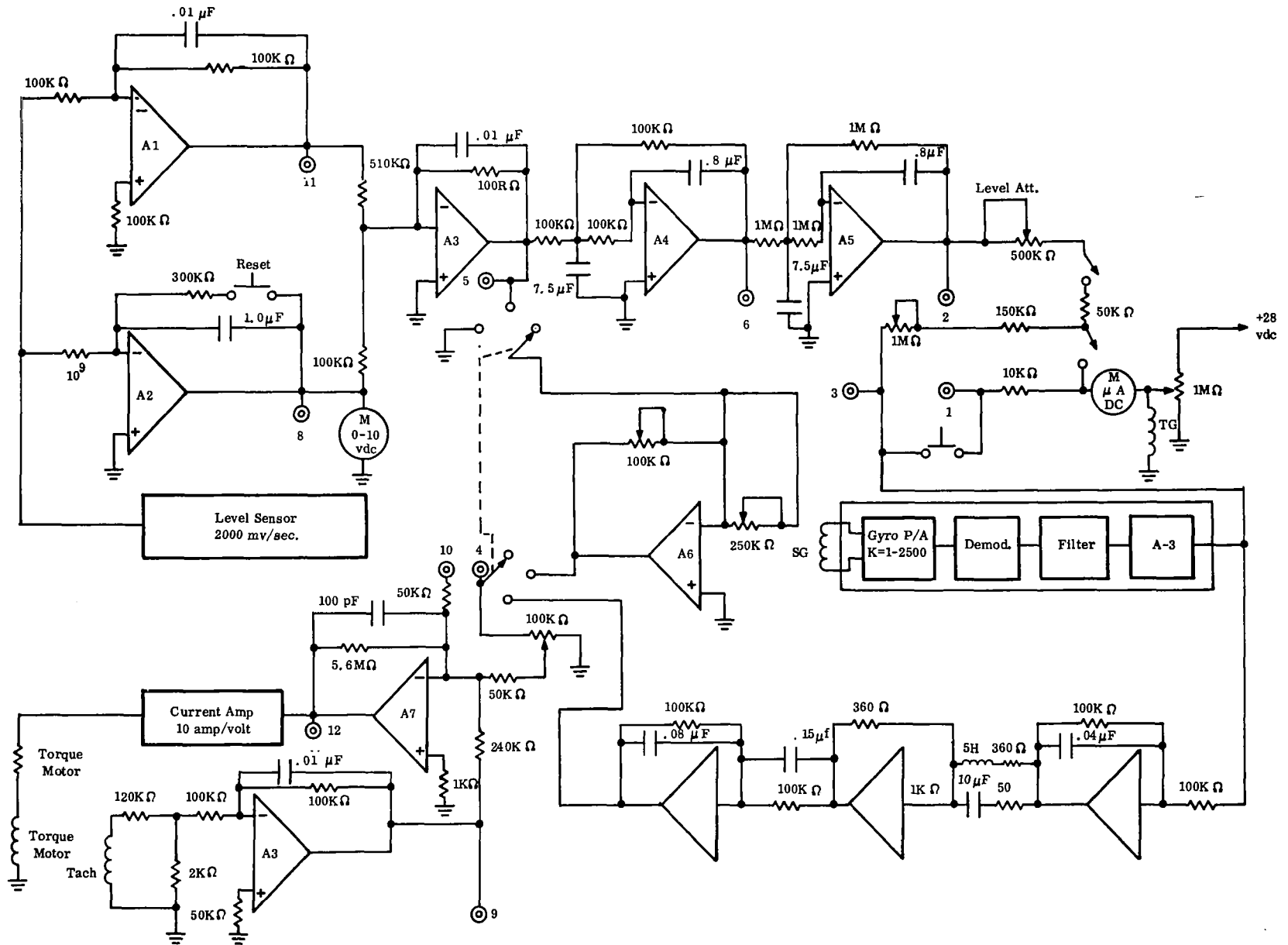
Figure 4-2. Schematic of Electronics Used in Experimental Platform

121

Ground Motion θ_0

Structure Dynamics

$$\frac{1 + 0.1\frac{S}{170}}{1 + 0.1\frac{S}{170} + \frac{S^2}{170^2}}$$

Error Angle δ

Tiltmeter

$$2\frac{\text{volt}}{\text{sec}}$$

Tiltmeter Filter

$$\frac{0.196\left(1 + \frac{5.1 \times 10^{-3}}{S}\right)}{(1 + 2.5S + 6.25S^2)(1 + 0.25S + .0625S^2)}$$

S

$\dot{\delta}$

Gyro Torquer

$$\frac{50\frac{\text{sec}}{\text{sec}}}{\text{ma}}$$

$$\frac{.02\frac{\text{ma}}{\text{volt}}}{1 + R_1/10^4}$$

$$2.06 \times 10^5 \frac{\text{sec}}{\text{rad}}$$

$$\frac{10^{-5}}{2.25}$$ **Mech Advantage**

$$\frac{h}{S(1 + \tau_g S)}$$

Gyro Dynamics

$$0.167\frac{\text{mv}}{\text{sec}}$$

Gyro Sig. Gen.

1000

Preamp & Demod Goerz

$$10^{-6} \text{ to } 6.7 \times 10^{-6}\frac{\text{ma}}{\text{mv}}$$

$$\frac{1}{S}$$

Potentiometer

$$.24\frac{\frac{\text{rad}}{\text{sec}}}{\text{volt}}$$

Motor

$+$

Potentiometer

$0 \text{ to } 1$

Test Signal

$$\frac{(1 + .015S)(1 + 0.004S + \frac{S^2}{140^2})}{(1 + .008S)(1 + .005S)(1 + .004S)(1 + 0.014S + \frac{S^2}{374^2})}$$

Servo Compensation

Gas Bearing:

$h = 8.8$
$\tau_g = 0.006$ sec

Ball Bearing:

$h = 4.4$
$\tau_g = 0.003$ sec

Figure 4-3.   Block Diagram of Experimental Servomechanism Levelling System

frequency at about 6 cps. A second Ideal-Aerosmith Tiltmeter was used to monitor the performance of the system. The indicated drift of the system as reported by the monitoring tiltmeter is plotted in Figures 4-4 and 4-5. With the exception of transients produced by disturbance torques, the tiltmeter used for control of the system reported deviations from level no greater than $\pm$ 0.05 arc seconds. The drifts indicated in Figures 4-4 and 4-5 therefore represent the disagreement between the two tiltmeters. The direction of the monitor tiltmeter is reversed in the two test runs, so that if there was an equal drift of the two instruments the drifts would add in one test and subtract in the other. The high frequency translational motions and erroneous signals produced by the sloshing of the mercury pools have been filtered in this data by a filter having a 10 second time constant.

As shown in Figure 4-5 the total drift of the platform and instruments over a fifteen day period was about 0.5 arc seconds with a maximum drift in a 24 hour period being about 0.2 arc seconds. There are a number of 24 hour periods in which the indicated drift was less than 0.1 arc seconds. A portion of this drift is due to the temperature and humidity sensitivities of the electronics of the tiltmeter. Checks of the sensitivity of the two tiltmeters were made before and after each run and were

123

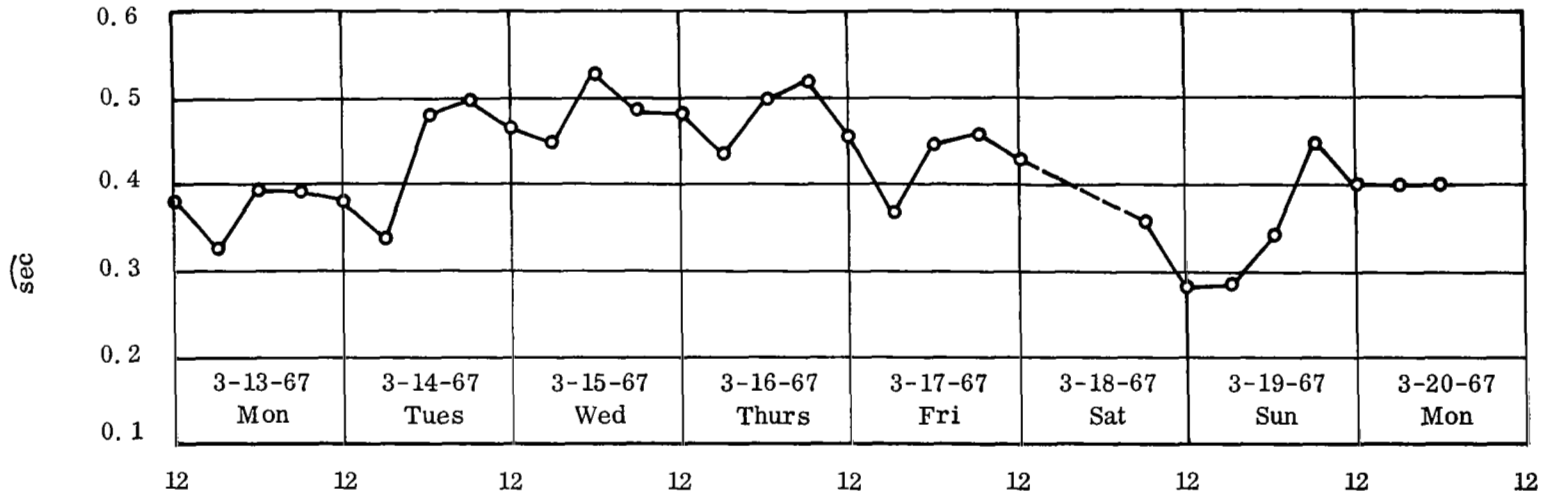Figure 4-4. Indicated Drift of Experimental Platform
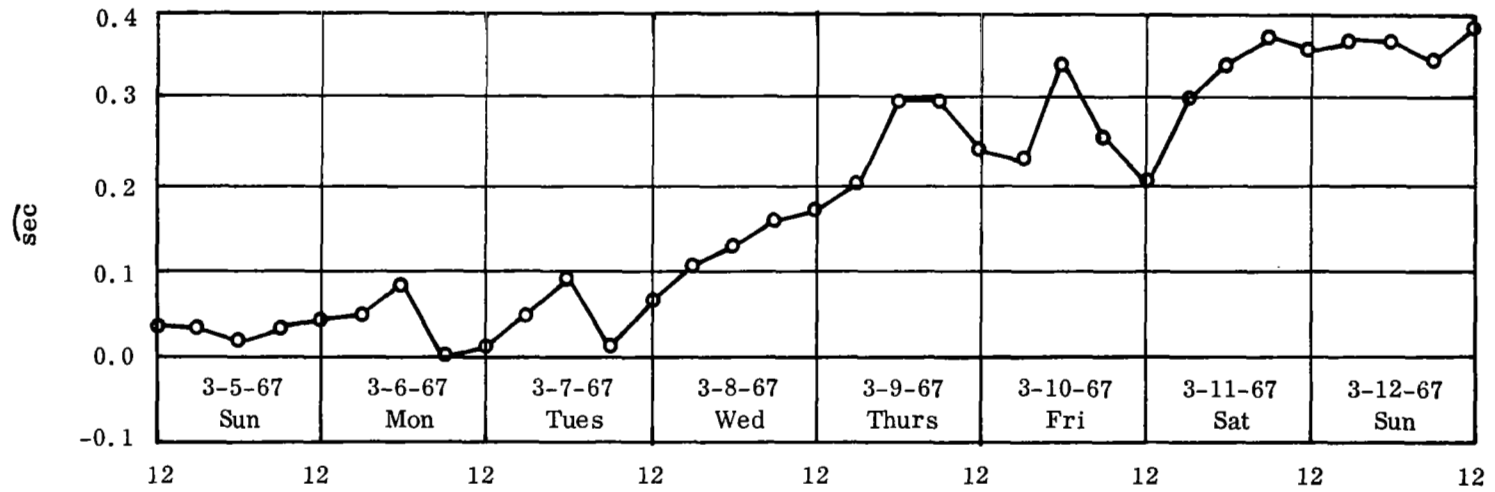
Indicated Platform Error Angle
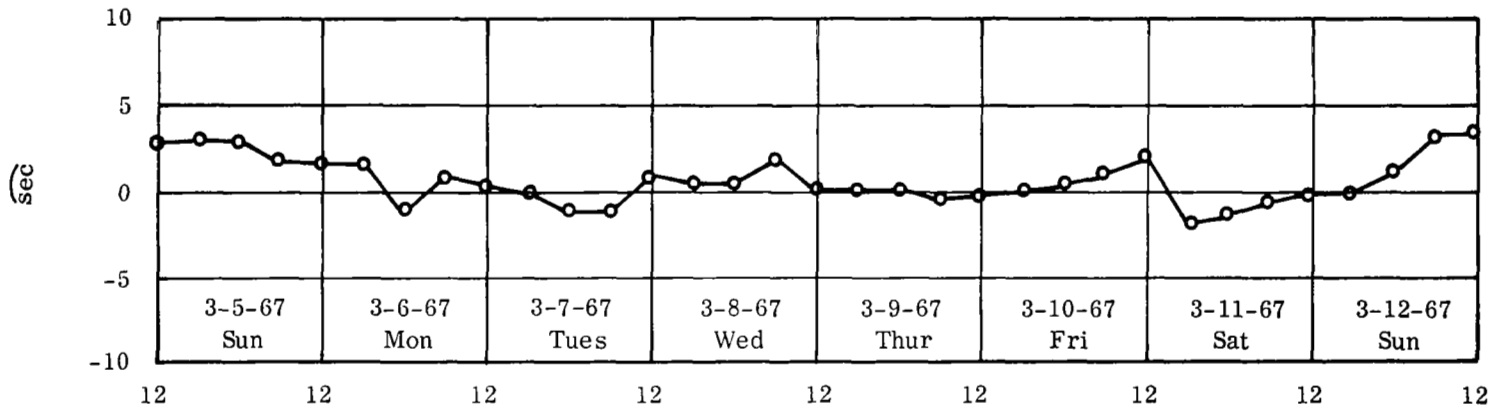
Ground Motion

Figure 4-5a. Indicated Drift of Experimental Platform

Indicated Platform Error Angle
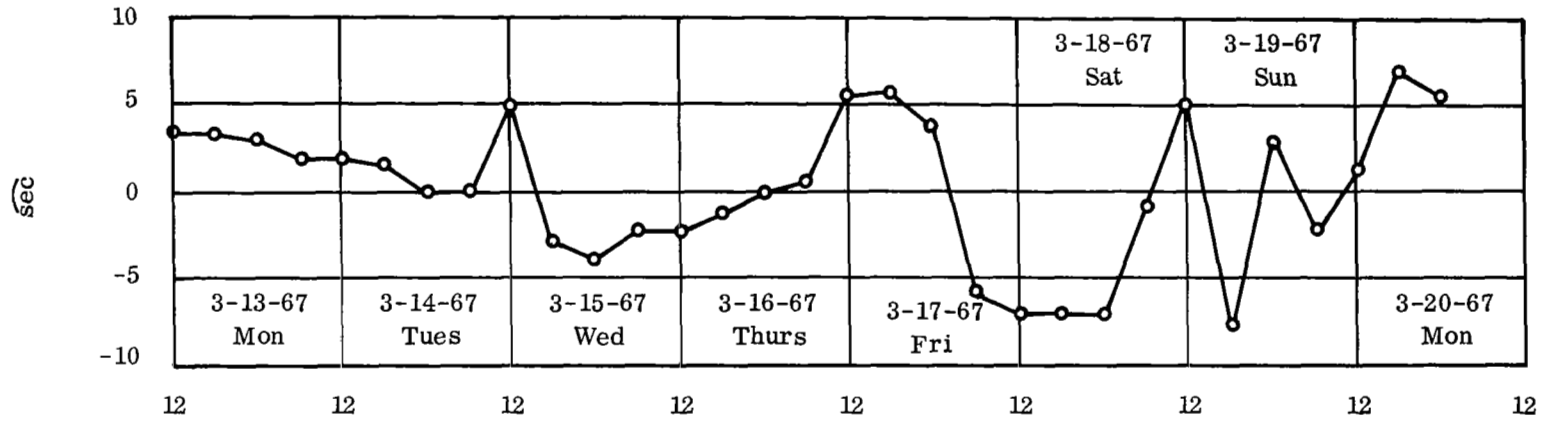
Ground Motion

Figure 4-5b. Indicated Drift of Experimental Platform

found in agreement with the manufacturers calibrations.

4.2 System Frequency Response

Measurements of the frequency response characteristics of the experimental model were made by driving the closed loop system with a sinusoidal voltage and measuring the voltage generated by the system to compensate for this disturbance. This frequency response characteristic is shown in Figure 4-6 and corresponds to the system response to noise inputs discussed in Section III. The resonant amplification of the noise response is attenuated between 10 and 27 cps by the second order lead compensation network indicated in Figures 4-2 and 4-3. As discussed in Section III this type of compensation reduces the system response to noise inputs below the resonant frequency at the expense of increasing the power required to drive the system and increasing system susceptibility to high frequency noise. The characteristics given here represent the best experimental compromise that was achieved. The response of the system to base motions is estimated from the experimentally determined frequency characteristic given in Figure 4-6 by:

$$\frac{\delta(s)}{\theta_o(s)} = \frac{(1-\delta(s))}{n(s)}\left(\frac{1 + 2\beta \frac{s}{\omega_n}}{1 + 2\beta \frac{s}{\omega_n} + \frac{s^2}{\omega_n^2}}\right)$$

127
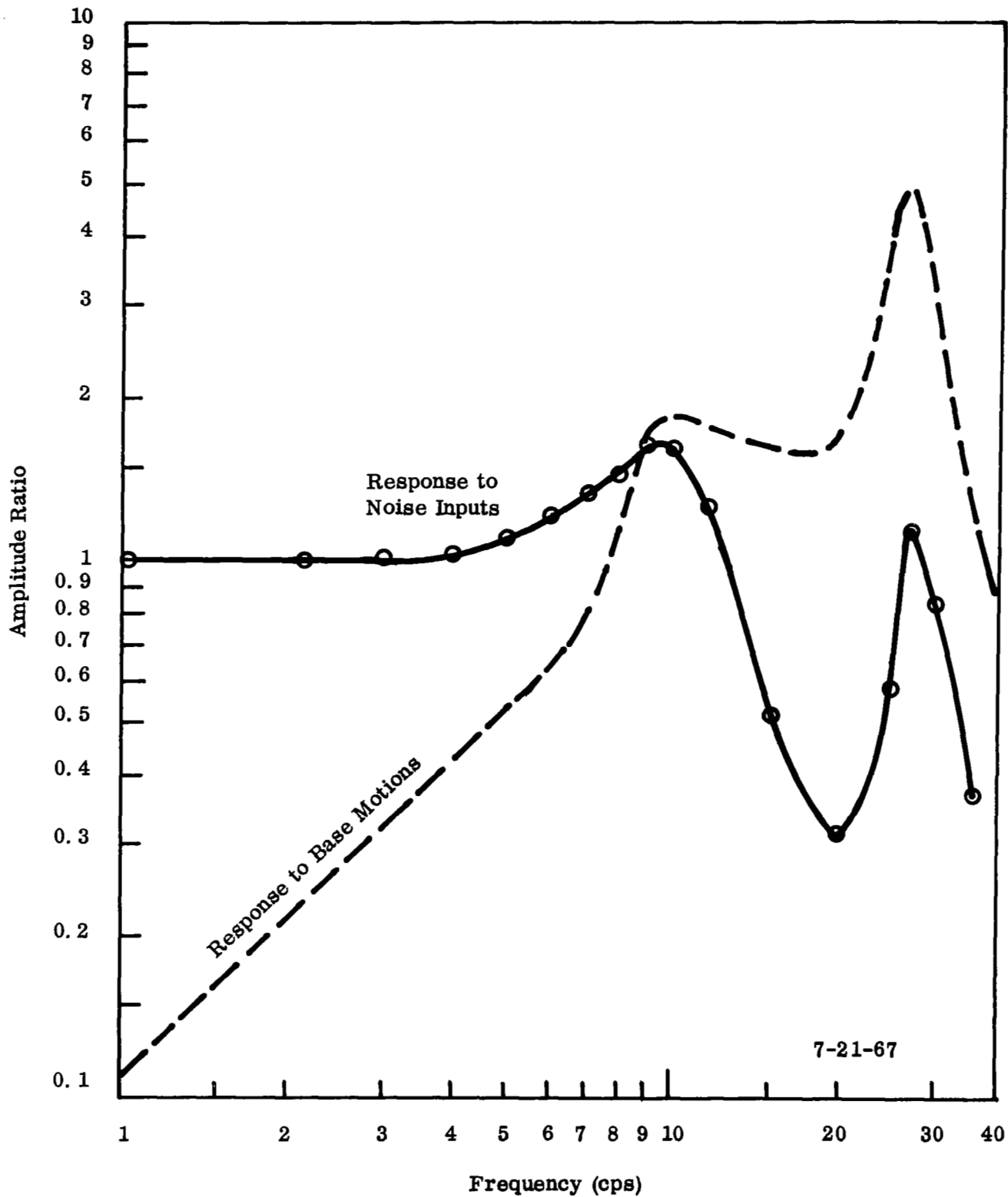
Figure 4-6. Response of Experimental System to Noise Signals and Base Motions

and is estimated in Figure 4-6.

The low frequency isolation of the servomechanism system and the high frequency inertia isolation system discussed in Section III combine to provide a transmissibility of less than 1 at all frequencies as indicated in Figure 4-7. A considerable improvement of the system attenuation of ground motions is expected with the use of the stiffer drive mechanism discussed in Section III.

4.3 Low Frequency System Performance.

At low frequencies the primary errors in the performance of the system are due to the random drift rate of the gyroscope instrument used to control the system as indicated by Figures 2-7 and 2-8. In addition, there are errors produced by the tiltmeter response to horizontal acceleration. In order to provide thermal isolation of the gyroscope, the instrument was initially mounted in a temperature controlled box which was mounted on plastic stand-offs. Drifts of the height of these stand-offs due to material creep and temperature changes in addition to the drift of the gyroscope instrument itself resulted in a noise response of the system of about 0.04 arc seconds peak to peak as indicated in Figure 4-8. The amplitude and frequency of this response appears to be independent of time of day and of the variations in the translational

Figure 4-7. Calculated Transmissibility of Experimental Servomechanism System
Mounted on Inertia Isolation System to Ground Motions

Platform Error Angle Gas Bearing Gyro 5-9-67
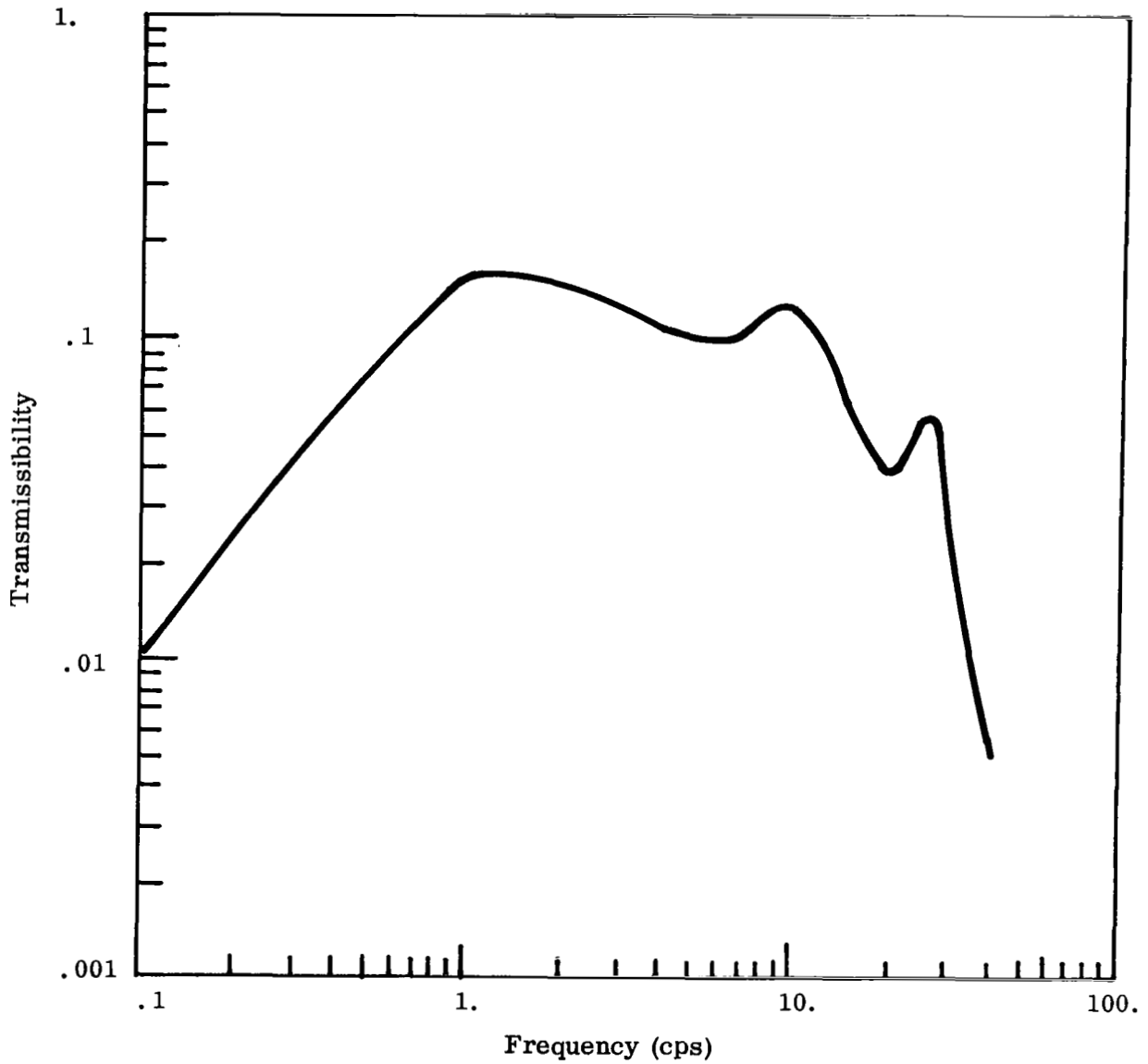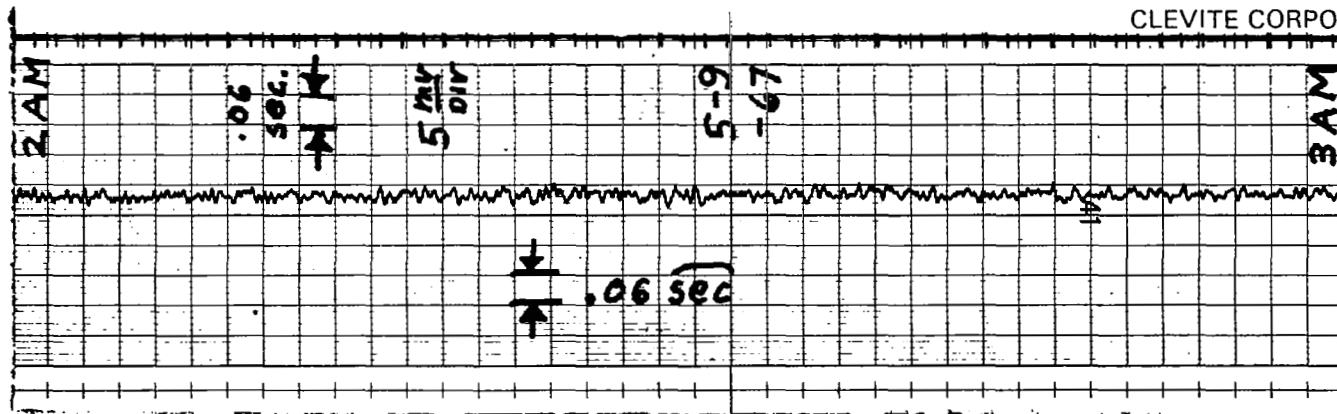Gyro Supported By Plastic Standoffs

131
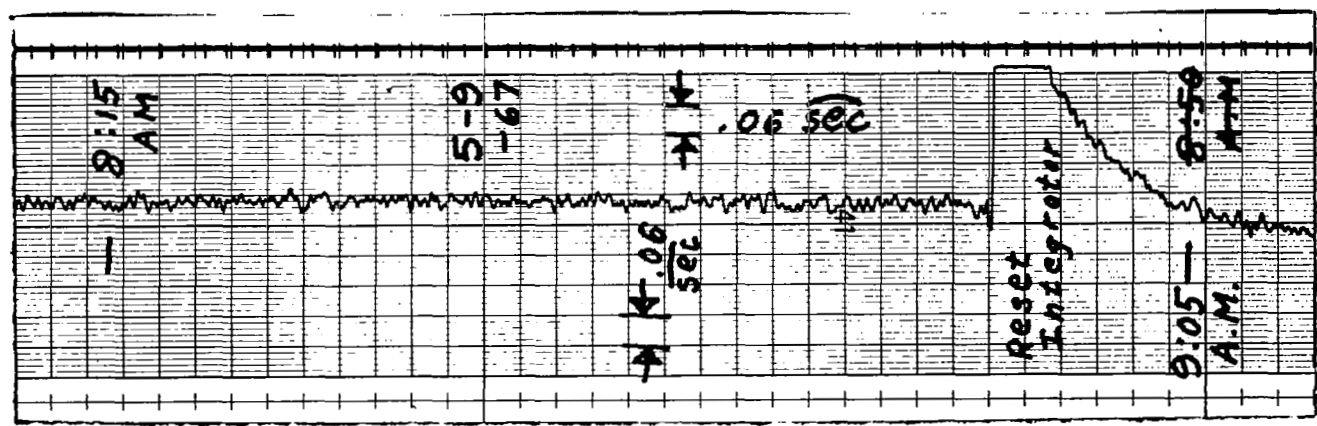
Platform Error Angle Gas Bearing Gyro 5-9-67
Gyro Supported By Plastic Standoffs

Figure 4-8.   Low Frequency Performance of System with Gas Bearing Gyroscope

acceleration environment of the laboratory. The transient response due to discharging the integrator capacitor shows the 200 second time constant associated with the system's compensation of long term gyro drift rate. During the course of the tests there was a failure of a power lead of the gas bearing instrument. The instrument was replaced by an available ball bearing gyroscope. Figure 4-9 shows the difference in platform error produced by the larger noise and drift rate associated with the ball bearing gyroscope instrument. The slow drift that is seen in Figure 4-9 was later found to be due to a d.c. drift of the integration amplifier. The effects of this drift were reduced by increasing the sensitivity of the tiltmeter electronics and reducing the bias level of this amplifier. In the course of attempting to locate this d.c. drift, however, it was found that a factor of two reduction in the noise response of the system was achieved by simply removing the plastic stand-offs as shown in Figure 4-10. As indicated by Figure 4-11 the gyro drift rate of the instrument is strongly sensitive to changes in temperature. The transient responses shown in Figure 4-12 are the result of changing the ambient temperature of the gyro by about $1^{\circ}F$. After improvements in the instrument and the temperature control the low frequency noise produced by the ball

Platform Error Angle for Gas Bearing Gyro   5-10-67

Platform Error Angle for Ball Bearing Gyro   5-11-67
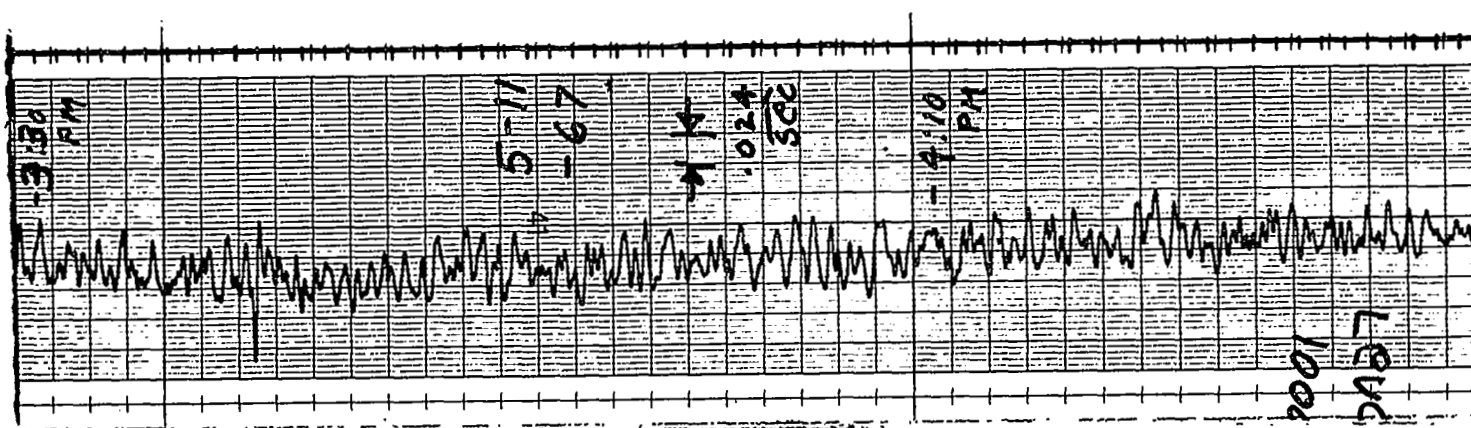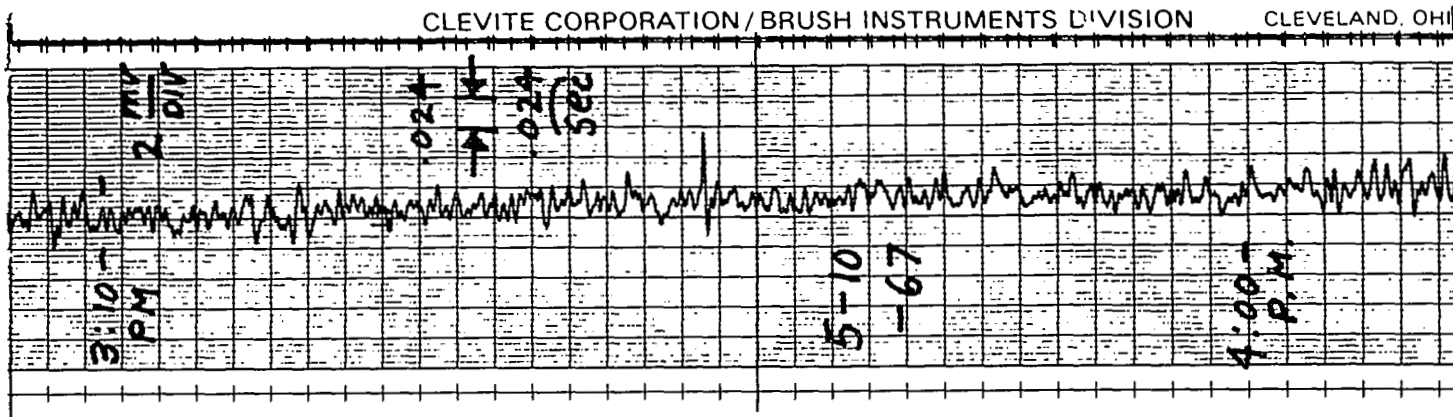
Figure 4-9.   Comparison of Platform Performance with Ball Bearing and with Gas Bearing Gyroscope
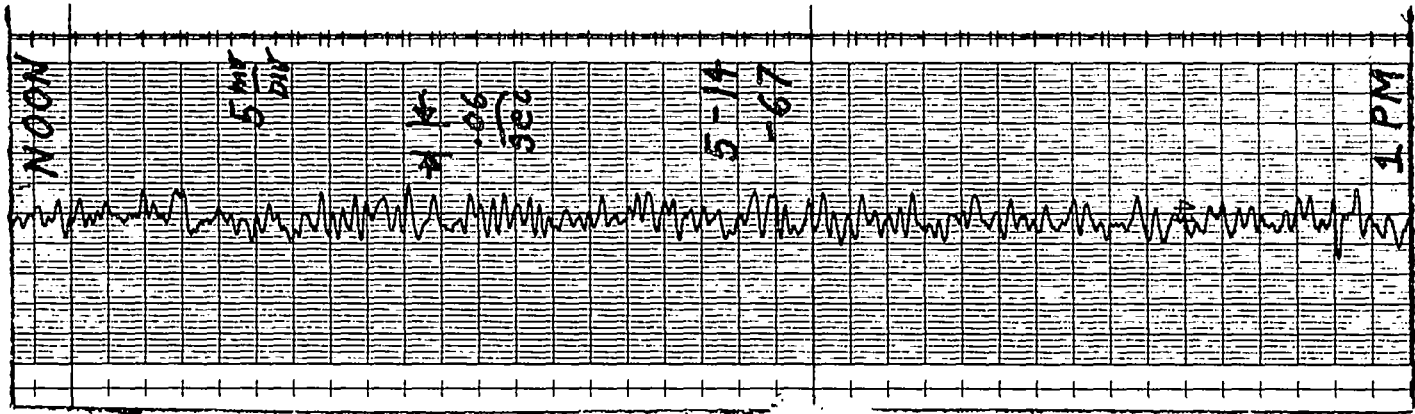
Platform Error Angle Ball Bearing Gyro
Gyro Supported By Plastic Standoffs

134
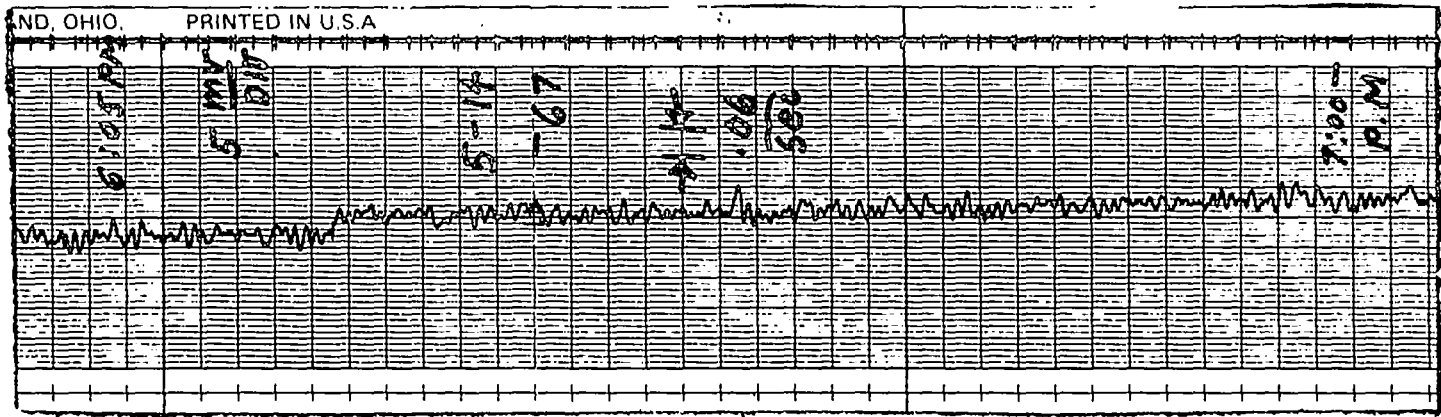
Platform Error Angle Ball Bearing Gyro
Plastic Standoffs Removed

Figure 4-10.   Effect of Plastic Standoffs on System Performance
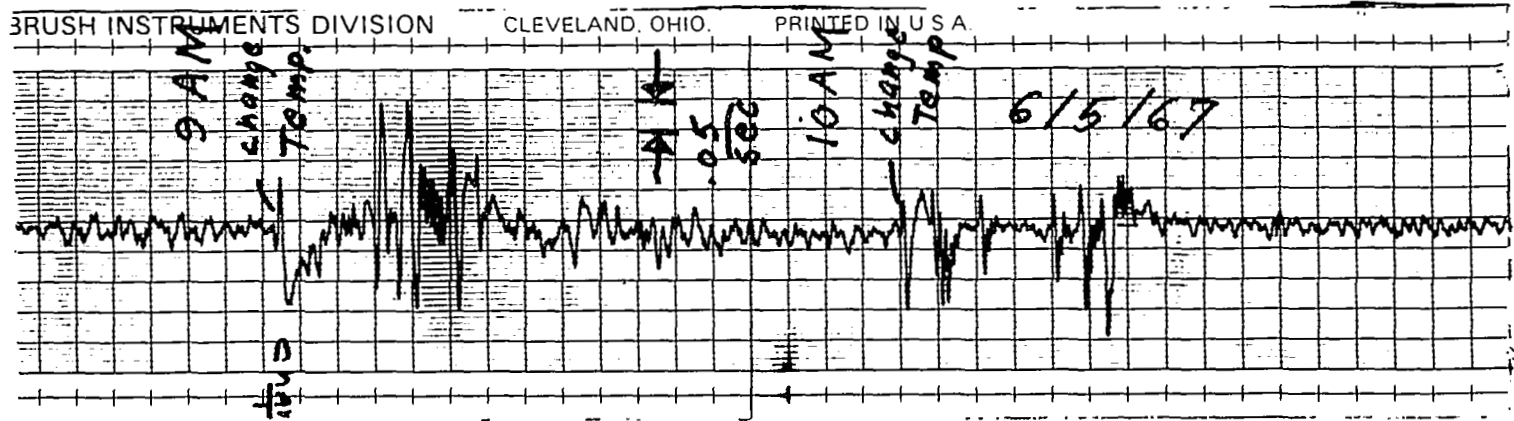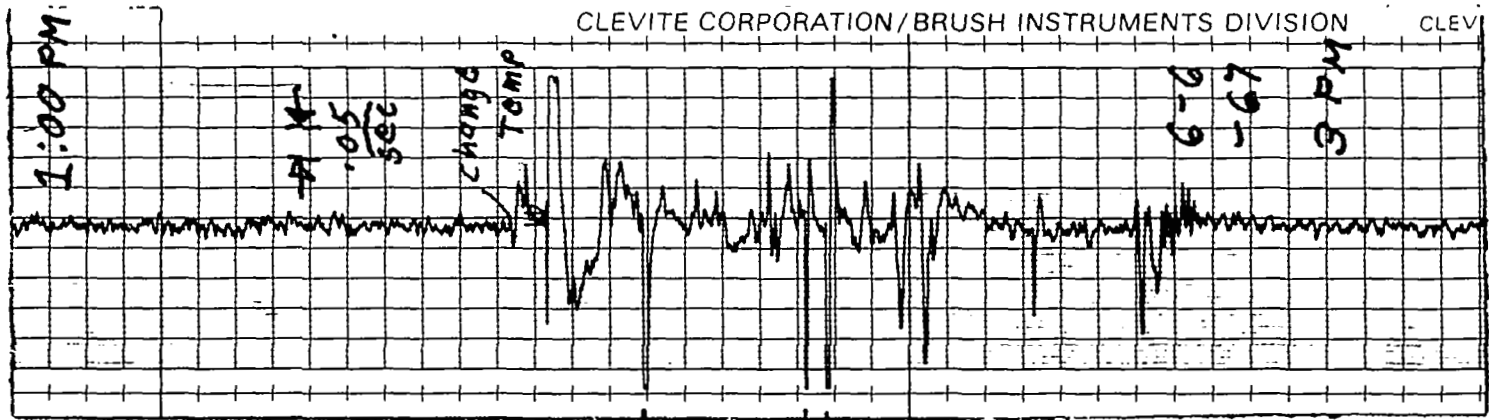
Platform Error Angle-Ball Bearing Gyro
Effect of Temperature Change on System Performance

Figure 4-11. Platform Error Angle-Ball Bearing Gyro Effect of Temperature Change on System Performance
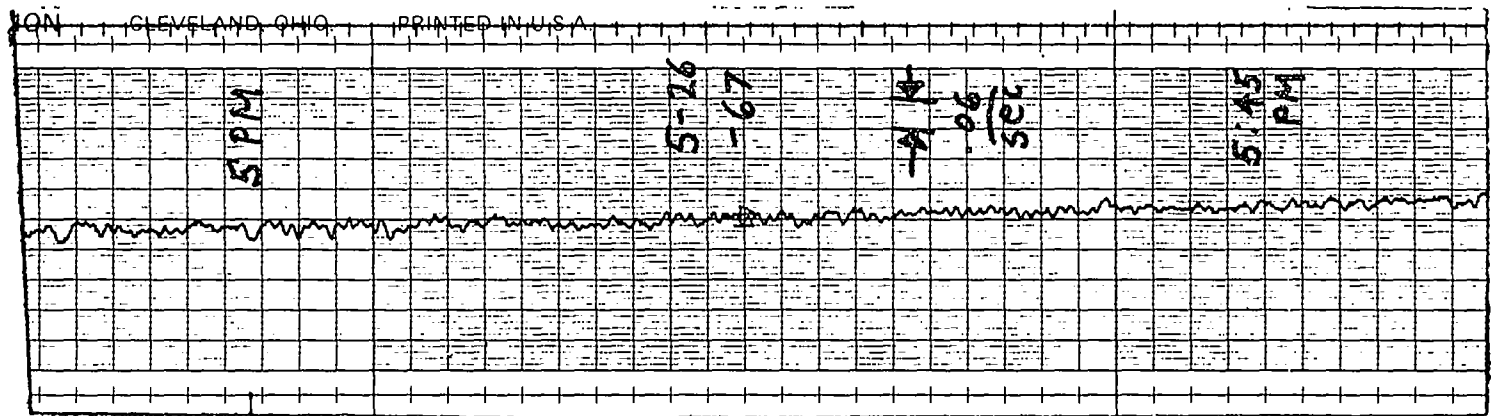
Platform Error Angle After Improvements in Gyro Mounting
and Temperature Control.
Ball Bearing Gyro

Figure 4-12.   Platform Error Angle After Improvements in Gyro Mounting and Temperature Control.
Ball Bearing Gyro

bearing gyro was reduced to about 0.03 arc second peak
to peak disregarding the long term drift produced by the
integration amplifier. Figures 4-13 and 4-14 show that
the long term drift is reduced by increasing the tiltmeter
sensitivity and removing the amplifier d.c. bias.
Figure 4-13 also shows the effect of a sudden unexplained
bias change in the gyro and the system's ability to com-
pensate for the change. In the course of testing several
unexplained platform excursions began to appear which
occurred at random intervals. The frequency of these
excursions increased as the tests continued and are
believed to represent a deterioration in the instrument
bearings. The unit on July 27th had been operating for
over 2000 hours which is near the normal expected life of
ball bearing instruments. Gas bearing instruments have
been reported to show no major deterioration with opera-
ting time.

4.4 Summary

The tests conducted on the experimental system
demonstrate that a servomechanism system having an effec-
tive natural frequency of 9 cps can be built using exist-
ing hardware and that a stiffer drive mechanism is
required to achieve the desired 25 cps response discussed
in Section III. As predicted in Sections II and III the
principal limitation on low frequency performance is the
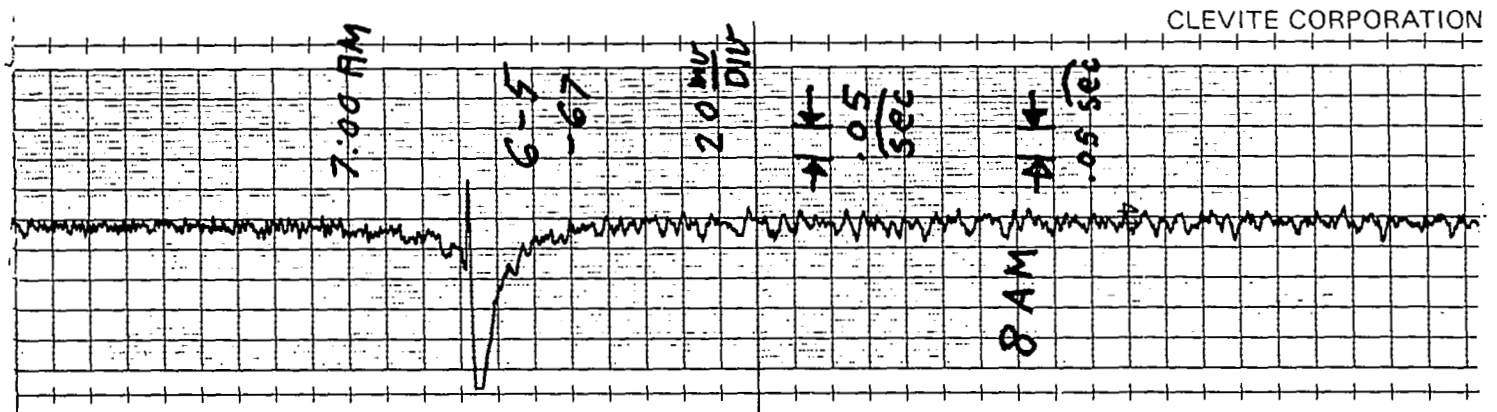
Platform Error Angle-Ball Bearing Gyro
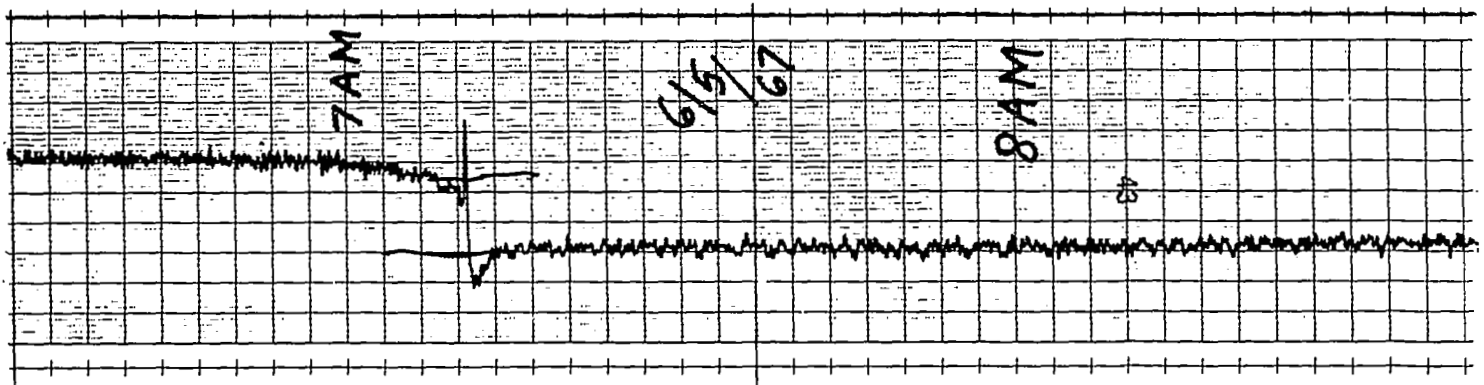
Gyro Compensation Torque

Figure 4-13.   Effect of Sudden Change in Gyro Drift Rate

Platform Error Angle

Ball Bearing Gyroscope

Suspected Friction Changes in Ball Bearing
with Performance Deterioration with Time
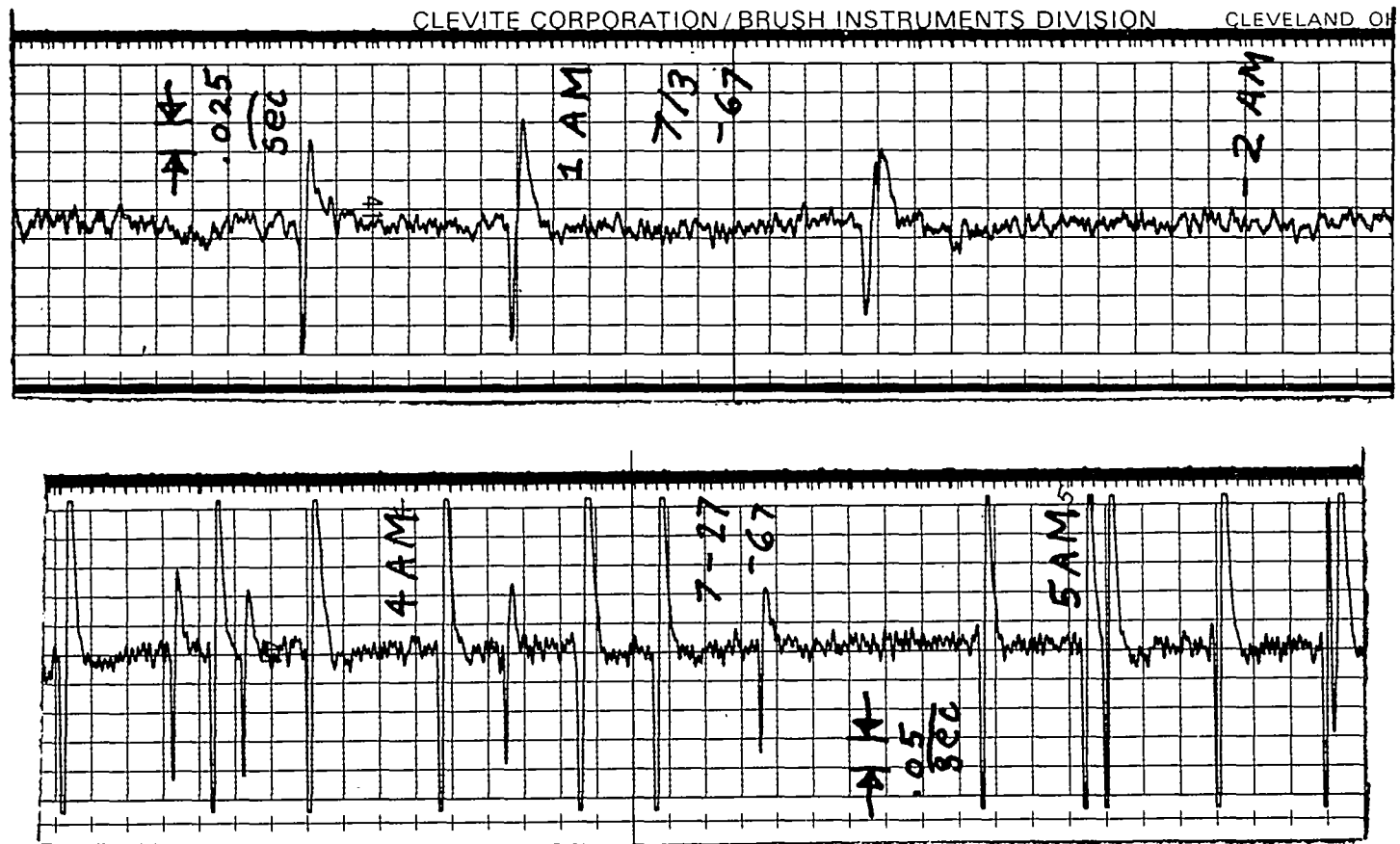
Figure 4-14. Suspected Friction Changes in Ball Bearing with Performance Deterioration with Time

noise and drift rate produced by the gyroscope instrument.
The experimental system indicates noise levels of about
0.03 arc seconds peak to peak can be achieved with exist-
ing and readily available instruments. A major advantage
of the experimental system over other existing systems
is its ability to resist torque loadings and transient
disturbances. A man sitting on the platform resulted in
deflections of the drive of about 3 arc seconds while the
resulting maximum platform error indicated by the level
was of the order of 0.2 arc second.

APPENDIX A

Calculation of Optimum Frequency Characteristics

of Levelling Servomechanism.

Section II requires the operator L(s) that will
yield a minimum rms value of the system error angle
under the conditions:

$$\overline{\delta^2} = \int_0^\infty \Phi_{\delta\delta}(f)\ df \qquad\qquad (A-1)$$

$$\Phi'_{\delta\delta}(\omega) = |L(j\omega)|^2 \Phi'_{11}(\omega) + |1-L(j\omega)|^2 \Phi'_{22}(\omega) \qquad (A-2)$$

Disregarding the requirement of physical realizability
the optimum characteristic of L(jω) is given by:

$$L(j\omega) = \frac{\Phi'_{22}(\omega)}{\Phi'_{11}(\omega) + \Phi'_{22}(\omega)} \qquad\qquad (A-3)$$

This frequency characteristic generally cannot be
obtained in a stable system but serves as a measure of
the best conceivable performance that can be expected.
That is, with the given spectra it is not possible to
obtain a smaller value of $\overline{\delta^2}$.

The best physically realizable system can be
obtained for rational spectra (spectra which can be
reduced to the ratio of two polynomials in ω^2) by the
Bode and Shannon approach to the design of the optimum
linear filter. The optimum frequency characteristic is:

$$L(s) = \frac{1}{\Phi_{ii}^{''+}(s)} \left[\frac{\Phi_{22}^{''}(s)}{\Phi_{ii}^{''}} \right]_+ \qquad (A-4)$$

where:

$$\Phi_{ii}^{''}(s) = \Phi_{11}^{''}(s) + \Phi_{22}^{''}(s)$$

$$\Phi_{22}^{''}(s) = \text{Function obtained by substituting } s = j\omega$$
$$\text{in spectral density } \Phi_{11}^{'}(\omega)$$

The quantities $\Phi_{ii}^{''+}$ and $\Phi_{ii}^{''-}$ are obtained by factoring
$\Phi_{ii}^{''}$ in the form:

$$\Phi_{ii}^{''} = (\alpha_1+s)(\alpha_2+s)(\alpha_3+s)..(\ ) (\beta_1-s)(\beta_2-s)....$$

and defining:

$$\Phi_{ii}^{''+} = (\alpha_1+s)(\alpha_2+s)(\alpha_3+s).....$$

142

$$\Phi_{ii}^{''-} = (\beta_1-s)(\beta_2-s)(\beta_3-s)\ldots\ldots$$

The notation $\left[\ \right]_+$ represents the partial fraction expansion of the quantity disregarding those fractions whose denominators would result in an unstable system (e.g., $\left(\frac{1}{\alpha - s}\right)$).

A.1 Best Frequency Characteristic for System Using Only Level Transducers.

Section 2.2 requires the optimum characteristic $L(j\omega)$ for:

$$\Phi_{\delta\delta}'(\omega) = |(1-L(j\omega))|^2 \Phi_{\theta\theta}'(\omega) + |L(j\omega)|^2 \Phi_{aa}'(\omega)$$

$$(2-16)$$

Figure 1-1 gives the reference spectra between 10^{-5} and 1 cps as:

$$\Phi_{\theta\theta}(f) = \frac{10^{-3}}{f^2}(1+10f^2)\ \frac{\widehat{sec}^2}{cps}$$

$$\Phi_{aa}(f) = \frac{10^{-15}\left(1 + \frac{f^4}{10^{-8}}\right)}{\left(1+\frac{f^2}{10^{-2}}\right)}\qquad g^2/cps$$

143

Substitution of:

$$\omega = 2\Pi f$$

$$s = j\omega$$

and converting the acceleration to arc second units gives the spectral densities as:

$$\Phi_{\theta\theta}''(s) = \frac{10^{-2}}{-s^2} \ (3.94 - s^2)$$

$$\Phi_{aa}''(s) = \frac{1.08 \ (1.56 \times 10^{-5} + s^4)}{(0.3944 - s^2)}$$

which gives:

$$\Phi_{ii} = \frac{0.0156 - 0.0434s^2 + .01s^4 - 1.08s^6}{-s^2(.3944 - s^2)}$$

which is factored as:

$$\Phi_{ii} = \frac{1.08(.438+s)(.438-s)(s^2 + .604s + .274)(s^2 - .604s + .274)^2}{(\varepsilon + s)(\varepsilon - s)(.628 + s)(.628 - s)}$$

thus:

$$\Phi_{ii}^+ = \frac{1.039(.438+s)(s^2 + .604s + .274)}{(\varepsilon + s)(.628 + s)}$$

144

and

$$\left[\frac{\Phi_{\theta\theta}}{\Phi_{ii}}\right] = \frac{10^{-2}(1.98+s)(1.98-s)(.628-s)}{1.039(\varepsilon+s)(.438-s)(s^2-.604s+.274)}$$

The only term in the partial expansion without roots in the right half of the complex plane is:

$$\left[\frac{\Phi_{\theta\theta}}{\Phi_{ii}}\right]_+ = \frac{3.94 \times .628 \times 10^{-2}}{1.039 \times .438 \times .274\,s}$$

$$= \frac{0.198}{s}$$

The optimum frequency characteristic is then obtained as:

$$L(s) = \frac{(0.628+s)(.198)}{1.039(0.438+s)(s^2+.604s+.274)}$$

which reduces to:

$$L(s) = \frac{\left(1+\dfrac{s}{.628}\right)}{\left(1+\dfrac{s}{.438}\right)\left(1+1.15\left(\dfrac{s}{.523}\right)+\dfrac{s^2}{(.523)^2}\right)}$$

by replacing s with jω we obtain the result given in Equation (2-19).

A.2 Optimum Filter for Level Sensor in Servomechanism Using Both Level Sensors and Gyroscopes for Control.

Section 2.3 gives the error angle of the system for frequencies less than 1 cps as:

$$\delta(s) = L_2(s) \frac{a_x}{g} + (1-L_2(s)) \, \epsilon_g(s)$$

with the requirement that $L_2(s)$ be selected to produce a minimum rms error angle.

For frequencies below 1 cps the acceleration power spectral density is in arc second units:

$$\Phi_{aa}''(s) = \frac{1.08(1.56 \times 10^{-5} + s^4)}{(0.3944 - s^2)}$$

the gyro drift angle power spectral density is obtained from Figure 2-5 as:

$$\Phi_{gg}''(s) = \frac{10^{-5}(3.94 \times 10^{-5} - s^2)}{s^4}$$

The algebraic manipulations outlined above result in:

146

$$L_2(s) = \frac{3.47 \times 10^{-3}(5.76 \times 10^{-3}+s)(0.628+s)}{(s+6.28 \times 10^{-3})(s+.124)(s^2+.128s+.0159)}$$

Further algebraic manipulation of Equations (2-22) through (2-26) results in:

$$L_o(s) = \frac{0.117(.628+s)\left[\dfrac{5.75 \times 10^{-3}}{s}+1\right]}{(1+8.6s+33.3s^2)}$$

Since the acceleration spectrum at 0.1 cps is more than 4 orders of magnitude above the gyro error there is little practical purpose served by the lead introduced at 0.1 cps by the (0.628+s) factor. The optimum filter is therefore taken as:

$$L_o(s) = \frac{0.0735\left[1+\dfrac{0.00575}{s}\right]}{1+8.6s+33.3s^2}$$

as given by Equation (2-20).

A.3 Optimum High Frequency Characteristic for Servomechanism Using Both Level Sensors and Gyroscopes for Control (Without Passive Isolation).

For frequencies above 0.001 cps the power spectral density of the gyro drift angle is:

147

$$\Phi_{gg}^{"}(s) = \frac{2.54 \times 10^{-7} (39.44 - s^2)}{-s^2}$$

and the angular vibration spectral density of the ground motion is approximated by:

$$\Phi_{\theta\theta}^{"}(s) = \frac{24.3 \times 10^3}{-s^2} \frac{(3.944 - s^2)}{(394.4 - s^2)(6166 - s^2)}$$

this spectrum agrees with Figure 1-1 with the exception that it falls off at 4 orders of magnitude per decade after 12.5 cps while Figure 1-1 falls off at 4½ orders of magnitude per decade. This simplification is permissible since the reference spectral densities are estimates of the environment and the density given here is more severe than the reference spectra.

Proceeding in the same manner as above the optimum frequency characteristic obtained as:

$$L_3(s) = \frac{(1 + s/2)\left(1 + \frac{1.28s}{556}\right)}{\left(1 + \frac{s}{1.985}\right)\left(1 + 1.41 \frac{s}{556} + \frac{s^2}{(556)^2}\right)}$$

Since the lag-lead characteristic $\left(\frac{1 + s/2}{1 + s/1.985}\right)$ has a negligible effect on the system performance the required filter is taken as:

$$L_3(s) = \frac{1 + \frac{1.28s}{556}}{(1 + 1.41s/556 + \frac{s^2}{(556)^2})^2}$$

A.4 Optimum High Frequency Characteristic for Servo-mechanism Using Both Level Sensors and Gyroscopes With 1 CPS Passive Isolation.

The power spectral density of the gyroscope drift angle for frequencies above .001 cps is as above:

$$\Phi''_{gg}(s) = \frac{2.54 \times 10^{-7}}{-s^2} \, (39.44 - s^2)$$

the angular vibration spectral density of the ground motion transmitted through the .1 cps passive vibration isolation system is approximated as:

$$\Phi''_{\theta\theta} = \frac{24.32 \times 10^3 \times (2\pi)^2 (3.94 - s^2)}{(394.4 - s^2)(6166 - s^2)((2\pi)^2 - s^2)}$$

The algebraic manipulations indicated above result in:

$$L = \frac{(s+1.99)(s^2 + 184s + 11715)}{(s+1.985)(s+134)(s^2 + 133s + 14380)}$$

As above the lag-lead characteristic at 2 rad/sec has no significant effect and the optimum filter is:

149

$$L(s) = \dfrac{1 + \dfrac{1.7s}{108} + \dfrac{s^2}{(108)^2}}{\left(1 + \dfrac{s}{134}\right)\left(1 + \dfrac{1.11s}{120} + \dfrac{s^2}{(120)^2}\right)}$$

REFERENCES

1. Weiher, T. E.: Progress in Test Pad Stability. AIAA/ION, Guidance and Control Conference, Minneapolis, Minn., August 16–18, 1965.

2. Test Pad Stability. AIAA/JACC, Guidance and Control Conference, Seattle, Washington, August 15–17, 1966.

3. Mathis, L. O., Stephens, J. R., and Wright, S.C.: The Design and Construction of an Inertial Test Facility, AlAA/ION, Guidance and Control Conference, Minneapolis, Minn., August 16–18, 1965.

4. Preskitt, S. V., and Fix, J. E.: Six Degree of Freedom Test Podium at the United States Air Force Standards Calibration Laboratory. Technical Report No. 63–46, The Geotechnical Corporation, Garland, Texas, May 1963.

5. Tsutsumi, K.: A Ground Tilt Isolation Platform. Report No. E-1508, M.I.T. Instrumentation Laboratory, January 1964.

6. DeBra, D. B., Mathieson, J. C., and Van Patten, R.A: A Precision Table Levelling System. AIAA/JACC, Guidance and Control Conference, Seattle, Washington, August 15–17, 1966.

7. Pepi, J. S., and Cavanaugh, R. D.: Performance Characteristics of an Automatic Tilt Stabilization and Vibration Isolation System. AIAA Guidance Control and Flight Dynamics Conference, Huntsville, Alabama, August 14–16, 1967.

8. Cavanaugh, R. D.: Air Suspension and Servo-Controlled Isolation Systems, Section 33 of Shock and Vibration Handbook, Harris, C. M., and Crede, C. E. Editors, McGraw Hill Book Company, New York, 1961.

9. Weinstock, H.: Limitations on Inertial Sensor Testing Produced by Test Platform Vibrations, Electronics Research Center, NASA Technical Note TND-3683, November 1966.

10. Truxal, J. G.: Control System Synthesis, McGraw Hill Book Company, New York, 1955.

11. Gardner, M. F., and Barnes, J. L.: Transients in Linear Systems, John Wiley and Sons, Inc., New York, 1958.

12. Ideal Aerosmith Tiltmeter, Dual Cistern Model DCTM-11, Ideal Aerosmith, Inc., Cheyenne, Wyoming.

13. Wrigley, W.: Single Degree of Freedom Gyroscopes. M.I.T. Instrumentation Laboratory, Report No. R-375, Cambridge, Mass., 1962.

14. C702590 Gas Bearing King II Floated Rate-Integrating Gyro, Kearfott Davison, General Precision, Inc., Aerospace Group, Little Falls, N. J., May 1965.

15. Analog Devices Operational Amplifiers, Analog Devices Company, Cambridge, Mass.

16. Inland Motors Torquer and Tachometer Catalogue, Inland Motors Catalogue, Inland Motors Corporation, Radford, Va.

17. Roark, R. J.: Formulas for Stress and Strain, McGraw Hill Book Company, New York 1954.

18. Crede, C. E., and Rusyicka, J. E.: Theory of Vibration Isolation, Shock and Vibration Handbook, Harris, C. M. and Crede, C. E., Editors, McGraw Hill Book Company, New York 1961.

19. Krach, F., Barry Controls Division of Barry Wright Corporation, Letters to Herbert Weinstock, NASA, Electronics Research Center, October and December 1966.

DEFINITION OF SYMBOLS

A_o	=	Effective area of large piston of micromotion drive.
A_{OA}	=	Gyroscope output angle.
a_x	=	Translational ground acceleration.
$B(s)$	=	Operational transfer function.
C	=	Viscous damping constant.
C	=	Electrical capacitance.
C_d	=	Viscous damping of single-degree-of-freedom gyroscope.
C_a	=	Air compliance of micromotion drive.
C_b	=	Bellows compliance of micromotion drive.
C_f	=	Fluid compliance of micromotion drive.
C_{TQ}	=	Torquer constant (torque per unit current).
C_{TCH}	=	Tachometer sensitivity (voltage per unit angular velocity).
E	=	Modulus of Elasticity.
F	=	Force.
f	=	Frequency.
f_n	=	Natural frequency of second order system.
f_v	=	Vertical natural frequency of servomechanism drive.
f_θ	=	Rotational natural frequency of servomechanism drive.
$G(s)$	=	Filter transfer function.
G	=	Effective integration gain of servoed air spring.
g	=	Specific force of gravity.

153

H	=	Gyroscope rotor angular momentum.
h	=	Gyroscope gain (output angle per unit input angle).
I	=	Area moment of inertia.
I_O	=	Platform moment of inertia.
I_{OA}	=	Gyroscope output axis moment of inertia.
J	=	Drive shaft moment of inertia.
j	=	$\sqrt{-1}$
K	=	Stiffness.
k_g	=	Gyroscope elastic restraint.
K_θ	=	Drive rotational stiffness.
K_ℓ	=	Drive translational stiffness.
L(s)	=	Filter transfer function.
M	=	Mass.
M_d	=	Disturbance Torque.
Mgl	=	Pendulousity.
N	=	Number of bellows convolutions.
n	=	Ratio of damper spring stiffness to main spring stiffness of filtered damper.
n(s)	=	Laplace transform of system noise signals.
p	=	Pressure.
q	=	Drive voltage.
R_O	=	Nominal bellows radius.
r	=	Radius.
s	=	Laplace transform operator.
t	=	Thickness of bellows.

V	=	Volume.
v	=	Voltage generated by control sensors.
v_a	=	Control sensor voltage per unit acceleration.
v_g	=	Control sensor voltage per unit gyro drift rate.
v_δ	=	Control sensor voltage per unit error angle.
x	=	Horizontal position.
y	=	Vertical displacement.
α	=	Ratio of air volume of micromotion drive to fluid volume.
α	=	Drive shaft angle.
β	=	Ratio of damping present in a second order system to critical damping for the system.
δ	=	Platform error angle.
ε_a	=	Angular tilt to produce specific force of translational acceleration.
ε_g	=	Gyro drift angle.
θ	=	Angular deviation from level of base.
ϕ	=	Angular motion produced by servomechanism drive.
τ	=	Time constant.
$\Phi_{aa}(f)$	=	Translational acceleration power spectral density.
$\Phi_{gg}(f)$	=	Gyro drift angle power spectral density.
$\Phi_{\theta\theta}$	=	Power spectral density of ground angular rotations.
$\Phi_{\delta\delta}$	=	Power spectral density of platform error angle.
$\Phi_{\delta\delta a}$	=	Power spectral density of error angle produced by horizontal accelerations.
ω	=	$2\pi f$
ω_n	=	$2\pi f_n$

155

BIOGRAPHY OF THE AUTHOR

Herbert Weinstock holds the degrees of Mechanical
Engineer and Master of Science in Mechanical Engineering
from the Massachusetts Institute of Technology and the
degree of Bachelor of Mechanical Engineering from the
City College of New York.

After receiving his bachelor's degree in June 1957,
Mr. Weinstock joined the staff of Allied Research Asso-
ciates Inc., Boston, Massachusetts where he was concerned
with the analysis of structures subjected to vibration
and shock loadings and with the design and testing of
special purpose vibration isolation systems. Mr. Weinstock
left Allied Research Associates in September of 1959 to
resume formal studies at M.I.T. where he received the
Master of Science degree in February of 1960. His master's
thesis was concerned with the effects of vibration on
gyroscope instruments.

In June of 1960, Mr. Weinstock became a member of the
staff of the M.I.T. Instrumentation Laboratory where he
conducted analytical and experimental studies of special
problems related to the design and evaluation of gyroscope

instruments. These problems included evaluations of the
effects of environmental conditions (e.g., temperature,
shock and vibration) on the performance of gyroscope
instruments and design of test methods for prediction of
instrument performance in final system application.
During this period, Mr. Weinstock continued his formal
studies at M.I.T. and received the degree of Mechanical
Engineer in June 1962.

Mr. Weinstock left the M.I.T. Instrumentation
Laboratory in November of 1965 to join the newly formed
Guidance Laboratory of the NASA Electronics Research
Center. He resumed his formal full time studies at M.I.T.
in February of 1966 and undertook the study described in
this document.

Mr. Weinstock is a member of the American Society of
Mechanical Engineers, Tau Beta Pi, Pi Tau Sigma and the
American Institute of Aeronautics and Astronautics where
he is serving as a member of the Test Pad Stability Sub-
committee of the Guidance and Control Committee.

PUBLICATIONS:

> "A study of the response of the Single-Degree-of-
> Freedom Integrating Gyroscope to Angular Vibrations."
> S.M. Thesis. M.I.T. Instrumentation Laboratory

PUBLICATIONS:
  (Cont)

      Report E-885, Jan. 1960.

      "Specification for the Permissible Motions of a Plat-
      form for Performance Evaluation of Single-Degree-of-
      Freedom Inertial Gyroscopes." M.I.T. Instrumentation
      Laboratory Report E-1267, Dec. 1962. Presented at the
      Symposium of A.I.A.A. Test Pad Stability Subcommittee
      at Dallas, Texas Feb. 1964.

      "The Description of Stationary Random Rate Processes."
      M.I.T. Instrumentation Laboratory Report E-1377,
      Jul. 1963.

      "Effects of Vibration on Gyroscope Instruments."
      M.I.T. Instrumentation Laboratory Report E-1399, Aug.
      1963. (Notes used for M.I.T. Special Summer Session
      Course 16.39S - Inertial Navigation Equipment Test
      and Evaluation. Aug. 1963.)

      "Laboratory Test Equations for the Evaluation of the
      Pendulous Integrating Gyroscope and The Linear Inte-
      grating Accelerometer." M.I.T. Instrumentation
      Laboratory Report E-1400, Aug. 1963.

      "Statistical Analyses of Sixteen Earth Reference Drift
      Runs of 4FBG Gyroscopes." M.I.T. Instrumentation
      Laboratory Report E-1486, April 1964.

      "Effects of High Acceleration on Ball Bearing Gyroscope
      Performance." M.I.T. Instrumentation Laboratory Report
      E-1568, May 1964.

      "Statistical Analyses of Five Inertial Reference Servo
      Runs." M.I.T. Instrumentation Laboratory Report E-1694,
      Nov. 1964.

      "Frequency Response Characteristics of a Typical Single-
      Degree-of-Freedom Integrating Gyroscope." With V.
      Marchese, M.I.T. Instrumentation Laboratory Report
      E-1721, Jan. 1965.

      "Effects of Assymetrical Temperature Distributions on
      Gyroscope Unbalance Torques." M.I.T. Instrumentation
      Laboratory Report E-1798, Jan. 1962.

"The aeronautical and space activities of the United States shall be conducted so as to contribute . . . to the expansion of human knowledge of phenomena in the atmosphere and space. The Administration shall provide for the widest practicable and appropriate dissemination of information concerning its activities and the results thereof."

— NATIONAL AERONAUTICS AND SPACE ACT OF 1958

NASA SCIENTIFIC AND TECHNICAL PUBLICATIONS

TECHNICAL REPORTS: Scientific and technical information considered important, complete, and a lasting contribution to existing knowledge.

TECHNICAL NOTES: Information less broad in scope but nevertheless of importance as a contribution to existing knowledge.

TECHNICAL MEMORANDUMS: Information receiving limited distribution because of preliminary data, security classification, or other reasons.

CONTRACTOR REPORTS: Scientific and technical information generated under a NASA contract or grant and considered an important contribution to existing knowledge.

TECHNICAL TRANSLATIONS: Information published in a foreign language considered to merit NASA distribution in English.

SPECIAL PUBLICATIONS: Information derived from or of value to NASA activities. Publications include conference proceedings, monographs, data compilations, handbooks, sourcebooks, and special bibliographies.

TECHNOLOGY UTILIZATION PUBLICATIONS: Information on technology used by NASA that may be of particular interest in commercial and other non-aerospace applications. Publications include Tech Briefs, Technology Utilization Reports and Notes, and Technology Surveys.

Details on the availability of these publications may be obtained from:

SCIENTIFIC AND TECHNICAL INFORMATION DIVISION

NATIONAL AERONAUTICS AND SPACE ADMINISTRATION

Washington, D.C. 20546